

THE BELL SYSTEM TECHNICAL JOURNAL

DEVOTED TO THE SCIENTIFIC AND ENGINEERING
ASPECTS OF ELECTRICAL COMMUNICATION

Volume 51

May-June 1972

Number 5

Copyright © 1972, American Telephone and Telegraph Company. Printed in U.S.A.

Where on the Moon? An Apollo Systems Engineering Problem*

Edited by J. O. CAPPELLARI, Jr.

(Manuscript received January 17, 1972)

Foreword

Bellcomm was established early in 1962 in response to a National Aeronautics and Space Administration (NASA) request to the Bell System for technical support of the manned space flight programs at the NASA Headquarters level. It was a small company, reaching a peak of 500 people in 1969, and was jointly owned by American Telephone and Telegraph Company and Western Electric Company. The initial cadre of technical people was drawn mainly from Bell Laboratories and Western Electric, with the administrative staff drawn mainly from Western Electric and the Operating Companies.

In its role as technical adviser to the Apollo Program Director, one of Bellcomm's major responsibilities was in the area of Apollo Program systems engineering, helping to insure that the total system being developed would, in fact, be able to successfully perform the planned Apollo missions. A significant part of this task involved insuring that

* Work performed for the National Aeronautics and Space Administration under Contract NASw-417

the missions, their objectives, and the required systems capabilities were sufficiently well identified in advance so that all of the Apollo Program objectives would be achieved in an orderly fashion. This issue of *The Bell System Technical Journal* is devoted to a description of one example of the work conducted at Bellcomm, that related to Apollo lunar landing site selection. Many people were involved in the site selection process over the years. However, only the names of the few who contributed directly to the preparation of this issue have been included in the list of contributors on page 1127.

Apollo missions have been priced by NASA in the range of one-third to one-half a billion dollars each. When the goal was to land on the Moon for the first time, almost any landing site was as valuable as another. However, for the second, third, and successive landings, where the objective was to help unlock the secrets of the Moon and the Solar System, the motivation was high to get the maximum useful information from every mission. If the systems approach was ever applied exhaustively, it was here, where Bellcomm and NASA left no stone unturned in trying to bring all sources of information to bear on the landing site decisions. Bellcomm's role was to assemble and interpret for NASA Headquarters all of the technical information pertinent to site selection. Data were obtained for this purpose from the Manned Spacecraft Center, the Marshall Space Flight Center, the Kennedy Space Center, and the scientific community; on important issues independent, and many times original, analyses were made by Bellcomm. The scientific rationale and objectives, and the Apollo systems's capability to safely meet the objectives were the basis for NASA's final selection between alternative sites.

With the successful completion of the Apollo 11 lunar landing mission, the original goal of the Apollo program was achieved. Soon thereafter Bellcomm began to phase out of the NASA work and on April 1, 1972, the organization was merged with Bell Laboratories, its work on the space program essentially complete.

Table of Contents

	<i>Page</i>
List of Figures	959
Abstract	961
I. INTRODUCTION	
1.1 Site Selection—A Systems Engineering Problem	961
1.2 Overview of the Site Selection Process	962
1.3 Survey of Major Constraints Affecting Site Selection	967
II. SATISFYING THE SCIENCE OBJECTIVES OF LUNAR EXPLORATION	
2.1 Lunar Exploration Goals	968
2.2 Preparing for the Selection of Apollo Landing Sites	972
2.2.1 Acquisition of Required Data	973
2.2.2 Site Selection for Apollo Missions 11 and 12	976
2.2.3 Site Selection for Apollo Missions 14 through 17	976
2.3 Mission Science Planning and Its Impact on Site Selection	979
2.3.1 Apollo Lunar Surface Experiment Packages	979
2.3.2 Orbital Science	983
2.3.3 Lunar Surface Traverse Capability	983
2.4 Lunar Science Results and Site Selection Implications	985
2.4.1 The Mare Basalts and Lunar Interior Composition	985
2.4.2 Regolith (Soil)	989
2.4.3 Breccias	990
2.4.4 Mare Soil "Foreign Components": Anorthosites and KREEP	990
2.4.5 Fra Mauro (KREEP+)	995
2.4.6 Lunar Chronology	995
2.4.7 Lunar Surface Processes	998
2.4.8 Global Aspects of the Moon	1001
2.4.9 Lunar Carbon, Organic Matter, and "Life"	1003
2.4.10 Tektites and Meteorites	1004
2.4.11 Origin of the Moon	1005
III. APOLLO SYSTEM CAPABILITIES	
3.1 The Apollo Missions	1006
3.1.1 Development Missions	1006
3.1.2 Lunar Exploration Missions	1007
3.1.3 General Mission Description	1008
3.2 Lunar Accessibility	1009
3.2.1 Introduction	1009
3.2.2 Mission Design Requirements and Constraints	1011
3.2.3 Launch Vehicle Considerations	1028
3.2.4 Launch Operational Considerations	1031
3.2.5 Methods of Determining Accessibility	1034
3.3 Lunar Module Descent Considerations	1043
3.3.1 Basic Shaping and Constraints	1044
3.3.2 Navigation	1048
3.3.3 Landing Site Redesignation	1050
3.3.4 Landability	1052
3.3.5 Evolution of LM Descent Requirements	1053
IV. SUMMARY	1054
APPENDIX A	
Lunar Lighting	
A.1 Introduction	1055

	<i>Page</i>
A.2 Photometric Quantities.....	1056
A.3 Visual Psychophysics.....	1059
A.4 Lunar Photometry.....	1062
A.5 Visibility Analyses.....	1067
A.6 Apollo Mission Launch Opportunities.....	1073
APPENDIX B	
LM Descent Hardware and Trajectory Details	
B.1 Hardware Description.....	1074
B.2 Guidance Equations.....	1076
APPENDIX C	
Lunar Orbital Navigation	
C.1 Introduction.....	1080
C.2 Observational Data.....	1081
C.3 Dynamical Formulation.....	1081
C.4 Data Reduction.....	1085
C.5 Real-Time Procedures.....	1087
APPENDIX D	
The Bellcomm Apollo Simulation Program	
D.1 Introduction.....	1090
D.2 Structure.....	1092
D.3 The Simulator.....	1093
D.4 Modes of Operation.....	1093
D.5 Program Modifications.....	1094
APPENDIX E	
Mass and Performance Tradeoffs	
E.1 Introduction.....	1098
E.2 Tradeoffs.....	1099
E.3 Limit Masses.....	1102
APPENDIX F	
Apollo Landing Sites	
F.1 Introduction.....	1108
F.2 Fra Mauro Region (Apollo 14).....	1108
F.3 Hadley-Apennine Region (Apollo 15).....	1110
F.4 Descartes Region (Apollo 16).....	1110
F.5 Alphonsus (Apollo 17 Candidate Site).....	1113
F.6 Gassendi (Apollo 17 Candidate Site).....	1114
F.7 Taurus-Littrow (Apollo 17).....	1116
APPENDIX G	
Aborts.....	1117
REFERENCES.....	1122
CONTRIBUTORS TO THIS ISSUE.....	1127

List of Figures

<i>Fig.</i>	<i>Title</i>	<i>Page</i>
1	Historical development of the site selection process.....	963
2	Mechanics of the site selection process (Apollo missions 16 and 17). . .	964
3	Landing sites in the Apollo operational zone.....	967
4	Geologic provinces of the near side of the Moon.....	970
5	Site landability.....	975
6	Apollo landing site locations.....	977
7	The Apollo 12 landing site.....	978
8	Apollo landing site photography.....	980
9	Layering in the west wall of Hadley Rille.....	986
10	Potassium versus potassium/uranium values for meteorites, tektites, the Earth, and the Moon.....	988
11	Simplified phase diagram for the Apollo 11 basalts.....	989
12	Chemical anomalies in mare soil.....	991
13	Exotic components ejected by meteoroid impact from highlands into mare soil.....	992
14	Generalized lunar cratering and thermal history.....	999
15	Translunar trajectory types.....	1012
16	General lunar accessibility.....	1013
17	Powered descent initiation antenna coverage for Descartes.....	1017
18	Tradeoff of ΔV versus time required for rendezvous.....	1022
19	First two burns of the CSM rescue rendezvous sequence used after abort from powered descent.....	1023
20	The final rendezvous sequence.....	1024
21	Effect of requirements and constraints on SPS propellant.....	1026
22	Relationship between launch window range and duration.....	1031
23	Typical translunar trajectory plane inclination versus declination.....	1032
24	Spacecraft performance as function of launch date and injection opportunity (Copernicus landing site).....	1034
25	J-mission opportunities to Hadley.....	1036
26	Summary of J-mission opportunities.....	1037
27	End-of-mission ΔV reserve.....	1041
28	Typical accessible regions.....	1042
29	Lunar surface accessible in March 1972.....	1043
30	Accessible area by launch date in March 1972.....	1044
31	Lunar surface accessible in December 1972.....	1045
32	The LM descent trajectory.....	1046
33	The visibility and landing phases.....	1047
34	View from the Commander's window.....	1050
35	Contours of constant ΔV penalty for landing site redesignations.....	1052
36	Threshold visibility as a function of angular diameter and contrast.....	1059
37	Lunar photometric geometry.....	1063
38	Integrated lunar surface brightness.....	1064
39	Lunar photometric functions.....	1066
40	Descent guidance logic.....	1077
41	LM descent thrust profile.....	1079
42	Pitch angle versus time.....	1080
43	Tracking configuration.....	1082
44	Spacecraft onboard optical coordinate system.....	1082
45	L1 lunar gravity field equipotential surfaces (near side).....	1084
46	L1 lunar gravity field equipotential surfaces (far side).....	1085
47	Typical sighting sequence.....	1089
48	Spacecraft mass increase resulting from increased experiment mass.....	1103
49	Launch vehicle propellant increase resulting from increased spacecraft mass.....	1103
50	LM performance status.....	1106
51	LM performance status.....	1106
52	CSM performance status for Hadley mission.....	1107

<i>Fig.</i>	<i>Title</i>	<i>Page</i>
53	The Fra Mauro Formation.....	1109
54	The Hadley-Apennine region.....	1111
55	Lunar Orbiter IV photograph of the Descartes region.....	1112
56	Geological sketch map of the Descartes region.....	1113
57	Crater Alphonsus with candidate landing area shown by circle.....	1114
58	Crater Gassendi with candidate landing area shown by circle.....	1115
59	Panoramic camera photograph of the Taurus-Littrow region showing the Apollo 17 landing point.....	1116
60	Apollo 15 minimum ΔV abort requirement.....	1119
61	Apollo 15 minimum return to Earth times for translunar aborts.....	1120
62	Apollo 15 return to Earth requirements from lunar orbit.....	1121

Where on the Moon?

An Apollo Systems Engineering Problem

Abstract

The selection of an appropriate sequence of landing sites on the Moon for the Apollo lunar landing missions was a classical systems engineering problem involving analysis of scientific and engineering factors, hardware and software development and production constraints, time-varying budget considerations, real-time alterations because of mission successes and failures, and evolving scientific and engineering objectives and mission priorities. The Apollo site selection process is examined from a systems engineering viewpoint, particularly as it involved Bellcomm in its role of technical coordinator and adviser to the Apollo Program Director. Significant technical parameters affecting the decision-making process are identified and discussed; they include lunar lighting, landing site approach terrain, landability, science requirements, trajectory mechanics, navigation, mass and performance, safety, and scheduling.

The site selection process was a powerful focal point for organizing to achieve the goals of the Apollo Program. In particular, the interlacing of the scientific and engineering requirements and constraints was made manageable through the concept of lunar accessibility, which was an extremely useful tool in guiding the selection of sites with high scientific value.

The historical development and functional aspects of site selection are presented in order to give an overview of the process; and the impact on site selection of the significant parameters and their interactions is discussed in detail.

I. INTRODUCTION

1.1 Site Selection—A Systems Engineering Problem

The first goal of the Apollo Program was to demonstrate a capability of landing men on the Moon and returning them safely to Earth. Beyond this was the goal of systematic scientific exploration of the lunar surface with a view toward learning more about the origin and history of the Moon, and by extrapolation, about the Earth and the Solar System. These objectives were first translated into specific mission,

engineering, and science requirements, which then led to the selection of areas of the Moon which were of particular interest. These landing site preferences then had to be merged with the capability of the Apollo system to reach the areas of interest, to land there, and to return to Earth, each with required margins of safety. It should be understood that, as the specific mission objectives and requirements changed from mission to mission, so too, site selection developed a different meaning as the program progressed.

Bellcomm recognized early in the program¹⁻⁴ that the selection of lunar landing sites should be a pivotal activity, lying as it did at the strong interface between the capabilities of the system and the continuously evolving desires and objectives of the scientists involved in the lunar program. Bellcomm took the lead in defining the scope of the problem, initiated independent analyses in all problem areas pertinent to site selection, and provided strong, continuing leadership for the entire site selection activity. However, as with all such broad activities, the whole cannot exist without all of its constituent parts, and adequate recognition of much dedicated work by others is necessary for a true perspective of the site selection job.

1.2 Overview of the Site Selection Process

In order to gain some understanding of the site selection process, the historical development of site selection (Fig. 1) and the mechanics of the site selection process (Fig. 2) are described in this section. In the flow chart shown in Fig. 1, the top half of the chart traces the interaction with the Ranger, Surveyor, Orbiter, and previously completed Apollo missions; the bottom half traces the evolution of the scientific community involvement in site selection; while the center box notes the importance, particularly during the early stages of Apollo site selection, of Earth-based mapping.

Once the Apollo program had been initiated, and the lunar orbit rendezvous mode selected, the system design requirements were developed and considerable effort was spent working on trajectory strategy, launch strategy, and the identification of constraints. Trajectory feasibility studies, using these design requirements and agreed-upon ground rules and strategies, led to the definition by Bellcomm of an area on the front face of the Moon close to the lunar equator, later known as the Apollo zone, which was generally accessible for Apollo landing missions. The Apollo zone, so defined, was then combined with the information available from Earth-based lunar mapping, the lunar landing lighting constraints, and the launch vehicle recycling require-

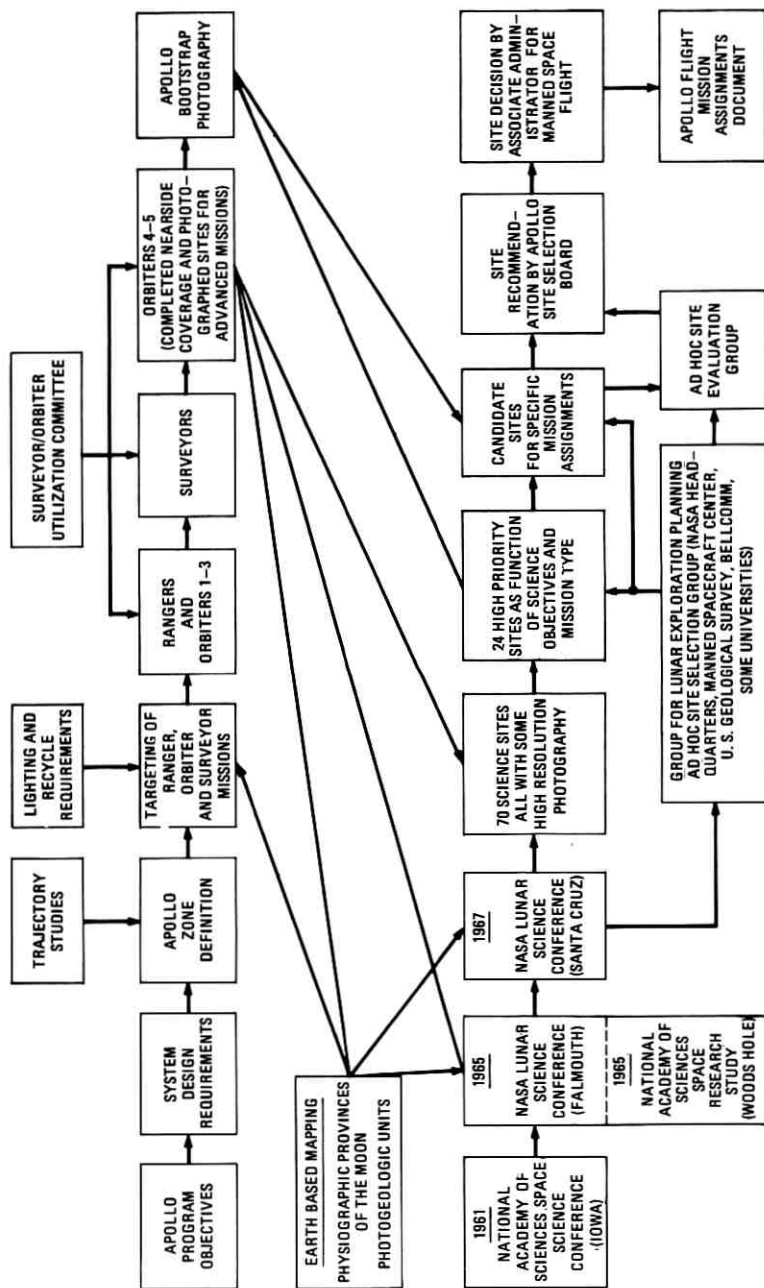


Fig. 1—Historical development of the site selection process.

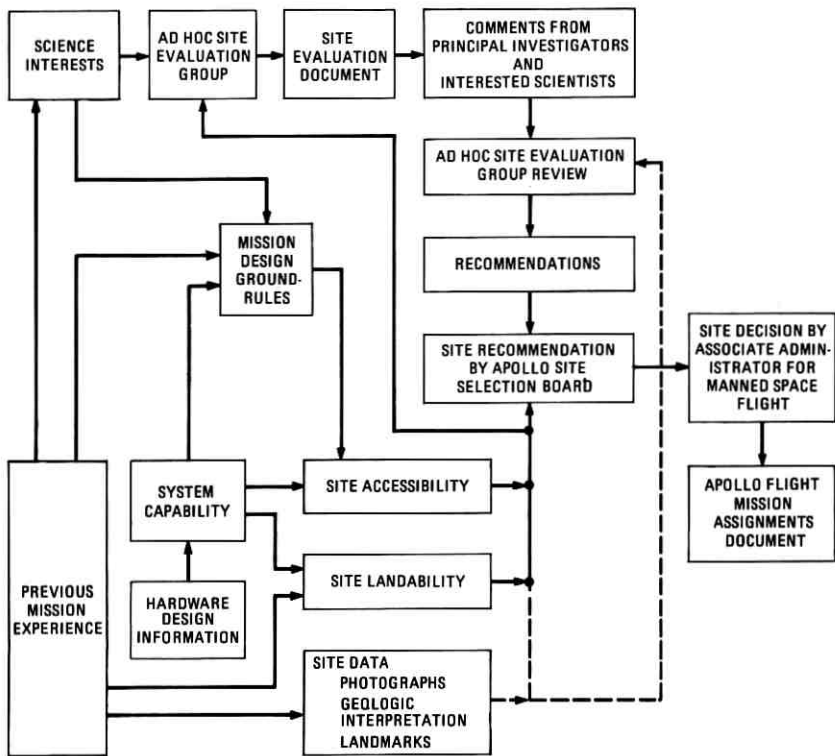


Fig. 2—Mechanics of the site selection process (Apollo missions 16 and 17).

ments to come up with recommendations for the targeting of specific Ranger, Surveyor, and Orbiter missions to gather data on lunar surface areas of interest for possible Apollo landing sites.⁵⁻⁷

These recommendations were taken into account, along with other (non-Apollo) scientific objectives, by the Surveyor/Orbiter Utilization Committee in their determination of specific targets for each mission.

The selection of the landing site for the first lunar landing mission (Apollo 11) was not directly influenced by scientific considerations, since the objective of this mission was to demonstrate a capability of landing men on the Moon and returning them safely to Earth. Following this, scientific considerations became more and more influential in site selection. The 1961 National Academy of Sciences Space Science Conference formulated a set of long-range planning goals for lunar

exploration. These were refined and updated at the 1965 National Academy of Sciences Space Research Study at Woods Hole, Massachusetts and at the 1965 NASA Lunar Science Conference at Falmouth, Massachusetts. The results of these conferences, along with the results of the photogeologic mapping program of the U. S. Geological Survey, were direct inputs to the targeting of Orbiters IV and V, which completed nearside medium-resolution photographic coverage and took high-resolution photographs of sites considered appropriate for advanced missions. The next significant conference was the 1967 NASA Lunar Science Conference at Santa Cruz, California. As a result of this conference, the Group for Lunar Exploration Planning was organized for the purpose of carrying out advanced studies related to lunar exploration and site selection. The group was made up of representatives from NASA Headquarters, the Manned Spacecraft Center, the U. S. Geological Survey, Bellcomm, and several universities. A set of 70 candidate science sites was established, which included all lunar sites for which high-resolution Orbiter photography existed. The Group for Lunar Exploration Planning was instrumental in condensing this set to 24 high-priority sites as a function of the science objectives and mission types. This smaller set was also the basis for selection of targets for Apollo bootstrap photography, which consisted of high-resolution photography during an Apollo mission of candidate sites for later missions. The final selection of a specific site for each mission was done by the Associate Administrator for Manned Space Flight, based on a recommendation from the Apollo Site Selection Board, chaired by the Apollo Program Director.

The second flow chart (Fig. 2) shows the typical functional interplay that occurred between the scientific interests and system capabilities during the site selection process. The specifics of this interplay varied somewhat from mission to mission; Fig. 2 shows the process for Apollo 16 and 17. The focal point for this interplay was the set of mission design ground rules for the mission under consideration. A major input to these ground rules was the system capability, i.e., hardware design information as modified by operational experience. Previous mission experience also influenced the mission design ground rules directly, as did the site data (photographs, landmarks, and geologic interpretation of lunar features) and the suitability of specific sites for landing missions (landability). Fundamental to all of these considerations was crew safety, which was a subjective matter, and its presence in the tradeoff provided additional complications.

The total set of mission design ground rules, together with the current

system (hardware and software) capability, were translated via trajectory analyses into accessible areas on the lunar surface. These accessible areas were then correlated with the candidate landing sites to determine which sites were available. This information was then fed back to the scientific community. Since many of the mission ground rules were matters of policy and judgment, strong scientific arguments with respect to a site could result in review and possible changes of the ground rules.

The scientific mission objectives were matched with candidate sites by the Group for Lunar Exploration Planning for Apollo 12 through 15 and by the Ad Hoc Site Evaluation Group (chaired by Bellcomm) for Apollo 16 and 17. Following this, a Site Evaluation Document was made available for comments and recommendations from principal investigators and interested scientists. This feedback from scientists was evaluated, together with available site data, to provide a set of recommendations to the Apollo Site Selection Board. The board then considered these recommendations, along with site accessibility and site landability, for the candidate sites before arriving at a recommendation for the mission under consideration. The final site selection decision, along with mission objectives and major design parameters for each mission, was then made by the NASA Associate Administrator for Manned Space Flight, and promulgated via the Apollo Flight Mission Assignments Document⁸ which was prepared for NASA by Bellcomm. The Site Selection Board recommendation was accepted for all of the Apollo missions.

The site selection process was a complex technical tradeoff conducted among representatives of a large community of diverse interests. There were concerns about the capabilities of the inanimate portions of the system (hardware and computer software), concerns about human performance of the ground and flight crews, and concerns about efficient utilization of the flights to further scientific and technical knowledge. Within each of these broad areas there were, again, diverse positions, particularly in the area of science; here the advice, frequently contradictory, of many individuals had to be brought together, since there was no single spokesman for the "scientific community." Although site selection did contain many political and "human" problems, it was not the solution of these that made it a classical example of systems engineering, but rather, the fact that so many of the purely technical considerations could be brought together for a coherent and meaningful tradeoff.

1.3 Survey of Major Constraints Affecting Site Selection

One of the first constraints that limited the area available for landing was the requirement to maintain communications with the astronauts during lunar surface operations and during the critical lunar landing and ascent (lunar launch) phases. This resulted in the early elimination of sites on the far side of the Moon.

A second major constraint was that imposed by the design and sizing of the launch vehicle and spacecraft coupled with the lunar orbit rendezvous mission mode. The first landing mission was flown with a requirement on the translunar trajectory such that, if the main spacecraft engine had become inoperative following translunar injection (the start of the coasting flight from Earth to Moon), the spacecraft would have swung around the Moon and returned to the Earth with acceptable reentry conditions, requiring only minor trajectory corrections using the Command and Service Module (CSM) attitude control system. The consequence of using this type of trajectory was that the surface area accessible for landing was confined to a region close to the lunar equator, the Apollo zone (Fig. 3). This rectangular zone was a gross average over time and certain engineering uncertainties, but was a very useful tool in this early time period. Relaxing this constraint expanded the accessible region to include the middle latitudes.

Another significant constraint was that associated with lunar lighting (Appendix A), which was complicated by the fact that the Moon exhibits very little color variation or contrast. The best lighting conditions occurred when the Sun was low enough on the horizon to reveal rough terrain by shadowing, but not so low that the landing area was within shadow; in addition, the Sun needed to be behind the astronauts in order to avoid glare. The net result was a requirement for landing in the early lunar morning such that any given landing site had the proper lighting only one day per month. In addition, the lifetime of the space vehicle propulsion subsystems after initial propellant loading was

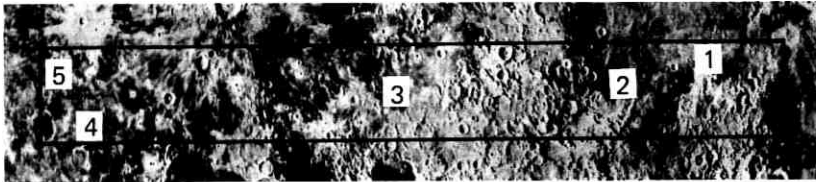


Fig. 3—Landing sites in the Apollo operational zone.

about 110 days, allowing, at best, only three monthly launch periods. Thus, it was desirable to provide as many launch opportunities as possible to insure flight of the hardware during the system's lifetime. For the first lunar landing mission, multiple launch opportunities for a given month were provided by using several sites separated in longitude. Additional launch opportunities were provided for later missions by planning to launch one day early and waiting in lunar orbit, or landing a day later than nominal (tolerating a higher Sun at landing).

Another important consideration in the selection of sites was the terrain roughness at the site and along the approach path to be followed by the Lunar Module (LM) during descent to the lunar surface. Adequate terrain clearance and the interaction between the terrain and the landing radar/descent guidance system were important for safety, as well as landing accuracy. Obviously, there had to be a sufficiently large, smooth area, adequate for landing, at any site selected.

The navigation and guidance system was the keystone which linked the trajectory mechanics and the landing site to make a landing at a desired site a physical reality. The mission consisted of several phases: translunar, lunar orbital, lunar descent, lunar ascent, and transearth. Of these, the lunar orbital and lunar descent phases presented the greatest challenge for guidance and navigation, particularly as the requirement for pinpoint landings evolved.

Up-to-date mass and performance data was important in the ongoing site selection process, since it made possible an assessment of the propulsion capability as compared with the requirements to reach given sites.

In the sections to follow, the impact of each of these facets and their interactions with site selection will be examined in detail. A survey of the Table of Contents should be useful in understanding how the material has been organized.

This article was written shortly before the Apollo 16 mission; however, because of the lead times involved, the Apollo 17 site had already been selected, completing the Apollo site selection process.

II. SATISFYING THE SCIENCE OBJECTIVES OF LUNAR EXPLORATION

2.1 *Lunar Exploration Goals*

The most significant value of the Moon as an object for exploration is that it offers an opportunity to investigate the early history of the Solar System. This epoch of history has been obliterated on the Earth due to vigorous modification from the time of its birth, mainly by

volcanism and by water erosion and its consequences. The Moon, on the other hand, provides accessibility to that record because of its physical state, and because it is not in a state of continuous internal evolution similar to that of the Earth. Therefore, exploration of the Moon could provide answers to first-order questions concerning the formation and evolution of the Earth-Moon system.

In order to understand the Moon's origin, evolution, and relationship to the Earth, it is necessary to (i) characterize the major lunar surface units, (ii) understand the processes that modify the lunar surface and interior, and (iii) decipher the physical and body properties of the Moon. Manned lunar landings are especially well suited to achieve these objectives by sampling and studying lunar surface materials, as well as by emplacing instruments and conducting geophysical experiments on the Moon.

A preliminary history of the evolution of the lunar surface was delineated by systematic mapping and classification of its materials. Efforts by the U. S. Geological Survey during the 1960's resulted in a classification of the major provinces of the near side of the Moon (Fig. 4). The units depicted constitute the major subdivisions of lunar surface materials. This classification serves as a basis for deciphering the historical record of the formation and evolution of the various types of materials.

The major lunar surface geologic units defined by the U. S. Geological Survey are characterized as mare (sea), terra (highland), and crater materials. Different units under these classes are assigned to one of four systems of a relative-age scale that were defined by the classification of the units within and around Mare Imbrium, but that have Moonwide application:

- (i) Pre-Imbrian—materials formed during a period of cratering and formation of mare basins older than Imbrium; includes oldest surface materials.
- (ii) Imbrian—materials deposited during the formation of the Imbrium basin, as well as most of the mare materials that fill Imbrium and other basins.
- (iii) Eratosthenian—materials of craters like Eratosthenes whose rays are no longer visible, and some post-Imbrian mare units.
- (iv) Copernican—materials of craters with visible ray systems; includes the youngest surface materials, which were exposed from approximately the time of formation of the crater Copernicus to the present.

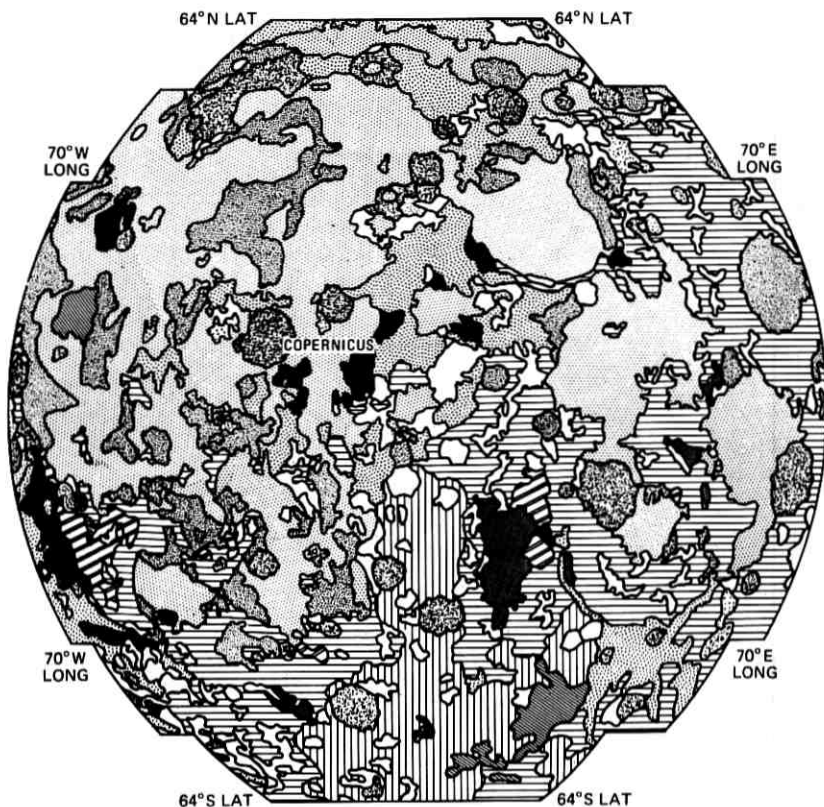


Fig. 4—Geologic provinces of the near side of the Moon (after J. F. McCauley and D. E. Wilhelms).

The relative age of a given surface unit was deduced by studying its spatial relationships to the surrounding units, supplemented by counts of crater density on their surfaces, i.e., the more craters, the older the unit. For example, the Apollo 11 and 12 sites were both in mare materials; however, the Apollo 11 site was characterized by a larger number of subdued craters in the 200-meter to 600-meter size range, and therefore its surface material was thought to be relatively older than that of the Apollo 12 site. This was confirmed by isotopic age dating techniques on the returned samples, as discussed in Section 2.4.6.3.

From the outset, it was clear that there were more interesting sites than there were Apollo missions. Sites important to deciphering the history of the Moon and unraveling its compositional variations included some in mare material and many in highland materials.

UNIT

INTERPRETATION AND HISTORY

	IMPACT CRATERS > 50 km	<p>IMPACT CRATERS LATER THAN THE IMBRIUM EVENT AND ITS ASSOCIATED BLANKET AND STRUCTURES. AGE RANGE FROM EARLIEST IMBRIAN TO COPERNICAN.</p>	
	MARE PLATEAUS		
	YOUNGER MARE		
	OLDER MARE		
	DARK MANTLES		
	LIGHT TERRA PLAINS		
	HILLY AND FURROWED TERRA		
	HILLY AND PITTED TERRA		
	BASIN DEPOSITS AND STRUCTURES		<p>MOSTLY FLOWS OF DARK TO INTERMEDIATE ALBEDO IN NEAR-SIDE MULTI-RING BASINS AND SMALLER BASIN RELATED DEPRESSIONS OR CRATER FLOORS. MARE PLATEAUS: LATER AGGREGATES OF VOLCANIC LANDFORMS, CONES AND DOMES PREDOMINATE; PYROCLASTICS AND FLOWS OF SAME OR POSSIBLY SLIGHTLY DIFFERENT COMPOSITION THAN MARIA. YOUNGER MARE: RELATIVELY THIN FLOWS, GENERALLY DARKER, LESS CRATERED, DISTRIBUTION PATCHY. DARK MANTLES: THIN VENEERS OF VERY DARK PYROCLASTICS; MOSTLY COVER LIGHTER TERRA UNITS, NEAR MARE-TERRA CONTACTS. LIGHT PLAINS: MORE CRATERED THAN MARIA, FILLS BASINS AND TERRA DEPRESSIONS; IMPACT LIGHTENED OLD MARE OR COMPOSITIONALLY DISTINCT OLDER VOLCANIC FILL UNIT. IMBRIAN TO COPERNICAN IN AGE.</p>
	CRATERED LIGHT TERRA PLAINS		<p>TERRA MODIFIERS. HILLY AND FURROWED: MOSTLY SUBDUED LINEAR STRUCTURES RESEMBLING FISSURE CONES. HILLY AND PITTED: ROLLING PLAINS AND PLATEAU UNIT, MANY CLOSELY SPACED RIMLESS PITS ON SURFACE. EMBAYS PRE-IMBRIAN CRATERS BUT CUTS IMBRIUM SCULPTURE. MOSTLY IMBRIAN IN AGE.</p>
	TERRA, UNDIVIDED	<p>RECOGNIZABLE EJECTA BLANKETS AND PARTS OF ENCOMPASSING STRUCTURAL RINGS AND RADIALLY LINEATED TERRAIN OF ORIENTALE, IMBRIUM AND NECTARIS BASINS. PRE-IMBRIAN TO MIDDLE IMBRIAN.</p>	
	TERRA, DENSELY CRATERED	<p>HEAVILY CRATERED PLAINS FILLING LOCAL DEPRESSIONS IN TERRA. MOST SUPERPOSED CRATERS LOWER IMBRIAN. PRE-IMBRIAN EQUIVALENT OF LIGHT TERRA PLAINS.</p>	

Fig. 4—(continued)

The sampling of the maria was a somewhat easier problem because only two major types of mare materials are noted on the Moon. Those labeled eastern maria (because of abundance in the eastern half of the Moon) are somewhat younger than the western maria, and both are younger than most highland materials.

The highlands, however, are composed of numerous surface units, and their study required more thought. In addition to the variations of surface materials, there was the problem of deciphering the composition of subsurface materials.

Four sources were available for sampling the lunar crustal materials:

- (i) Ejecta from impact craters—the larger the crater, the greater the depth to which material will be excavated. The deepest

samples occur around the margins of the circular mare basins of impact origin. The Fra Mauro (Apollo 14) site, which is composed of ejecta from the Imbrium basin, and the ejecta blanket of the crater Tycho in the southern lunar highlands are good examples of this type of material.

- (ii) Central peaks of large impact craters—terrestrial studies indicated that the central peaks are composed of material that was lifted above its original stratigraphic position by a vertical distance of approximately 10 percent of the crater's diameter. The central peak of Copernicus is an example.
- (iii) Large scarps which were originated by displacement along faults—samples from the lower part of fault scarps may be composed of material that solidified many kilometers below the surface. The Apennine mountain front is an example.
- (iv) Volcanic ejecta blankets around explosive or maar-type craters—terrestrial experience indicated that the most varied and deepest samples of Earth materials are brought to the surface as xenoliths or deep-seated fragments, around volcanic craters. The Davy Rille (crater chain) is a good example, since it may contain such deep-seated inclusions in the ejecta blankets of its chain of craters.

Site selection for the Apollo landings progressed through its various stages with all the above considerations in mind. The knowledge gained from each successive mission affected considerations for candidate sites for following missions, as will be discussed in Section 2.2.

2.2 *Preparing for the Selection of Apollo Landing Sites*

One could say that the foundations of site selection for a manned lunar landing were initiated three hundred years ago, when Galileo Galilei inaugurated observations of the Moon's surface through his crude telescope. Selenography, or the study of lunar surface features, progressed through the building of larger and better telescopes, the development of modern remote sensing techniques, and, more recently, the launching of automated spacecraft.

The developments most pertinent to Apollo landing site selection took place during the ten years preceding man's first steps on the Moon. The intent, in this section, is to retrace the stages of this effort, to develop site selection history, and to describe briefly the candidate landing sites for Apollo missions.

2.2.1 Acquisition of Required Data

Detailed mapping of the near side of the Moon began in 1961 under the sponsorship of NASA. This work was conducted by the U. S. Geological Survey, Branch of Astrogeology. It involved systematic geologic mapping, based on telescopic observations and study of photographs by specially trained geologists, on topographic base maps prepared by the Aeronautical Chart and Information Center at a scale of 1:1,000,000. These photogeologic maps depicted the sequence of formation of observable features of the lunar surface and provided for a geological interpretation of the Moon's history as initially proposed by Shoemaker and Hackman⁹ and later modified by other investigators. These maps formed the basis for continuing study.

In 1964 and 1965, television pictures sent back in real time by Rangers VII, VIII, and IX provided the first closeup views of the lunar surface. The final frame of each mission, taken immediately before impact, had a resolution of 1 to 3 meters (compared with the 300 to 500 meters resolution claimed for the largest telescopes under the best seeing conditions). The Ranger pictures served to confirm that the lunar maria were reasonably smooth and topographically simple lunar surface areas.

A tentative Apollo operational zone was defined in 1965 at the instigation of Bellcomm, which proposed limits extending from 45° East to 45° West longitude and 5° North to 5° South latitude (Fig. 3). These limits were determined by such factors as Earth-Moon communications, propulsion systems performance, tracking, and launch date uncertainty. Although the defined zone was too simple to reflect accurately the bounding constraints, it was adequate for establishing Apollo's needs for communication to the Orbiter and Surveyor programs, which were potential sources of useful data. In August of 1965, a Surveyor/Orbiter Utilization Committee, chaired by Edgar Cortright, was formed to establish mission objectives and to select targets for the Surveyor and the Orbiter spacecraft that were scheduled to be launched. These missions also provided maximum support to the manned Apollo missions to the Moon. Simultaneously, in response to a Bellcomm recommendation, the Apollo Site Selection Board (chaired by then Major General Samuel C. Phillips, the Apollo Program Director) was formed to evaluate all factors that would influence the final selection of a landing site for man's first visit to another body in our Solar System, and to recommend specific sites to NASA's Associate Administrator for Manned Space Flight, Dr. George E. Mueller.

The successful Surveyors I, III, V, and VI were targeted to points lying within the Apollo zone; they landed within, or very near, what were later selected as potential Apollo landing sites. These flights demonstrated beyond reasonable doubt that the lunar surface would permit a successful LM touchdown, and that the lunar maria would not present landing hazards that a piloted spacecraft could not avoid. Because of the success of these missions, the last flight in the series, Surveyor VII, was targeted to a point outside the Apollo zone (the northern rim of the crater Tycho) in order to study a highland region. It showed that at least a part of the highlands would be hospitable for landing from the standpoint of surface roughness and bearing strength.

Lunar Orbiters I through V, which flew during the period of the later Surveyor missions (1966 to 1967), provided the photographs needed for all the initially selected candidate Apollo landing sites and for many of the sites under consideration for the remaining Apollo missions. The first three Orbiters concentrated on high-resolution (1 to 3 meters), photographic coverage in the Apollo zone. Because of their success, Orbiter IV was programmed to take moderate-resolution photographs of the Moon's entire near side and some of its far side. Orbiter V photographed additional Apollo sites, a number of candidate science sites, and significant features outside the Apollo zone on the Moon's near side; it also completed moderate resolution coverage of the Moon's far side.

In order to support Apollo site selection, the Orbiter photographic systems and the orbital parameters of the missions were designed to produce the following:

- (i) Photographs with 1-meter ground resolution, capable of enabling one to detect a cone 0.5 meter high with a base diameter of 2 meters
- (ii) Stereo coverage for detection of 6-meter-by-6-meter areas with slopes of 7 degrees or greater
- (iii) Approach path photographs covering the last 40 kilometers of the LM approach
- (iv) Oblique views, where possible, to approximate the pilot's view of the landing sites.

Photographs with the above specifications were obtained for 32 sites in the Apollo landing zone. The Mapping Sciences Laboratory of the Manned Spacecraft Center, Houston, was responsible for analysis of these photographs to determine the "landability" of each site. Analysis

included measuring the areas within each site covered by craters, positive obstructions, and excessively steep slopes (Fig. 5). A numerical factor was then assigned to each site, expressing its "landability."

From the original 32 sites, eight sites that best met the above constraints were selected. In January of 1968 these were further reduced to five sites (Fig. 3). Within these five sites, target landing areas (ellipses of various sizes representing landing error probabilities) were carefully chosen to minimize the landing hazards for the LM. Approach path landmarks and terrain features within the ellipses were identified for pilot recognition. A relief model of Apollo Site 3 (in Sinus Medii, near the center of the lunar disc) was constructed at a scale of 1:2000 for use with the LM simulators to practice final approach procedures. Map packages at a scale of 1:5000 were prepared for all the sites and included photographs and geological maps of the entire ellipse.

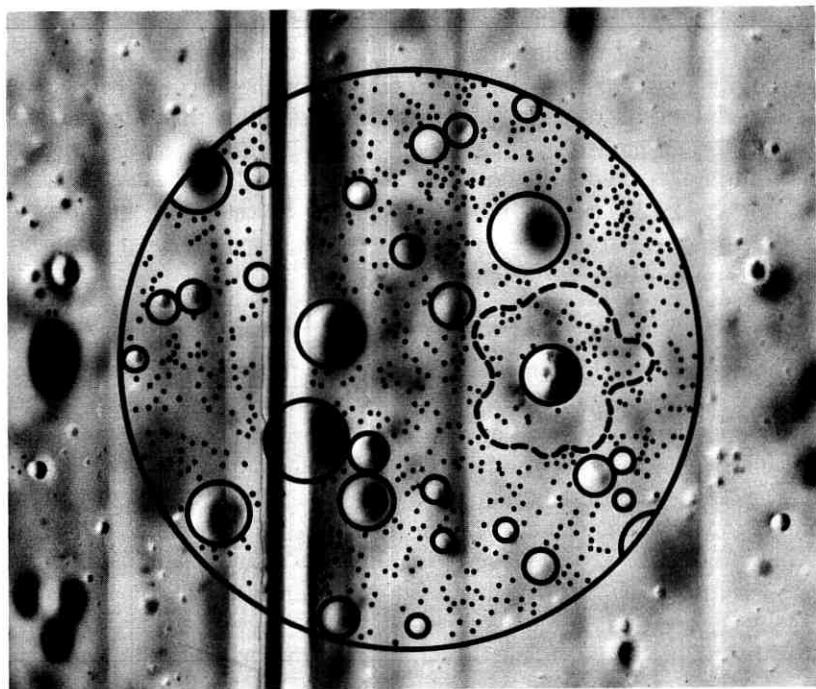


Fig. 5—Site landability. The landable surfaces within a 1-kilometer radius circle at the Apollo 11 site lie outside the circles and dots. (The prominent vertical fold-mark slightly left of center is a result of an imperfection in the original Orbiter photograph.)

2.2.2 Site Selection for Apollo Missions 11 and 12

The Apollo Site Selection Board recommended Apollo Site 2* in Mare Tranquillitatis (Sea of Tranquillity) as the prime site for Apollo 11 (Fig. 3). Apollo Site 3 in Sinus Medii (Central Bay) and Site 5 in Oceanus Procellarum (Ocean of Storms) were selected as backups in case a launch hold and recycle occurred (Fig. 3). These recommendations were approved by the Associate Administrator for Manned Space Flight. In May of 1969, Apollo 10 flew a preview mission of the Apollo 11 flight, descending to within 15 kilometers of Apollo Site 2. The astronauts reported that it appeared acceptable for landing.

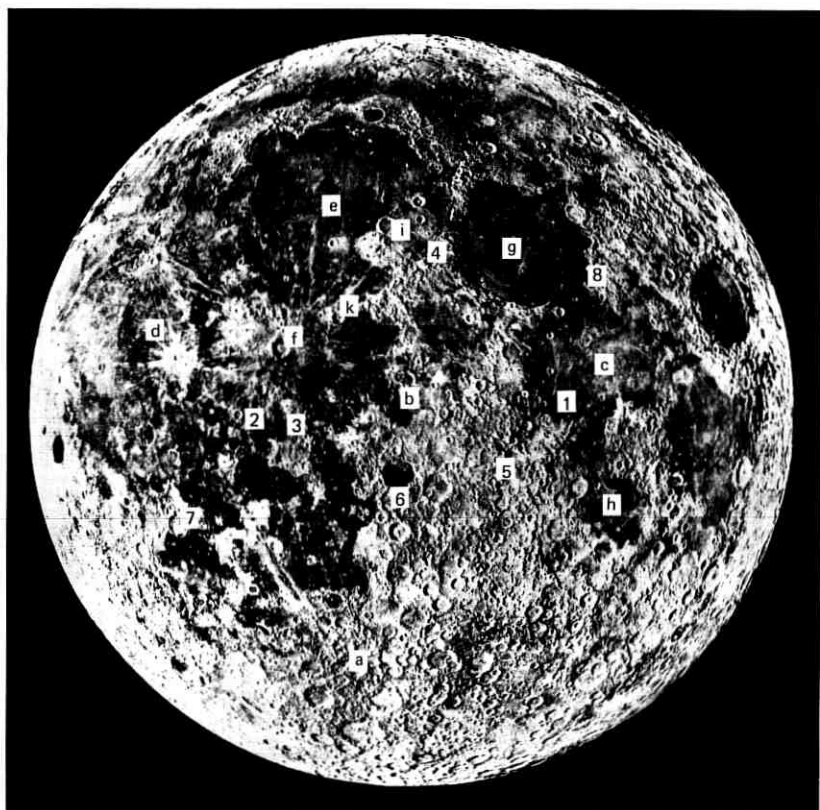
On July 20, 1969, the Apollo site selection process passed its final test. Neil Armstrong and Edwin Aldrin landed the spacecraft *Eagle* at the southern edge of Apollo Site 2, in the Moon's Sea of Tranquillity.

The landing site selected for Apollo 12 (Figs. 6, 7, and 8) was chosen with the objective of perfecting pinpoint landing techniques by targeting for a site near Surveyor III. The landing ellipse was selected with Surveyor III at its center. The landing constraints for this site were similar to those of Apollo 11. However, since the Apollo 12 landing site was at 23° West (Fig. 6), only one site farther west could be selected as a backup (Site 5, Fig. 3), providing launch opportunities on only two days each month. A relief model of the landing site was prepared for training astronauts Conrad and Bean. Apollo 12's eventual touchdown less than 200 meters from Surveyor III demonstrated conclusively the accuracy capability of the Apollo system and justified plans for more ambitious future missions.

2.2.3 Site Selection for Apollo Missions 14 through 17

Following the achievements of Apollo 11 and the pinpoint landing demonstration of Apollo 12, a lunar exploration program was planned based on scientific rationale. Representatives from all relevant fields of science assisted in the selection of landing sites for this phase. Following the NASA-sponsored "Summer Study of Lunar Science and Exploration," which was held at Santa Cruz, California in August, 1967, the Group for Lunar Exploration Planning was established, and was a major contributor to these efforts. Sites recommended by the Group for Lunar Exploration, subject to operational constraints, were reviewed by the Apollo Site Selection Board, chaired by Dr. Rocco Petrone, the Apollo Program Director succeeding General Phillips. Final approval

* Site numbering was not unique; therefore, Site 2 relative to the five candidate sites for Apollo 11 does not necessarily correspond to sites labeled "2" on other figures.



APOLLO SITES

- | | |
|-------------------------------------|------------------------------------|
| 1— APOLLO 11 SITE | 5— DESCARTES (APOLLO 16 SITE) |
| 2— APOLLO 12 SITE | 6— ALPHONSUS |
| 3— FRA MAURO (APOLLO 14 SITE) | 7— GASSENDI |
| 4— HADLEY—APENNINE (APOLLO 15 SITE) | 8— TAURUS—LITTROW (APOLLO 17 SITE) |

REFERENCE POINTS

- | | |
|-------------------------|------------------------|
| a— CRATER TYCHO | f— CRATER COPERNICUS |
| b— SINUS MEDII | g— MARE SERENITATIS |
| c— MARE TRANQUILLITATIS | h— MARE NECTARIS |
| d— OCEANUS PROCELLARUM | i— PALUS PUTREDINIS |
| e— MARE IMBRIUM | k— CRATER ERATOSTHENES |

Fig. 6—Apollo landing site locations.

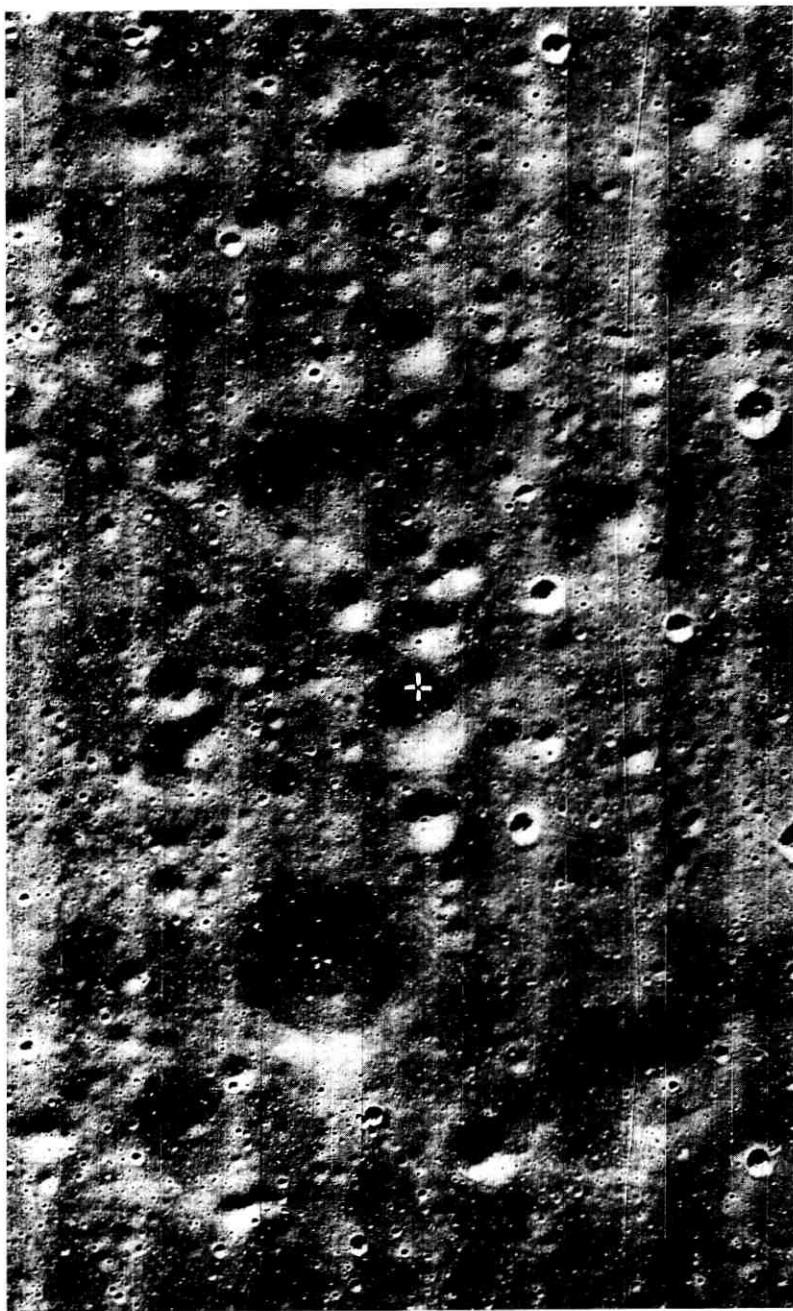


Fig. 7—The Apollo 12 landing site. The cross marks the location of the Surveyor III spacecraft.

was given by Dale D. Myers who succeeded Dr. Mueller as Associate Administrator for Manned Space Flight.

The philosophy of site selection for Apollo missions 14 through 17 was based largely on photogeological interpretations of the lunar surface units, relative values of achievable scientific objectives at each of the candidate landing sites, and results of previous missions. Therefore, site selection for these missions was a continuous process, with flexibility to allow for changes based on data returned by previous missions. Sites that were considered for missions 14 through 17 went through a screening process similar to that for the sites for the first and second lunar landings. Initially, a set of 21 sites (later expanded to 24) was selected from the original list of 72 sites. Further selection was delayed because of the continuing need for flexibility, with about 12 sites being considered as candidates.

The Apollo 14 (Fra Mauro Formation)* and Apollo 15 (Hadley-Apennine) sites (Fig. 8) were complimentary. They were selected to study materials related to the Imbrium Basin. The Apollo 14 site was on the ejecta blanket, while the Apollo 15 site was on the rim of the basin. The site chosen for the Apollo 16 mission was in the Descartes region, located on a rise forming a ridge with respect to the surrounding highlands, while the site finally chosen for Apollo 17, Taurus-Littrow, was on a young volcanic valley floor surrounded by old highlands. Detailed characteristics of the landing sites for Apollo missions 14 through 17 are summarized in Appendix F.

2.3 *Mission Science Planning and Its Impact on Site Selection*

The prime science objective of all the Apollo lunar landing missions was the acquisition of lunar samples; consequently, in the site selection process, this was always the dominant factor in arriving at the relative scientific merit of the sites considered. However, on occasion, two or more candidates for a specific mission had roughly equal sample priority; or it was evident that the same sites would be candidates for a subsequent mission. It was under these circumstances that secondary factors entered the site selection considerations and affected both the site for a specific mission and the sequencing of sites in the overall program.

2.3.1 *Apollo Lunar Surface Experiment Packages*

The Apollo Lunar Surface Experiment Packages (ALSEP) were self-contained instrument packages which included passive seismometers,

* The Fra Mauro site was originally selected for the Apollo 13 mission. Because of the high scientific interest in this site, it was reselected as the site for Apollo 14 when Apollo 13 was unsuccessful.

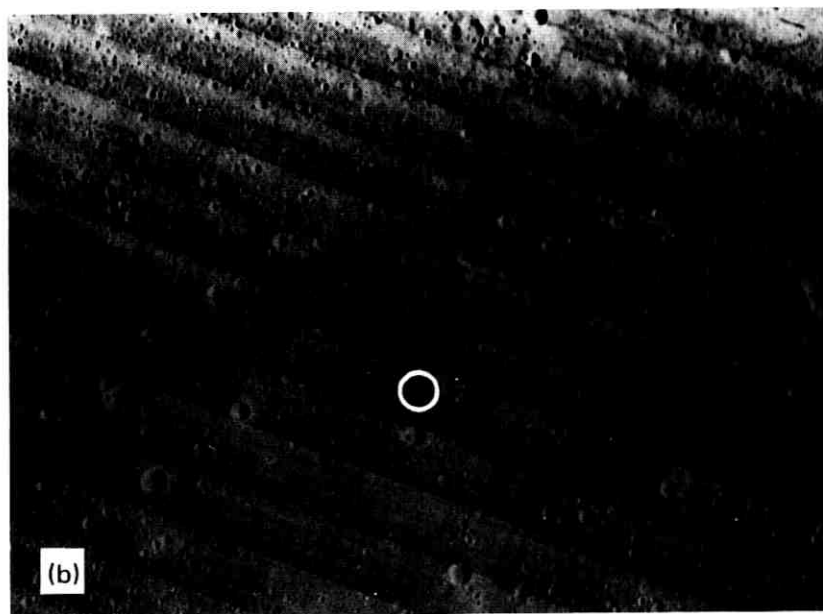
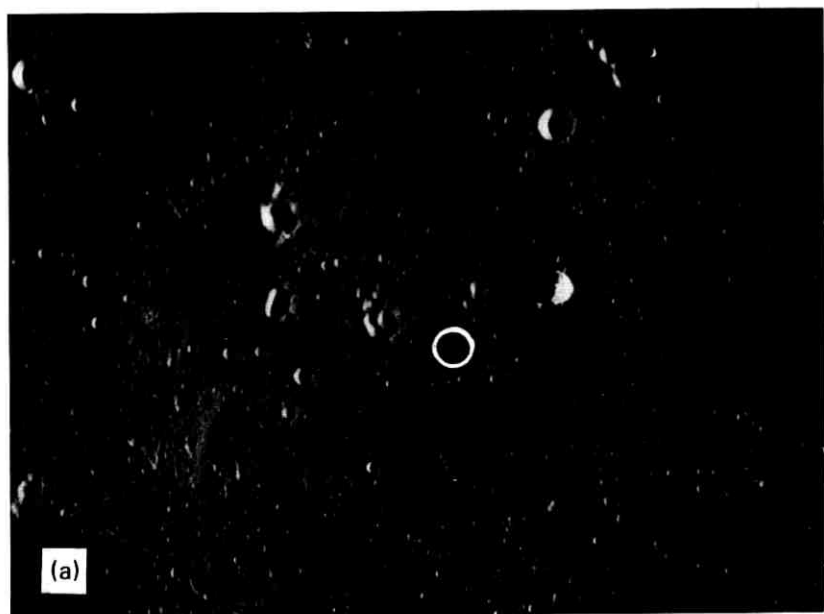


Fig. 8—Apollo landing site photography. (a) Apollo 11: Mare Tranquillitatis. (b) Apollo 12: Oceanus Procellarum.

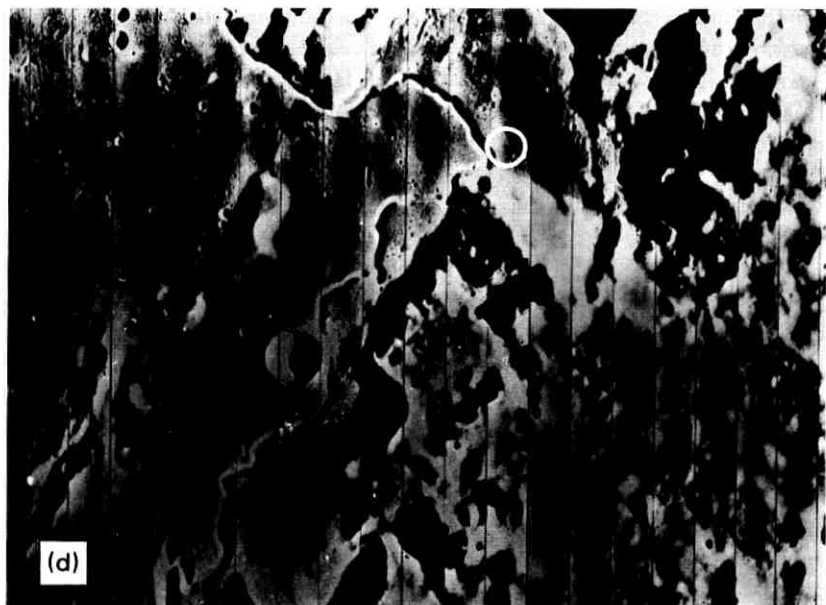
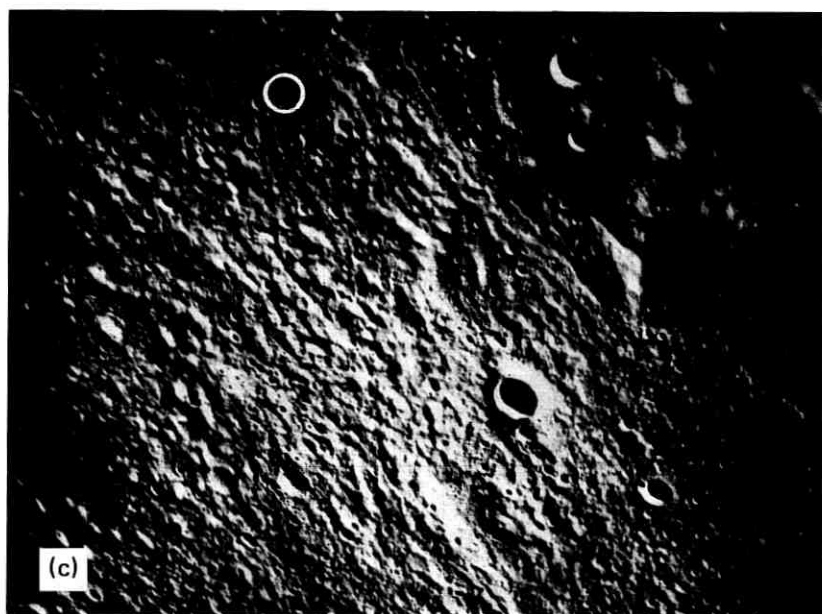


Fig. 8 (continued)—Apollo landing site photography. (c) Apollo 14: Fra Mauro. (d) Apollo 15: Hadley-Apennine.

active seismic experiments, magnetometers, heat flow probes, and various solar wind, ionospheric, and atmospheric experiments. Although not originally part of the ALSEP proper, the Laser Retroreflector is also considered here. An ALSEP for a specific flight usually carried only four to five of the above experiments, but the particular instrument complement was determined long before selection of the site. Certain of the experiments, for example the solar wind spectrometer, were site independent and had little effect on the site selection deliberations. Others, however, depended on the site characteristics. Two of the site-dependent experiments which had a significant influence on site selection were the Passive Seismometer and the Laser Retroreflector.

The Passive Seismometer was designed to detect Moon-quakes, both of internal origin and those caused by meteoroid and spacecraft impacts. Detection meant pinpointing the location of seismic events in position (X, Y, Z) and time. In order to resolve ambiguities in space and time, it was obviously necessary to have a network of stations which allowed triangulation on the events. The sensitivity and timing resolution of the seismometer determined a minimum spatial separation, while the Apollo mission interval and limited ALSEP lifetime demanded that successive missions establish an operational network. Thus, when Apollo 12 and 14 established one leg of a network, the Apollo 15 site location became critical. The two final contenders for the Apollo 15 site assignment were Marius Hills and Hadley-Apennine. They were grossly different geologically, but had roughly equal weight for their sampling objectives. However, a glance at Fig. 6 shows that the Hadley-Apennine site yielded both a better triangulation network and an opportunity to receive seismic signals which had traveled through the highlands.

The Laser Retroreflectors were arrays of glass corner cubes designed to reflect Earth-originated laser pulses back to the transmitting telescope. Extremely accurate timing of the round-trip travel time made it possible to accurately measure the instantaneous telescope-retroreflector distance (to a fraction of a meter, assuming no uncertainty in the speed of light), and eventually to determine the Moon's motion which, in turn, is a function of its internal physical properties. Like the seismic experiments, the success of Laser Retroreflector experiments depended on establishment of a triangulation network. After the Apollo 11 and 14 deployments, resulting in reflectors separated in longitude but both roughly equatorial, it was obvious that a high-latitude site was desirable in order to better resolve lunar libration components. In that regard,

Hadley-Apennine was clearly preferable to Marius Hills, another strong contender.

2.3.2 *Orbital Science*

Orbital science affected site selection in two grossly different ways; one concerned future site photography, and the other, the degree of coverage of the lunar surface available with the orbital paths leading to the site. Prior to Apollo 15, photography alone was accomplished from lunar orbit; and that was from the Command Module (CM). The scientific value of CM orbital photography was recognized, but it was obvious that almost any orbit would overfly interesting lunar features, and thus site selection was not affected strongly. However, among leading site candidates for subsequent missions were several for which adequate operational photography did not exist. Of particular interest was the candidate highland site, Descartes, which was on the orbital ground track of Apollo 13, which was targeted to Fra Mauro. At the time of the Apollo 13 flight, the Apollo 14 mission was tentatively set for Littrow. After the accident aboard Apollo 13 prevented a lunar landing mission, the decision had to be made whether to attempt again to go to Fra Mauro or to proceed to Littrow. The fact that a Littrow flight would not allow photography of the high-priority highland site, Descartes, was instrumental in retaining Fra Mauro for Apollo 14. An additional factor was that a judgment was reached that existing photography of Hadley-Apennine was adequate. Hadley-Apennine was a site which was scheduled to be photographed on the Littrow mission.

The orbital science capability was greatly expanded on Apollo 15, which carried a large photography complement; a Laser Altimeter; Gamma-Ray, X-Ray, α -Particle, and Mass Spectrometers; and a subsatellite which was ejected into a separate lunar orbit. In the choice between Marius Hills and Hadley-Apennine for the Apollo 15 site, it was clear that because of the higher latitude (about 26 degrees), the orbital inclination of a Hadley-Apennine mission would result in much greater ground coverage for the Command and Service Module instruments than would the Marius Hills site (about 15 degrees latitude). This, combined with the benefits to the Passive Seismic and Laser Retroreflector experiments, was the determining scientific factor in making the decision to go to Hadley-Apennine on Apollo 15.

2.3.3 *Lunar Surface Traverse Capability*

The science planning for each Apollo site selection involved detailed analysis of the objectives at the site and evaluation of the potential

for accomplishing those objectives. Basically, this meant analyzing the capability (time and distance) to traverse from the Lunar Module touchdown point as constrained by the considerations discussed in Section 3.3 to points on the lunar surface selected to meet the scientific objectives of the mission. Early missions (Apollo 11 and 12) were area targets in the sense that the science return would be about the same no matter where in the mare terrain landing took place. Many sites, however, had objectives which would require traverses to specific points, and most of the sites had several points of interest separated by several kilometers. These considerations led to a desire to have an extensive traverse capability (about 10 kilometers per extravehicular activity) in order both to reach objectives and to find the best sampling locations.

The influence of traverse planning can better be appreciated by considering the arguments and the relative sequence of the candidate sites Fra Mauro, Copernicus, and Hadley-Apennine in the Apollo flight mission assignments after the Apollo Site Selection Board meeting of March, 1970. At that time, these sites were associated with Apollo 13, 16, and 19, respectively (the actual flight assignments were influenced by accessibility also, but only the relative sequences are considered here).

Apollo 12 had successfully demonstrated the pinpoint landing capability. Fra Mauro was essentially a single-objective site with the desired sampling point, Cone Crater, a little over 1 kilometer from the landing point, which was clearly within walking distance of the LM. Consideration of Copernicus, however, showed that the prime objective, the central peaks, was beyond walking capability of an Apollo 14-type mission but was within walking distance on the proposed Apollo 16 mission, which was to have more extravehicular activities and an improved life support system. At that time, the Lunar Roving Vehicle was scheduled for Apollo 16 and would have been very useful at Copernicus. The possibility existed, however, that the Lunar Roving Vehicle would not meet the schedule, thus making it mandatory that one be able to get to the central peaks on foot.

The proposed mission to Hadley-Apennine had two major sampling objectives—the mountain front and the rille. Both of these were line targets, as contrasted with point targets at Fra Mauro and Copernicus, in the sense that one could not predict with confidence where the best sampling location would be found. Additionally, at the particular landing point under consideration at that time, the rille and mountain front were many kilometers apart. The net conclusion was that the Hadley-Apennine site should be assigned to a flight where one was reasonably confident a Lunar Roving Vehicle would be carried.

2.4 *Lunar Science Results and Site Selection Implications*

Analysis of lunar samples from Mare Tranquillitatis (Apollo 11), Oceanus Procellarum (Apollo 12), Fra Mauro (Apollo 14), Hadley-Apennine (Apollo 15), and Mare Fecunditatis (Luna 16) resulted in an outpouring of data and interpretations at a rate unparalleled in the Earth and planetary sciences. Part of the site selection procedure was to continually synthesize models and processes from those lunar science results in order to re-evaluate science objectives and to attempt to match candidate sites with corresponding gaps in our developing knowledge. In this section, a brief resume of the important scientific results from these missions and examples of how these results influenced site selection are presented. Much of the material which follows is condensed from a review¹⁰ which contains greater detail and a comprehensive bibliography. The Apollo 15 data are based upon very preliminary analyses and were not available until after the Apollo 16 site was selected.

2.4.1 *The Mare Basalts and Lunar Interior Composition*

The full-Moon photomosaic (Fig. 6) and landing site pictures (Fig. 8) show that the Tranquillitatis, Procellarum, Hadley-Apennine, and Fecunditatis sites are all, at least in part, in typical mare terrain, which is characterized by large expanses of low-albedo (7 to 10 percent) material of low relief. Pre-space-age photogeologic studies indicated that the mare material must have been relatively fluid in order to have smoothly filled so much of the pre-existing topographically low areas. Such a characteristic of mare fill admitted to many diverse hypotheses regarding the composition and origin of the fill, including that it is water-lain sediment, "dust" electrostatically transported from surrounding highlands, or igneous rock derived from lava and/or ash flows.

Analysis of the returned lunar samples leaves no doubt that the major surface rock-forming units of the maria are basalts or minor variants thereof, basalt being grossly defined as a fine-grained (0.1 to 0.5 millimeter average diameter) crystalline igneous rock, whose essential mineral phases are pyroxenes (silicate solid-solutions characterized by end-members CaSiO_3 , MgSiO_3 , and FeSiO_3) and calcic plagioclase (a silicate solid-solution of $\text{CaAl}_2\text{Si}_2\text{O}_8$ and $\text{NaAlSi}_3\text{O}_8$ with the calcium end-member dominating). Other minerals conspicuous in many of the basalts are ilmenite (FeTiO_3), olivine (a silicate solid-solution with end-members Mg_2SiO_4 and Fe_2SiO_4), and cristobalite and tridymite (polymorphs of SiO_2). Minor amounts of elemental iron, troilite (FeS), and numerous "accessory" minerals occur.

Typical terrestrial basalts are extruded and crystallize at temperatures in the 1000 to 1100 °C range. Heating experiments on the lunar basalts and on simulated lunar rocks indicate a similar temperature of extrusion. Certain characteristics of the basalts, namely the small crystal size, presence of glass, relatively large number of vesicles (spherical voids once filled with gas), compositionally zoned crystals, and minor amounts of metastable minerals, point to rapid, near-surface crystallization. Thus, it is hypothesized that the basalts were extruded upon the lunar surface as thin (several meters) lava flows. It is not surprising then, that at Procellarum as many as four to six distinct basalt lava flow units were penetrated by the craters at the Apollo 12 landing site, such craters ranging up to 30 to 40 meters in depth. Since the maria are estimated to be as much as 10 kilometers thick, it was speculated that they must consist of anywhere from hundreds to thousands of individual thin lava flows. One of the objectives at the Hadley-Apennine site was to photograph the 350-meter-deep rille in order to obtain direct evidence of such layering. As shown in Fig. 9, that evidence was obtained.

Comparing the chemistry of lunar basalts with terrestrial continental basalts, one first notes that the lunar basalts are high in iron and low



Fig. 9—Layering in the west wall of Hadley Rille. This 500-mm photograph shows the multiple layers representing a sequence of lava flows (arrow). The individual layers seen here generally range from about 1 to 10 meters in thickness.

in silicon relative to the terrestrial basalts. The net result is to lower the viscosity of the silicate melt. Experimental work showed that the lunar lavas were about an order of magnitude less viscous than a typical terrestrial flow. All else being equal (cooling rates, supply rates), and allowing for the reduced lunar gravity, a lunar lava should spread over a greater distance than a terrestrial flow; this possibly explains the large expanses (hundreds of square kilometers) of lunar terrain occasionally covered by individual flow units.

Relative to both "cosmic" and terrestrial abundances, lunar basalts are depleted in water and in the elements in Periodic Table Groups 1A and 1B through 7A which are considered to be relatively volatile. This apparent depletion of volatiles is accompanied by a corresponding anomalously high content of certain refractory elements, including titanium and the rare-earth elements. The problem is: just when and where did the lunar material undergo this relative loss and gain of elements? The evidence indicates that the lunar interior source material was depleted in volatiles before the lavas formed:

- (i) There is a complete lack of water-containing fluid inclusions in the basalts and an almost total lack of hydrated minerals.
- (ii) Lunar rocks are characterized by a low potassium-to-uranium ratio (K/U) (1000 to 3000) compared with Earth ($\sim 10^4$) and chondritic meteorites (~ 5 to 10×10^4) (Fig. 10), and by a high U^{238}/Pb^{204} (~ 500 to 2500) compared with Earth (~ 10) and chondritic meteorites (~ 0.1). The potassium and lead are relatively volatile under usual igneous conditions, while the uranium is relatively refractory. However, since the uranium abundances in the mare basalts are not abnormal, it was concluded that potassium and lead were preferentially lost.

When combined with age data (Section 2.4.6), the preceding information leads to a more general conclusion that there is and, since lunar origin, always has been a depletion of volatiles and enrichment of refractories in the outer region of much of the Moon.

Since only a very small part of the Moon has been sampled, however, one could argue that somewhere volatile-rich material will be found. Geologic reasoning leads to a prediction that the best place to look for volatiles is in areas of explosive volcanism. Several potential areas of explosive lunar volcanism have been identified, one being the dark-halo craters within the larger crater Alphonsus (Fig. 57).

Data bearing on the mineralogic composition of the lunar interior, the presumed source region of the basalts, are equivocal. The basalts

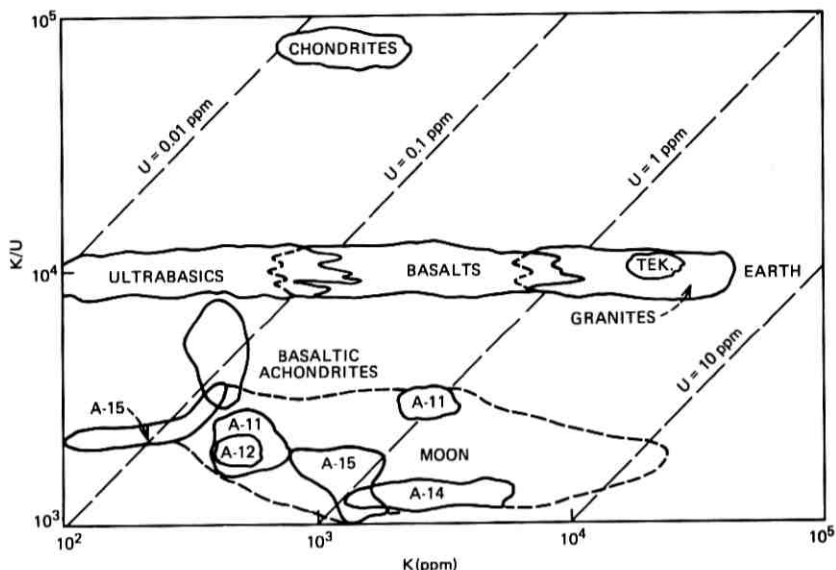


Fig. 10—Potassium versus potassium/uranium values for meteorites, tektites, the Earth, and the Moon. The potassium variation spans most rock types. The coherence of the K/U ratio for a given source indicates that rock-forming processes do not significantly change the K/U ratio initially present in planetary bodies. The consistent differences support the view that neither tektites nor meteorites are derived from the Moon, and that the Moon did not fission directly from the Earth.

(density ~ 3.4 g/cc) transform to a high-density mineral assemblage (density ~ 3.7 g/cc) at pressures equivalent to a ~ 300 -kilometer depth (Fig. 11). Such a transformation was predicted after the Surveyor analyses indicated the basaltic nature of mare fill. This phase change is incompatible with the lunar bulk density (density = 3.34 g/cc) and moments of inertia and thus it was concluded that the interior is not basaltic. Consistent with this, the basalts appear to be a partial melting product of interior material and, as deduced from chemical studies, a nonrepresentative sample at that.

Gaining a knowledge of the interior composition was obviously critical to the development of valid models of lunar chemical evolution. Three types of lunar features offered the potential for obtaining interior samples directly. First, one could go to a mountain front, such as was done on Apollo 15 at Hadley-Apennine, bordering a large mare basin; such fronts are thought to be fault blocks exposing material from several kilometers depth. Indeed, it appears that Apollo 15 returned samples not seen before and which came from regions now covered by the basalts.

Second, one could go to the central peaks of large impact craters such as Copernicus or Gassendi (Fig. 5S). It is thought that the central peaks represent "rebound" material from ~ 5 to 10 kilometers initial depth below the pre-impact surface. The third possibility for obtaining deep samples consisted of the explosive volcanic features already mentioned above in connection with volatiles. On Earth, analogous features frequently contain subsurface rocks brought explosively to the surface from depths up to 100 kilometers.

2.4.2 Regolith (Soil)

Prior to unmanned lunar exploration, consideration of the fact that the lunar surface must be continually pelted by meteoroids and of the peculiar ability of the lunar surface to scatter incident light preferentially in the return (180 degrees) direction led to commonly accepted predictions that much of the surface is covered by a fragmental debris layer or regolith (a term commonly used interchangeably with soil).

Indeed, analyses of the returned regolith samples gave conclusive evidence that it is produced primarily by the meteoroid impact-induced fracturing or comminution of previously coherent basaltic rocks. The evidence consisted of: a small median particle size (on a weight basis)

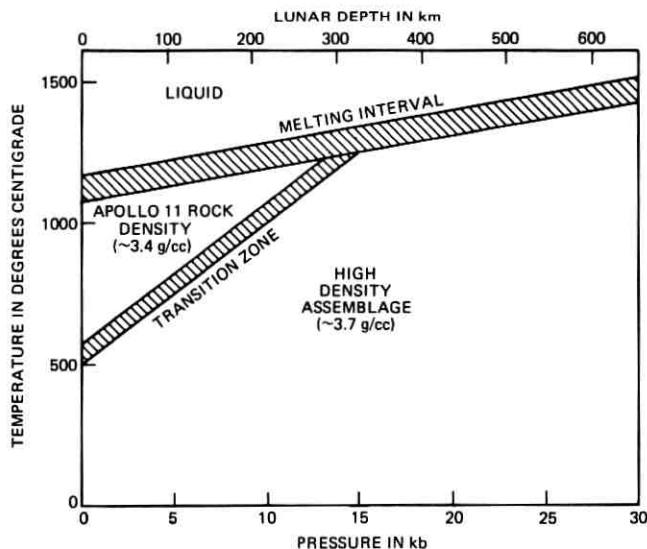


Fig. 11—Simplified phase diagram for the Apollo 11 basalts. The observation that the basalts cannot exist as the low-density phase below ~ 300 kilometers is evidence that the entire Moon (bulk density = 3.34 g/cc) cannot be basaltic.

of ~ 60 microns; the presence of angular fragments of basaltic rocks and glass or glass-covered rock; the occurrence of shock features, impact pits, or craters, and a minute number ($\ll 1$ percent) of small particles of meteoroid debris; the re-aggregation of particles into coherent rocks called breccias; and the observation of surface soil and rocks coated with meteorite-produced glass-spatters.

Pre-Apollo observations indicated that apparent regolith thickness increases with increasing surface crater density, but at a decreasing rate because of the "buffering" action of the debris layer which prevents generation of totally new debris by any impact not penetrating the regolith. This consideration led to predictions that, on the average, the mean grain size should increase with depth and that the uppermost layers should be well mixed or gardened. Indeed, such was seen in many of the regolith core samples. Efficient mixing of the regolith is attested to by the observation that there is no general decrease in solar wind gas content as a function of depth. Solar wind gas is initially acquired, of course, only at the very surface of the Moon.

The observation that there was indisputable multiple layering in several core samples caused some confusion. It was pointed out that these layers were not well-mixed and that small meteoroid impacts could not have homogenized or gardened the layers, i.e., the deposition rate exceeded the gardening rate. Clearly, this is a statistical sampling problem. The regolith was formed by a large number of cratering events and, in fact, the one core showing the best layering was taken on a crater rim where the effect of the cratering event is still preserved.

2.4.3 *Breccias*

Many of the rocks and abundant fragments in regolith fines from all sites are weakly to strongly indurated agglomerates of rock fragments and regolith fines called breccias. Aside from the induration, one finds that the gross mineralogy, texture, particle-size distribution, and noble gas content of many of the mare breccias is similar to that of the unconsolidated regolith, leading to an interpretation that many breccias are local regolith material indurated to varying degrees during meteoroid impact events.

2.4.4 *Mare Soil "Foreign Components": Anorthosites and KREEP*

When the mare soil major element chemistry was compared with rock chemistry, it was found that at all mare sites the regolith was consistently deficient, relative to the rocks, in iron and titanium and contained

an excess of aluminum (Fig. 12). In addition, the Procellarum soils contained a large excess of rare-earth elements.

This suggested that mare regolith contains one or more foreign components, one of which was indeed found "in the flesh." First, there were varieties of basaltic fragments in the regolith which did not have large rock equivalents. These, however, appeared minor in amount. More obvious were truly exotic fragments (constituting 5 percent of the coarse fragments) which contained large amounts of plagioclase, moderate amounts of pyroxene, but very little olivine and ilmenite. These particles are commonly referred to as anorthosites (Fig. 13).

The anorthosite chemistry was very similar to that determined at the highlands site Tycho by the Surveyor alpha-backscattering experiment. This observation led several investigators to propose that the anorthosite fragments may arrive in mare regions as ballistic impact ejecta from the highlands. Consistent with such distant sources was the high degree of shock seen in many of the anorthosite chips. The percentage of crystalline plagioclase component in the regolith increased from ~5 per-

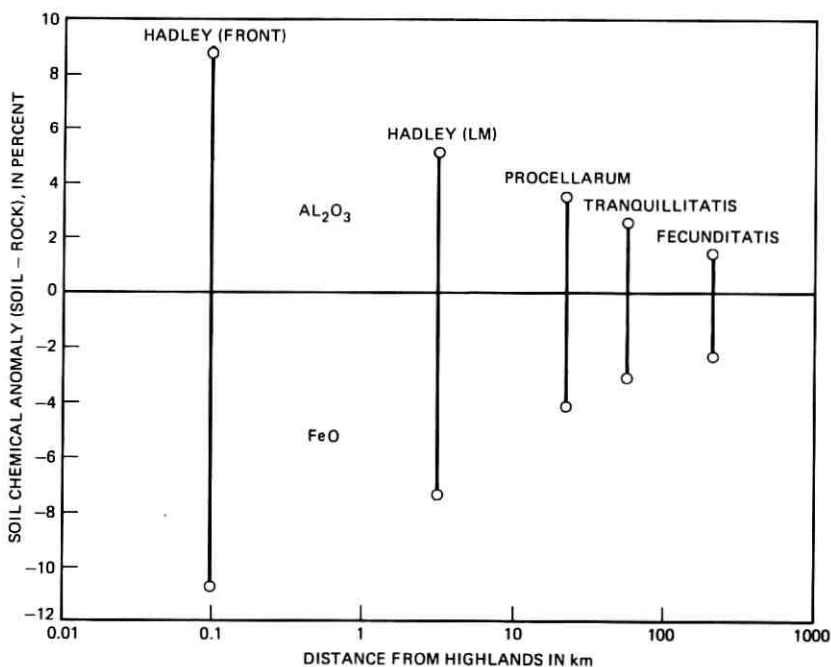


Fig. 12—Chemical anomalies in mare soil. The increase in the anomaly with decreasing distance from highlands indicates highland components high in Al_2O_3 and low in FeO . (See Fig. 13 also.)

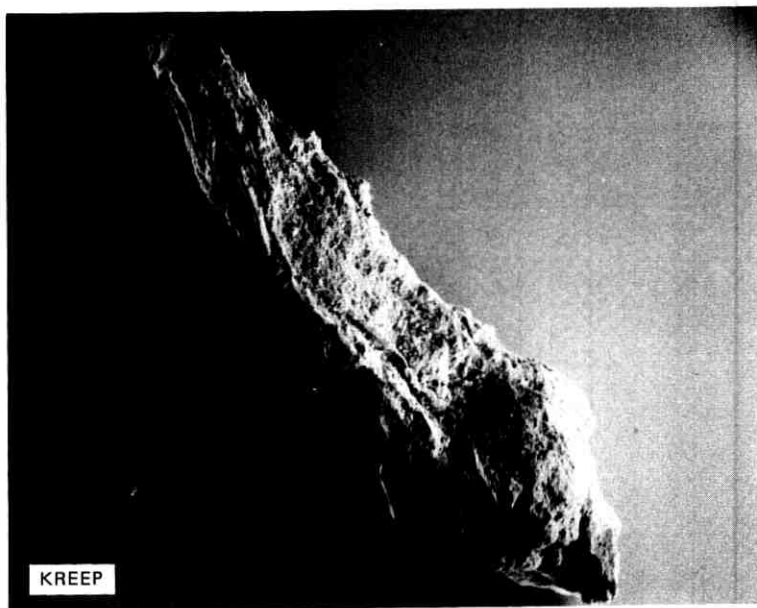
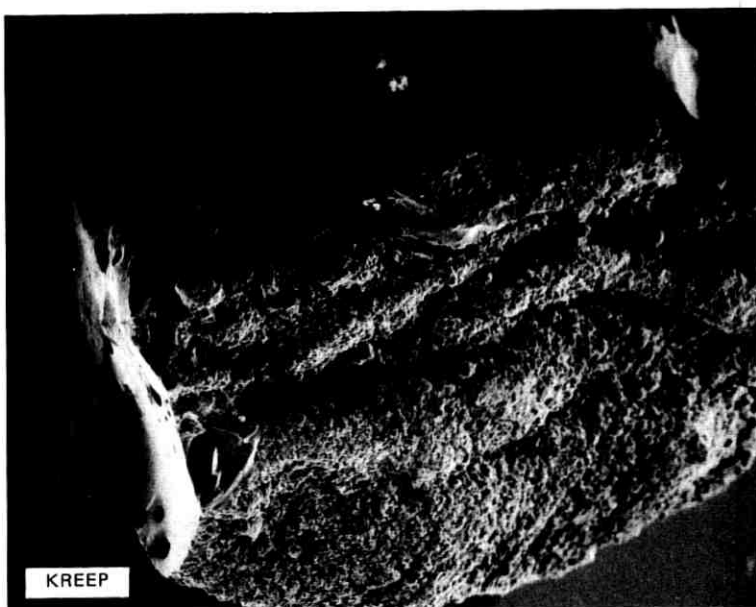


Fig. 13—Exotic components ejected by meteoroid impact from highlands into mare soil. The light-colored anorthositic fragments commonly exhibit glassy, ropy, and contorted textures indicative of impact origin. These particles are low in FeO and high in Al_2O_3 relative to the mare basalts. (Fig. 12.)

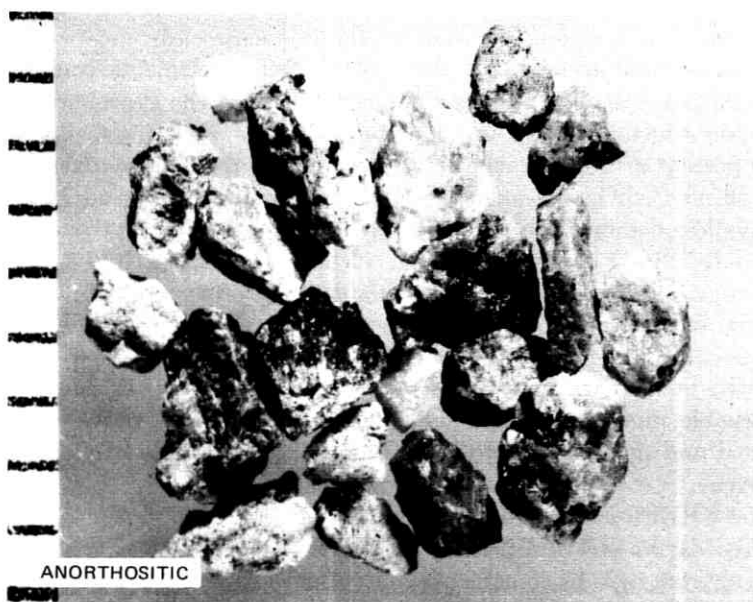
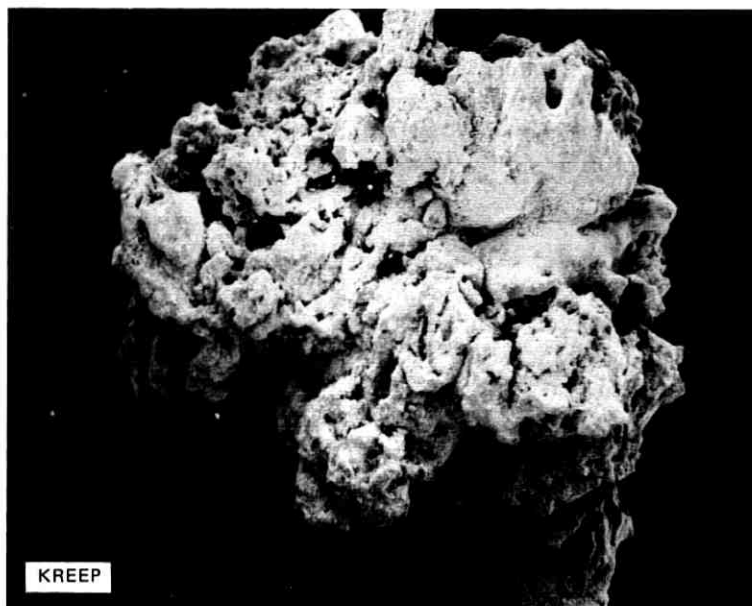


Fig. 13—(continued)

cent in the 1 to 10 millimeter chips, to ~ 15 percent (crystalline) in the < 37 -micron fraction. The 40 percent glass in the < 37 -micron fraction also contained a high percentage of anorthosite component. Recognizing that the size fraction below 37 microns contained ~ 40 percent by weight of the regolith, one could roughly account for the excess aluminum and depletion of iron and titanium.

Certain observations led to hypotheses that the anorthosite fragments were genetically related to the mare basalts. Associated calculations indicated that, if this is true, there must exist masses of plagioclase-rich rocks several times the mass of mare basalts—not an insurmountable problem if large regions of the lunar highlands are anorthositic.

Obviously, it was necessary to sample the highlands directly. The Apollo 15 mission to Hadley-Apennine was a first step in that direction, for the Apennine Mountain front was clearly non-mare. Preliminary analyses of Apollo 15 samples showed that Apennine material is rich in the anorthosite component—in fact, one rock returned was > 99 percent plagioclase, thus a true anorthosite. Unfortunately, the anorthosite was part of a breccia, thus obscuring its ultimate origin. The need to sample highlands was instrumental in the selection of Descartes (Fig. 55) as the Apollo 16 site, and it also played a dominant role in the Apollo 17 site evaluations.

Chemical analyses of the anorthositic fragments clearly showed that they could not account for the high rare-earth-elements content of Procellarum soils. The prime foreign component at the Procellarum site was one which occurred in three forms: (i) as rock fragments with ~ 60 percent orthopyroxene (an orthorhombic variety of pyroxene with almost no CaSiO_3 end-member; clinopyroxene also occurred but was always less common), ~ 40 percent plagioclase, ~ 1 percent potassium feldspar, and ~ 1 percent rare-earth calcium phosphate; (ii) as a yellow-brown glass, often ropey and showing flow textures; and (iii) as glass-matrix breccias with impact-formed textures. The relatively high potassium (K), rare-earth elements (REE), and phosphorous (P) resulted in the acronym KREEP (Fig. 13). The few fragments with observable mineral textures indicated that the parent rock was fine-grained and not unlike basalt except for the dominance of the orthopyroxene.

The KREEP component was such that it could account for the range of Procellarum soil and breccia compositions by mixing it in amounts ranging from ~ 25 to 65 percent with normal Procellarum basalts. Since the KREEP had low iron and titanium content, there was no *a priori* need to invoke an anorthosite contribution in the Procellarum soil

and indeed, it was found that anorthosite content was minor compared with the KREEP content.

2.4.5 *Fra Mauro (KREEP+)*

The KREEP component at Procellarum was speculated to be derived from a lunar geologic unit called the Fra Mauro Formation, which occurs at the surface about 20 kilometers from the Apollo 12 Procellarum site, under the mare surface near the site, and probably in a ray crossing the site from the large crater Copernicus. It was this Fra Mauro Formation that was selected as the landing site for Apollo 14.

The Fra Mauro Formation (Fig. 53) could be quite convincingly argued to be an ejecta deposit resulting from the impact which created the large Imbrium basin. It was on this basis that it was selected for Apollo 14. It was expected that Fra Mauro material would show the spectrum of impact-associated alteration including shock and brecciation. Indeed, those attributes were observed in the suspected Fra Mauro material returned from the Procellarum site. The chemical analyses of Fra Mauro regolith and rocks showed the general equivalence with the Procellarum KREEP. It thus appeared certain that a large part of the upper crust of the Moon in the Imbrium region must be composed of KREEP-type material. Using reasoning similar to that concerning the mare basalts, it could be shown that these Fra Mauro-KREEP basalts represented a more extreme fractionation of the lunar interior than the mare basalts.

The Apollo 12, 14, and 15 chemical data significantly affected the site selection considerations. Consider that Copernicus was consistently a leading candidate for exploration on Apollo 15 to 17. The finding of probable Copernicus ray material at the Apollo 12 site and its equivalence to Apollo 14 samples indicated that there would be a high probability of duplication of results on a Copernicus mission. In addition, Copernicus, like the Apollo 12, 14, and 15 sites, is a "circum-Imbrium" site. Thus, it was felt to be highly desirable that remaining Apollo sites be as far as feasible from the Imbrium basin, and the initially attractive Copernicus crater was dropped from consideration.

2.4.6 *Lunar Chronology*

In the chronological ordering of a series of planetological events, it is possible to derive a relative and an absolute time scale. Both must indicate the same sequence of events but the relative scale, of course, contains no information about the absolute time of any event or of the length of any of the intervals involved. In deciphering lunar history

we were, prior to Apollo, limited to establishment of the relative scale. All prior estimates of an absolute scale were based upon assumptions concerning absolute rates of processes, such as cratering or erosion. Establishment of the absolute scale had to await highly accurate elemental and isotopic abundance data on returned lunar samples.

2.4.6.1 *Relative Age Dating of the Moon.* The lunar stratigraphic time scale, laboriously constructed by the U. S. Geological Survey, was based upon the premises that, in a comparison of two strata, unit A is younger than B: if unit A is seen to overlap B, if A transects or cuts B, if the relief of A is sharper than that of B, or if the impact crater density and regolith thickness on the surface A is less than on B. The relative time scale thus derived indicated that parts of the highlands form the oldest observable lunar terrain. After formation, the highlands recorded a period of random (time and space) formation of the great circular basins, one of the last being the Imbrium basin whose ejecta blanket, the Fra Mauro Formation (Apollo 14), provided a widespread stratigraphic marker unit. After basin formation, but before the major episodes of mare flooding, a relatively large number of highland basins, e.g., Descartes (Fig. 55), the Apollo 16 site, became flooded with a material with morphologic expression not unlike mare fill but of higher albedo. A period of mare flooding followed the filling of the upland basin. The major mare flooding appeared to have occurred during a "short" time interval, although it was recognized that mare surface crater densities vary by as much as a factor of $\sim 2\text{-}1/2$ to 5 from one mare to another. These ratios should be compared with a value of > 30 for the highlands to average mare crater ratio.

2.4.6.2 *Recent Pre-Apollo Estimates of Absolute Ages.* Estimates of the absolute ages of the various lunar units were dependent upon a multitude of assumptions concerning the meteoroid flux history, secondary craters, meteoroid energy-crater diameter scaling, possible volcanic craters, etc. The most recent pre-Apollo estimates, based on what were thought to be good assumptions, ranged all the way from an "average" mare age of ~ 3.6 billion years to 3 to 40 million years. The large difference between the estimates was due mainly to the fact that the 3.6-billion-year age was derived using a meteoroid flux based upon the number of craters observed on the terrestrial pre-cambrian shields (thus integrating over several billion years) while the young ages were based upon statistically short-term satellite and (suspect) observational data pertaining to the modern-day flux.

2.4.6.3 *Isotopically Derived Rock Crystallization Ages.* The age dates on lunar basalts were obtained by a variety of techniques, the most

reliable of which appear to have been obtained by the rubidium-strontium technique. Using this method, it was shown that Procellarum basalts are ~ 3.3 billion years, Fecunditatis ~ 3.4 billion years, Imbrium ~ 3.4 billion years, and Tranquillitatis ~ 3.7 billion years. The pertinent observation was that the volcanism that filled the mare areas seems to have all occurred in a geologically short time interval of $1/2$ billion years, some $3-1/2$ billion years ago. The Fra Mauro event itself was tentatively dated at ~ 4.0 billion years.

The exploration objectives of Apollo 16 and 17 were to extend the chronology, and evolutionary implications thereof, in both directions. Apollo 16 was targeted to land on one of the upland basin fill units which were believed, based on the crater counts, to be older than the mare. Proceeding in the other direction, an objective considered for Apollo 17 was to sample certain volcanic units which might be, again based on crater counts, as young as ~ 1 billion years (see Section 2.4.8.1 for implications). These relatively young deposits include certain of the possible explosive volcanics which might also yield the deep interior samples.

2.4.6.4 Soil Ages. The basalt ages reported above represent the time at which the basalts crystallized on the lunar surface. However, the regolith from all the mare sites and from Fra Mauro gave uranium-thorium-lead and rubidium-strontium apparent ages generally ranging from 4.4 to 4.7 billion years, an observation causing some confusion for those who wondered how one grinds up, for example, a 3.7-billion-year-old rock to make a 4.6-billion-year-old soil. The old apparent ages of the regolith were not necessarily bothersome in and of themselves, since under certain circumstances, rocks can retain a memory of earlier events. However, consideration of all the available data forced the conclusion that the regolith contains a genuinely old component not observed in, and related to, the basaltic rocks. This was dubbed the "magic" component and of itself had to give ages of ~ 4.4 to 4.6 billion years. (It should be noted that the interpretation of this age is extremely complex.)

A significant amount of detective work indicated that the "magic component" appears to be, in large part, none other than the KREEP basalt so prevalent at the Fra Mauro site.

2.4.6.5 Age of the Moon. There is as yet no crystalline rock sample which gives a rock crystallization age of greater than ~ 4.0 billion years. The Moon must, of course, be at least that old. The 4.4 to 4.7-billion-year regolith ages found at widely separated lunar locations indicated, however, that a major chemical fractionation occurred at that time.

Since 4.6 billion years is the accepted age of the Earth and most meteorites and since most models of Solar System origin envision it to be a rapid process, this is also generally accepted as the age of the Moon.

One of the major lunar objectives for Apollo 16 and 17 was to locate the older rocks for two significant reasons. First, it became obvious that a major part of lunar chemical evolution occurred between 4.0 and 4.6 billion years. The specific models which can be constructed for early lunar evolution generally fall into two categories: a spike-type (rapid) evolution at 4.6 billion years, and a continual-type (slower) evolution over the period 4.0 to 4.6 billion years. Clearly, a gap in ages between 4.0 and 4.6 billion years would favor the former. The second reason for desiring old rocks was to find evidence for "extinct" radioactivity (radioactivity with a half-life of $\sim 10^8$ years, which is long relative to the period of formation of the Moon but short relative to the total lunar history). From such data, it is possible to deduce such things as the time interval involved in the formation of the Solar System and its component planetary bodies.

It was clear that many "old" samples needed to be acquired before achieving any confidence in which model of early evolution was the more likely. Equally clear was the high probability that, in the final missions, it would not be possible to acquire sufficient samples to do so; however, it would be a start and, once again, it was in the heavily cratered highlands that one hoped to find the desired samples.

2.4.7 *Lunar Surface Processes*

A prime objective of the Apollo lunar program was to establish modes and rates of lunar surface modification. It has long been known, for example, that with increasing exposure to the space environment, initially sharp features become subdued, rocks "disappear," bright rays fade, and the regolith thickens. External agents believed to be responsible for these effects were the meteoroid flux and both solar and galactic radiation.

Calculations of meteoroid-induced rock erosion and regolith generation rates suffered from the same uncertainties as did calculations of absolute ages estimated on the basis of assumed cratering rates. Experiments aimed at studying surface alteration by cosmic rays or solar wind suffered mainly from the inability to properly simulate the lunar vacuum, atomic particle energies and fluxes, and micrometeoroid impacts. Sufficient radiometric age determinations on the old mare surfaces and on young rock surfaces (ejected onto the mare surfaces by geologically recent impacts) have now been carried out to make possible reasonably good estimates of process rates.

2.4.7.1 *The Meteoroid Flux and Cratering Rates.* Correlation of mare surface ages with the crater densities leads to the inescapable conclusion that the flux of crater-producing bodies was extremely high during and soon after lunar origin. As shown in Fig. 14, the flux fell off rapidly in the first billion years, with a relatively low flux since 3.3 billion years being indicated. It appears that the cratering model which led to estimates of very young mare ages is incorrect in that either the modern flux is anomalously high or many of the built-in assumptions in the observations and calculations are wrong.

The derived meteoroid flux curve affected site selection in two rather different ways. The age values upon which it is based are clustered at an old age and covered a relatively short time interval of ~ 0.7 billion years. In order to gain the desired confidence in use of the curve as a tool in age dating the vast unexplored regions of the Moon, it is important

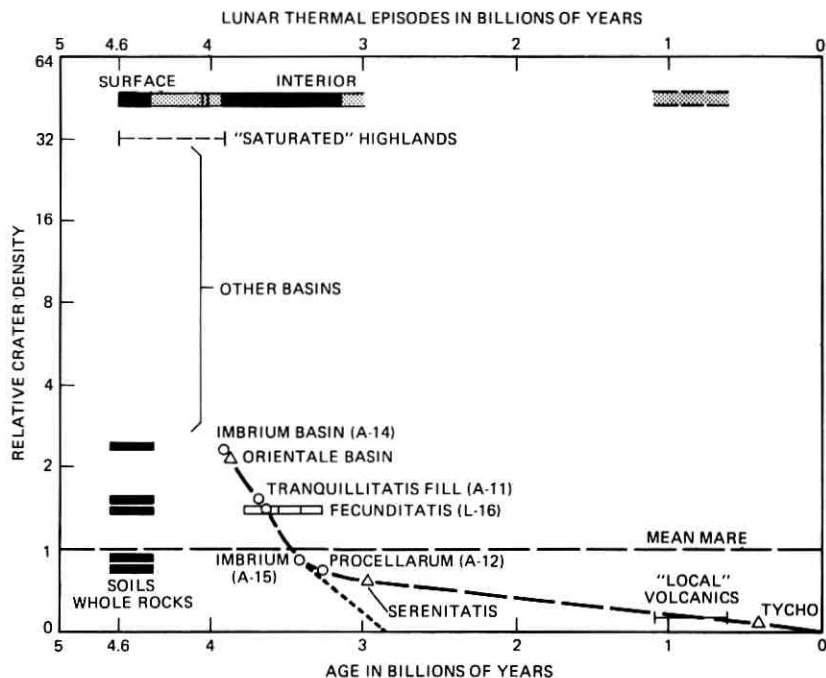


Fig. 14—Generalized lunar cratering and thermal history. Soil and whole rock ages indicate an early melting, possibly limited to the upper several hundred kilometers, and due to accretional energy. Mare volcanism appears to be a result of internal melting due to radioactive heating. Crater densities indicate that most volcanic activity ceased at ~ 3 billion years, with the possible exception of "local volcanics" whose real age is not known. The crater density curve at ~ 3 billion years is uncertain and could fall anywhere between the dotted and dashed lines, although the latter is thought to be more realistic.

that a genuinely young surface be dated. Such a surface is the ejecta blanket of the crater Tycho, estimated to be as young as 400 million years. Unfortunately, Tycho was dropped from consideration as a site for operational reasons. Another possible surface was the dark blanket-type deposit ($\sim 1/5$ the Procellarum crater density) such as seen in the Taurus-Littrow region (Fig. 59). The occurrence of this deposit at Taurus-Littrow was a significant factor in its selection as the Apollo 17 site.

The desire to obtain old samples was stressed in Section 2.4.6. Identifying sites which might contain old samples was not easy. A glance at the crater density curve indicates that highland sites exceeding 4.0 to 4.1 billion years tend to be saturated surfaces (so heavily cratered that new craters on the average destroy equal numbers of old ones) from which little, if any, relative age information can be obtained. Thus, arguments that obtaining old samples should be a major Apollo 17 lunar objective were diminished in effectiveness through the inability to distinguish between highland sites on the basis of age.

2.4.7.2 Surface Optical Properties and Alteration. The lunar surface has the unusual facility of scattering light preferentially back towards the source of illumination. A physical model and theoretical expression for the lunar photometric function (a mathematical expression for the reflective properties) indicated that the surface must be covered, to optical depths at least, with a highly porous, particulate soil (see Appendix A). Early estimates of the porosity of the "fairy-castle" structure were 90 percent with about a 60-micron upper limit on grain size. Indeed, the lunar soil consists of small particles with a mean grain size (by weight) of 60 microns with < 2 percent under 8 microns, not far from the theoretical prediction. The *in-situ* lunar soil density of 1.6 to 1.8 g/cc corresponds to bulk porosities of ~ 45 to 50 percent, the value predicted by radar backscatter models, but nowhere near the photometrically predicted 90 percent. However, the stereo lunar surface close-up photographs hinted at a much higher "cross-sectional" porosity for the optical layer which is all that one sees from Earth and the structure of which is destroyed by sampling.

Although major lunar albedo differences are attributable to compositional differences, the overall low lunar albedo and the disappearance of light colored rays with time require a lunar-wide darkening process. Pre-Apollo candidate processes included radiation damage, solar wind sputtering, and material deposited from impact-generated vapors. It now appears that none of these is the answer but, rather, that a process termed vitrification darkening is at work.

As shown in the laboratory, the albedo of lunar crystalline rock can be lowered by half or more when the rocks are vitrified, because of the darkening effected by dispersing titanium and iron in impact-produced glass. The titanium and iron in the rock were initially in discrete dark ilmenite grains in a matrix of lighter minerals. Support for this mechanism came from the observation that, relative to Procellarum, the lower albedo at Tranquillitatis correlates with higher titanium and glass content. Further, it was proposed that rays gradually disappear by progressive vitrification (and mixing with pre-existing soil) of initially highly crystalline ray material.

The information in the preceding paragraph led to increased confidence in the use of remotely-sensed data. For example, the low albedo of the blanketing deposit in the Taurus-Littrow region (Fig. 59) was interpreted as being caused by a high glass content of the soil (an alternative interpretation that the low albedo is due to the presence of darker rocks was ruled out by the Earth-based radar back-scattering data which showed the region to be relatively smooth on the centimeter scale). Since the crater density on the blanket is low, one cannot attribute the glass to meteoroid impacts, resulting in greatly increased confidence that the deposit is of explosive volcanic origin (terrestrial volcanic ash being glass-rich).

2.4.8 *Global Aspects of the Moon*

2.4.8.1 *Thermal Evolution.* The soil ages of ~ 4.6 billion years were evidence for a major chemical fractionation at that time which, in turn, implies large-scale melting. The relative age scale indicated that the next distinctly identifiable major igneous activity after the 4.6-billion-year event was the mare basaltic flooding. (The upland basin flooding noted in Section 2.4.6 occurred only a little earlier than mare flooding but is not as yet considered "major.") The isotopic age dating and crater statistics showed that mare volcanism started rapidly at, or slightly before, 3.7 billion years, peaked in the next $1/2$ billion years or so, and subsequently tailed off such that very little occurred after ~ 2.5 to 3.0 billion years. This implies a cool Moon today, a supposition supported by the nonequilibrium figure of the Moon, the persistence of mascons (large-scale positive gravity anomalies), the low level of lunar seismicity, and low interior electrical conductivity as deduced from magnetic sounding (eddy current response of the Moon to an applied magnetic field).

It became evident that the Moon had experienced two hot-cold cycles. The second cycle, mare flooding to the present, will be treated

first. An especially apt model of planetary igneous melting indicates that, if one starts with an unmelted Moon containing uniform relative concentrations of radioactive uranium, thorium and potassium, and preferentially concentrates the radioactivity in the melt, relative to the residual solid, such that it migrates upwards as volcanism occurs, then the intensity of volcanism will be sharply peaked in the early stages. This model indicates that *after* the onset of volcanism, peak volcanic activity is reached rapidly in $\sim 10^8$ years. The indicated die-off rates are slower, typically having "half-lives" of $\sim 3 \times 10^8$ years. The qualitative fit of this model to the lunar case was striking and provided circumstantial evidence that mare basalt generation and consequent basin flooding resulted from the buildup of radiogenic heat from uranium, thorium, and potassium.

Returning to the first hot-cold cycle, the hypothesized present low interior temperature and the cessation of mare volcanism at ~ 3 billion years are not compatible with an initially uniformly warm ($> 800^\circ\text{C}$) Moon; therefore, the 4.6 billion years melting required a near surface (presumably ~ 100 to 300 kilometers) heat source other than, or in addition to, long half-life radioactivity. The prime candidate for early heat generation is accretional (gravitational potential) energy associated with the infall of bodies forming the Moon.

Accretional heating would tend to result in a thermal profile peaked near the surface, thus allowing rapid cooling ($\ll 500$ million years, probably < 100 million years) and cessation of volcanism until mare basalt generation.

2.4.8.2 Remanent Magnetism and Lunar Core Considerations. Lunar basalts exhibited remanent magnetism which, if acquired as the basalts cooled below the Curie point of iron ($\sim 780^\circ\text{C}$), requires a magnetizing source field of several thousand gamma (Earth's field $\approx 50,000$ gamma).

Several source fields were considered. First, the ages of the basalts (3.2 to 3.7 billion years) ruled out a strong solar field associated with the formation of the Solar System at 4.6 billion years. Next, the Moon would have to have been $\lesssim 3\frac{1}{2}$ Earth-radii away from Earth to have experienced a sufficiently large geomagnetic field. Such a close approach is highly unlikely at 3.7 billion years and less likely at 3.2 billion years. Therefore, it is possible to conclude that the magnetizing field was indigenous to the Moon and that the Moon may at one time have had a liquid metallic core (presumably mostly iron) which could have behaved as a dynamo (an iron core of $\lesssim 0.2$ the radius of the Moon is not contrary to the moment of inertia data).

The geochemical evidence does not point towards the formation of an iron core:

- (i) Relative to Earth, the lower lunar bulk density indicates less free iron in the Moon, yet lunar basalts are richer in iron, suggesting that the lunar subsurface has not been greatly depleted in iron.
- (ii) Thermal models indicate that the deep interior has never been above the melting point.

The discovery of a small magnetic field (40 to 100 gamma) at Fra Mauro and of dozens of localized highland magnetized regions (an interpretation of Explorer 35 and Apollo 15 subsatellite-detected magnetic anomalies) indicated that remanent magnetism is a lunar-wide phenomenon. However, since there was no satisfactory explanation, it was concluded that the return of highland samples was of utmost import.

2.4.8.3 *Seismic Data and Lunar Layering.* Abundant evidence implied that large scale shallow layering should exist on the Moon: mare lava flows filling the basins, KREEP basalts overlying something else, and probable anorthositic highlands. Seismic data from deliberate spacecraft impacts showed some evidence of a velocity discontinuity at ~ 20 kilometers in the Procellarum mare region, but none at shallower depths. This lack of layering at shallow depths may simply have been due to intense fracturing and layer disruption caused by meteoroid bombardment. In that region the data did indicate, however, a generally low near-surface velocity rapidly increasing with depth, a complex seismic surface wave propagation, and an unusually high Q (low energy loss). These were interpreted to indicate scattering and/or dispersion in a self-compressed zone of fractured dry rock.

2.4.9 *Lunar Carbon, Organic Matter, and "Life"*

An extremely diligent search, using techniques with sensitivities unattainable only a few years ago, was made for evidence of lunar organic matter which might be indicative of proto-life chemical processes. Carbon analyses showed that the basalts contain ~ 25 to 75 ppm total carbon while the soils typically have higher contents of ~ 100 to 200 ppm. These relative carbon abundances, when combined with observations that carbon content increases with decreasing particle size and correlates with solar wind hydrogen content, lent support to the conclusion and supporting calculations, which showed that much of the soil carbon is derived from the solar wind. That there must also be a contribution from meteoritic carbon was attested to by evidence that ~ 10 to 20 ppm exists as carbide (not uncommon in meteorites), a level much higher than the carbide content of the rocks.

Searches for visible micro-organisms, dead or alive, were 100 percent

negative, as were attempts to find micro-organisms by culture techniques. On the other hand, there were reports of trace amounts (tens of ppb) of amino acids, porphyrins, and various chain and cyclic hydrocarbons. In view of the serious and obvious contamination problems, however, it was not felt that these findings were significant. Further, consideration of the harshness of the lunar environment (temperature extremes, meteoroid bombardment, high vacuum, lack of water, high solar and cosmic radiation) did not encourage the search for lunar organic compounds. Consequently, bio-oriented arguments relative to site selection ceased to have any weight.

2.4.10 *Tektites and Meteorites*

Tektites are highly siliceous, glassy objects found in as many as eight different broad terrestrial "strewn-fields." Over the years, evidence pro and con a terrestrial origin accumulated as did evidence for an extraterrestrial origin. The most favored extraterrestrial source was the Moon. There are, however, so many relative elemental abundance ratios, isotopic ratios (e.g., see Fig. 10), and radiometric age data that are grossly different in lunar material relative to tektites that it is difficult to believe that there is any common origin. Thus, the argument that the lunar crater Tycho is the source for one of the tektite fields was no longer counted as a valid reason for considering that site.

Arguments were also advanced in the past that a certain class of meteorites, the basaltic achondrites, might have a lunar origin. Most of this meteorite class show distinct brecciation, often of two or more generations, thought to have originated in impact events near the surface of a planetary body. Chemically, the basaltic achondrites resemble lunar mare basalts in being low in potassium and sodium, high in rare earths, and high in iron. They differ significantly, however, in their low titanium content (0.4 to 1.0 percent TiO_2). Mineralogically, the basaltic achondrites contain large amounts of orthopyroxene and small amounts of magnetite, neither of which exist in the lunar mare basalts. On an isotopic level, lunar basalts all have similar $\text{O}^{18}/\text{O}^{16}$ ratios which, in turn, are distinctly unlike those in basaltic achondrites. Recently presented new and redetermined U-Th-Pb ages of basaltic achondrites cluster near 4.6 billion years, much older than lunar basalt. The basaltic achondrite potassium/uranium ratio (Fig. 10) falls between Earth and lunar values. It was quite logically proposed that the gross geochemical and petrological similarities between lunar mare basalts and basaltic achondrites are simply indicative of similar processes

acting in different parts of the Solar System. On the Moon, however, the samples were collected in a geologic context, thus removing much of the speculation that accompanies interpretation of meteorite data.

2.4.11 *Origin of the Moon*

The soil model ages of 4.6 billion years indicated a major lunar-wide chemical fractionation at that time. By analogy with meteorite systems and the Earth, both of which formed at 4.6 billion years, it was concluded that 4.6 billion years is indeed the time of lunar origin.

Certain chemical differences between lunar and terrestrial rocks and meteorites, e.g., the lower lunar volatile and siderophile element content and higher refractory element content, were used to support hypotheses that:

- (i) The Moon fissioned from the Earth.
- (ii) The Moon was captured by the Earth.
- (iii) The Moon accreted from an assemblage of planetesimals orbiting the Earth.

Common sense might dictate stopping here, but it is felt that the sequence above is one of increasing probability. Fission proponents argue that fission occurred early, near the time of Solar System origin, with the Moon coming from an Earth which had already formed a core. This follows from a desire to explain the depletion of lunar siderophile elements as resulting from their incorporation in the iron of the Earth's core. Such an interpretation was not supported by the lunar siderophile abundance pattern which was distinctly non-Earthlike. Likewise, the K/U and U^{238}/Pb^{204} ratio argued against any direct commonality of lunar-Earth mantle chemistry but this was circumvented by postulating a severe post-fission heating of the Moon with subsequent loss of volatiles.

The spread of 1/2 billion years in mare ages did not support pre-Apollo interpretations that mare flooding represents the effect of capture and subsequent rapid tidally-induced heating of the Moon by the Earth (the Moon would rapidly move out of the region of strong heating). However, this simply caused proponents to place capture near the time of lunar origin.

A very complex model of how one might account for the observed chemical differences between the Moon and Earth was put forth. It depends basically upon formation of a hot massive silicate-containing atmosphere around the Earth. Upon cooling, the refractory silicates condensed into planetesimals in an inner ring around the Earth. The

more volatile compounds condensed further out, in cooler regions, and were ultimately swept away. The planetesimals (10^2 - 10^7 centimeters diameter) finally accreted to form the Moon.

In summary, all lunar origin models have become more complex in order to attempt to fit new chemical constraints. As a result, simple direct fission and simple binary planet formation models are rapidly disappearing, although some recent models may be viewed as variations on those themes. It would have been very desirable to be able to predict which of the candidate lunar sites, if any, held the answer to the lunar origin problem. However, at that time we did not have that ability (nor do we now); in addition, lurking in the back of one's mind was the fact that samples taken from tens of thousands of "terrestrial sites" have not enabled us to pin down the details of the Earth's origin. About the best that could be done was to select a site with as wide a variety of objectives as feasible and hope for the best; thus, a lunar site which promised a combination of old rocks, young rocks, and deep-interior samples ranked high in the Apollo 17 site evaluation process.

III. APOLLO SYSTEM CAPABILITIES

The capability of the Apollo system has been a constantly evolving property, with each mission adding its own increment in terms of new or modified equipment or mission procedures, and increased confidence in the reliability of the system components. This evolution directly impacted site selection, primarily through its effects on lunar accessibility (Section 3.2).

3.1 *The Apollo Missions*

3.1.1 *Development Missions*

The initial phase of the Apollo Program consisted of a series of missions, both unmanned and manned, to demonstrate and understand the capabilities of the Apollo system. These missions culminated in the first manned lunar landing. Early test missions (Little Joe II and Saturn I flights) were unmanned and were designed to qualify the spacecraft structural design. The principal objective of the unmanned Saturn IB (AS-201, AS-202, AS-203, and Apollo 5) and Saturn V (Apollo 4 and Apollo 6) flights was to qualify the space vehicle design for manned flights. Finally, the manned Saturn IB (Apollo 7) and Saturn V (Apollo 8, Apollo 9, and Apollo 10) test flights qualified both the flight systems and flight crews for lunar landing missions.

The climax of the development program was the long-anticipated

successful landing of the Apollo 11 Lunar Module *Eagle* in the Sea of Tranquility on July 20, 1969. The first two men to set foot on the Moon, Neil Armstrong and Edwin Aldrin, Jr., carried out limited selenological inspection, photography, survey evaluation, and lunar soil sampling. With their safe return to Earth on July 24, the national goal of successfully landing men on the Moon during the decade of the 1960's had been accomplished.

3.1.2 *Lunar Exploration Missions*

Following successful completion of the Apollo 11 mission, attention turned to the scientific exploration of the Moon. The remaining lunar landing missions were divided into two groups: the H series (Apollo 12, Apollo 13, and Apollo 14) and the J series (Apollo 15, Apollo 16, and Apollo 17).

3.1.2.1 *The H Missions.* These missions were to demonstrate precision landing capability, deploy scientific instrumentation on the Moon, expand the lunar surface exploration capability of the astronauts, and begin the systematic exploration of the Moon at sites selected for their scientific interest. In short, these missions were to provide as many advances as possible without requiring basic new hardware items. Apollo 12 (November 14 to 24, 1969) demonstrated a pinpoint landing capability by landing within walking distance of the Surveyor III spacecraft, sampled a mare area, deployed an Apollo Lunar Surface Experiment Package, and obtained photographs from orbit of candidate exploration sites. Apollo 13 (April 11 to 17, 1970) was to have landed at Fra Mauro, but an oxygen tank rupture necessitated an abort 56 hours after liftoff. Apollo 14 (January 31 to February 9, 1971) was targeted to Fra Mauro in a second attempt to explore this area. This time mission success was achieved, with a good scientific return.

3.1.2.2 *The J Missions.* These missions greatly extended the lunar surface exploration capability by providing a lunar roving vehicle, longer stay times on the surface and in orbit, and an improved life support system, leading to longer extravehicular activities. In addition, heavier scientific payloads were taken to the lunar surface, and extensive new science equipment was carried for use in lunar orbit. The launch vehicles in this series of missions were required to provide increased payload capability as necessary for the heavier payloads and associated spacecraft configurations. Apollo 15 (July 26 to August 7, 1971), the first of the J missions, dramatically demonstrated the improved exploration capability with the augmented surface mobility resulting from use of the Lunar Rover.

3.1.3 *General Mission Description*

The nominal lunar landing mission consisted of a series of distinct segments or phases. In case of difficulty at any phase, the mission could either be aborted or transformed into an alternative mission with new objectives, depending on the nature of the difficulty. The nominal mission proceeded as follows:

- (i) The spacecraft configuration was launched from Cape Kennedy, Florida, aboard a Saturn V three-stage launch vehicle. The third stage, the S-IVB, completed the boost into Earth orbit.
- (ii) After one or two revolutions, during which the spacecraft systems were checked out and the orbit was firmly established via Doppler tracking, the S-IVB stage was restarted to place the spacecraft on a translunar trajectory.
- (iii) Following translunar injection, transposition and docking were carried out, i.e., the Command and Service Module (CSM) was separated from the S-IVB/Lunar Module (LM), the CSM was turned around to enable CSM/LM docking, and the S-IVB was then separated from the now-docked CSM/LM. Following this, the CSM/LM continued to coast toward the Moon, while, depending on the mission, thrust was applied to the S-IVB to either send it on an escape trajectory from the Earth-Moon system or on a trajectory to impact the Moon in order to excite seismometers left there by previous missions.
- (iv) When the spacecraft reached the vicinity of the Moon, the Service Propulsion System (SPS), which was the main Command Module engine, deboosted the spacecraft into an elliptical lunar orbit, the pericyinthian (point of closest approach to the Moon) of which was on the far side of the Moon.
- (v) After approximately two revolutions, a second SPS burn, the descent orbit insertion maneuver, placed the CSM/LM combination in a lower orbit, with the pericynthian now on the front side of the Moon for direct access to the lunar surface by the LM.
- (vi) The LM separated from the CSM and used the LM descent propulsion system to descend under power to the lunar surface.
- (vii) Following lunar surface operations, the LM ascent propulsion system and reaction control system were used to launch from the lunar surface and rendezvous with the CSM.
- (viii) After transfer to the CSM was completed, the LM ascent stage was deorbited to impact the lunar surface, providing another input to the seismometers on the surface.

- (ix) After completion of the post-rendezvous CSM orbital activities, the SPS performed the transearth injection burn to inject the CSM into a transearth trajectory.
- (x) The Command Module separated from the Service Module 15 minutes before the entry interface, with Command Module touchdown occurring in mid-Pacific (the Service Module was consumed in the atmosphere).

3.2 *Lunar Accessibility*

3.2.1 *Introduction*

One of the fundamental issues which affected Apollo site selection was lunar accessibility; that is, given the system performance capability and mission design ground rules, what areas on the lunar surface could be reached on an Apollo mission? Reduced to its simplest terms, the site selection process was an iteration between the desirable sites based on scientific interests and the ability to fly missions to these sites. Needless to say, lunar accessibility was influenced by a number of factors, some of which arose from the capabilities and limitations of the Apollo system hardware (constraints) and others of which were generated by program management for reasons of flight safety, flight control, or operational facility (mission design requirements).

The question of lunar accessibility could be posed either of two ways, "Where can we land on the Moon on a given date?" or "When can we land at a particular site?" Both aspects will be considered, following an outline of the mission design process and a discussion of the mission design ground rules.

The mission design process included a multiparameter optimization of the trajectory for minimum propulsion requirements, subject to certain operational constraints. The process can be considered as beginning with the restriction on the lunar surface lighting conditions during the critical descent and landing phase of the Lunar Module. For most sites of interest, the Sun elevation angle at landing was required to be in the range of 5 to 25 degrees above the horizon.* Since the Moon rotates about 13 degrees per day, proper lighting conditions for landing at a particular site occurred only on one or two days during each lunar revolution. The lighting at landing essentially fixed the acceptable times of arrival at the Moon and the time of the lunar orbit insertion maneuver, since the timeline in lunar orbit prior to landing was essentially standardized to one day.

* The acceptable range varied from mission to mission, depending on landing site latitude, landing area topography, and LM descent trajectory geometry.

Working further back from the landing, the spacecraft propulsion and abort requirements which were imposed on the translunar trajectories basically limited the translunar time of flight to approximately three to four days duration. The faster the translunar flight time, the greater the energy of the translunar trajectory and, therefore, the greater was the demand on the Service Propulsion System (SPS) to insert the spacecraft into the desired lunar orbit. The available SPS propellant limited the duration of the translunar flight to a practical minimum of about three days. On the other hand, slower (lower energy) trajectories to the Moon required more propellant to handle aborts should the nominal mission become impossible. Since these trajectories were required to satisfy the abort capability ground rules, a maximum translunar flight time of about four days resulted. The specific limits on allowable translunar flight time varied slightly depending on the position of the Moon in its orbit and intended landing site but, in general, no more than a 24-hour variation in flight time was possible. The translunar time of flight and the translunar trajectory type largely determined the launch vehicle performance requirement for the mission. The launch-to-Earth-orbit performance requirement was independent of the lunar landing site, but the capability varied somewhat during the year as the average winds and temperatures encountered at Cape Kennedy vary. Launch opportunities occurred daily and were scheduled at the proper time to allow the translunar injection maneuver to occur essentially in the same plane as the Earth parking orbit.

Working forward from the lunar orbit insertion maneuver, the lunar orbit plane was selected so as to bring the spacecraft over the desired site at the time of landing, and to minimize the total SPS propellant requirements for performing:

- (i) the lunar orbit insertion maneuver itself (the most fuel demanding maneuver because both the CSM and LM were involved and the SPS tanks were initially full),
- (ii) a plane change maneuver to bring the CSM back over the landing site at the time of LM liftoff to facilitate rendezvous, and finally,
- (iii) the transearth injection maneuver which put the CSM on a trajectory targeted to enter the Earth's atmosphere with a prescribed flight path angle for a safe reentry.

For a given departure time from lunar orbit, the transearth flight time was quantized in increments of 24 hours by the requirement that the Earth landing occur at a predetermined location in the Pacific Ocean.

The SPS propulsion requirement to perform transearth injection was a function of both the duration of the lunar orbit stay and the transearth flight time.

The mission design requirements are covered in some detail in the following sections. It will be seen that the majority of these ground rules affected spacecraft propellant utilization, with the result that accessibility usually rested on the capability of the spacecraft systems to satisfy all the imposed requirements. The techniques used at Bellcomm for determining lunar accessibility will be described in Section 3.2.5.

3.2.2 *Mission Design Requirements and Constraints*

The requirements and constraints which led to the formulation of specific rules under which Apollo missions were designed¹¹ are described in this section. The general effect of these rules on SPS propellant consumption is also discussed, although, as mentioned earlier, a multi-parameter optimization was generally employed to determine a fuel optimum solution within the various constraints. Mission design requirements may be broadly classified as either general operational requirements for the nominal Apollo mission or contingency requirements to account for unexpected conditions, malfunctions, or system failures. General operational requirements included such factors as trajectory type, lunar orbit requirements, and photographic and scientific requirements. Contingency requirements included CSM capability to rescue a disabled LM in lunar orbit, CSM capability to move the splashdown point in case of adverse weather, and all mission abort requirements.

3.2.2.1 *Operational Requirements*

In describing the operational requirements, groupings are used that permit the simplest explanations of cause and effect. The trajectory itself is best subdivided into Earth, Earth-Moon (translunar), lunar, and Moon-Earth (transearth) phases. Spacecraft factors are emphasized in this section because they dominate the mission design; the launch phase, being uncoupled to a large degree, is treated further in Sections 3.2.3 and 3.2.4.

(i) *Translunar Trajectories.* As stated previously, the most significant SPS maneuver during the Apollo mission was lunar orbit insertion. Along with the Earth-Moon geometry at the time of the mission¹² and the location of the desired lunar landing site, which was reflected in mission design by the optimum lunar orbit orientation, the translunar trajectory had a major influence on the magnitude of the lunar orbit insertion maneuver. There was an evolution in the design of the trans-

lunar trajectories used during the Apollo program (Fig. 15). For the early manned lunar missions (Apollo 8, 10, and 11) the translunar trajectories were targeted such that, should lunar orbit insertion not be performed, the interaction of the spacecraft with the lunar gravitational field would bend the trajectory around the Moon to return the spacecraft to a safe entry in the Earth's atmosphere with only minor velocity corrections using the attitude control system. In order to make the lunar orbit insertion into the 110-kilometer circular parking orbit as efficient as possible, the pericyynthian of the translunar trajectory was targeted to about 110 kilometers. The Apollo 11 translunar trajectory severely curtailed the accessible area of the Moon. In planning the initial lunar landing, sites were restricted to lie within a box extending approximately ± 5 degrees in latitude about the lunar equator (Fig. 16). The box was also restricted to ± 45 degrees in longitude to allow adequate pre-landing and post-liftoff tracking. This area, which was a rough approximation

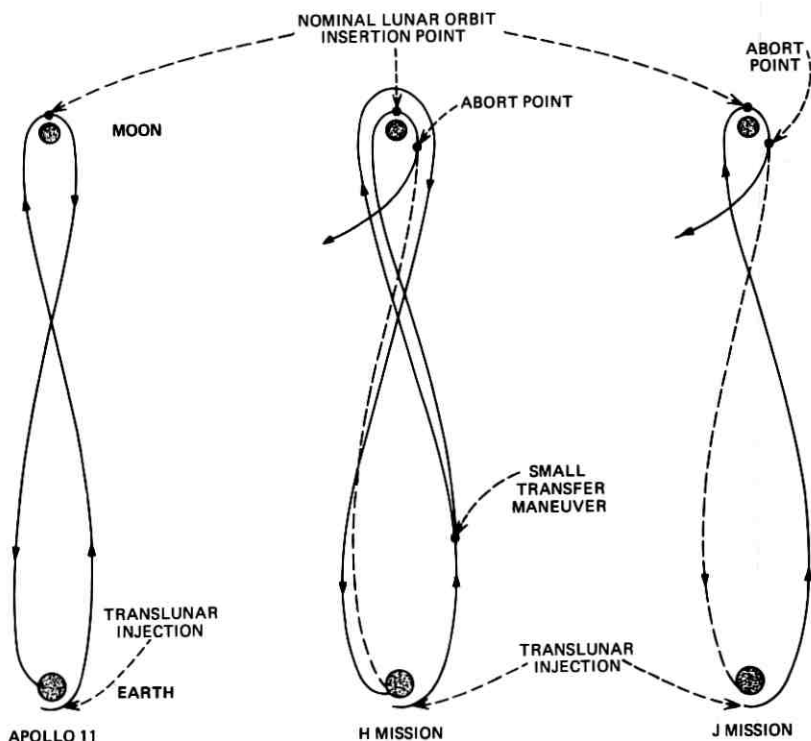
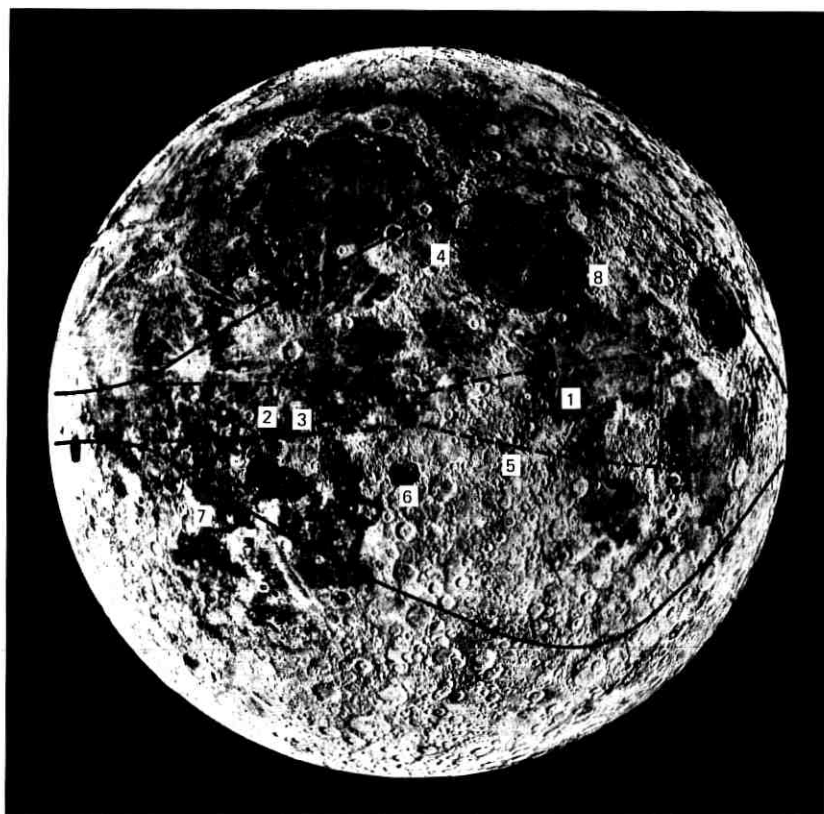


Fig. 15—Translunar trajectory types.



APOLLO SITES

- | | |
|-------------------------------------|------------------------------------|
| 1— APOLLO 11 SITE | 5— DESCARTES (APOLLO 16 SITE) |
| 2— APOLLO 12 SITE | 6— ALPHONSUS |
| 3— FRA MAURO (APOLLO 14 SITE) | 7— GASSENDI |
| 4— HADLEY—APENNINE (APOLLO 15 SITE) | 8— TAURUS—LITTROW (APOLLO 17 SITE) |
| — — — — — APOLLO 11 | ————— LATER MISSIONS |

Fig. 16—General lunar accessibility.

of the union of accessible areas during any month of the general period anticipated for the initial lunar landing, was used to limit site selection so that the initial lunar landing could be planned independently of the actual launch date. The characteristic shape of the accessible area for an Apollo 11 type trajectory was not that of a rectangle, but rather a "bow tie," as shown in the dashed contour line in Fig. 16.

Following the successful Apollo 11 landing, program emphasis shifted to lunar exploration and methods were investigated for expanding the

lunar surface areas accessible to Apollo landings. The translunar trajectory design was modified for the H missions (Apollo 12, 13, and 14) in order to open up the accessible regions (solid contour in Fig. 16—the longitude constraints from tracking are not included) and to reduce the demands on the SPS, thereby maintaining performance reserves despite growth in spacecraft mass because of increased scientific payload. The H-mission technique was to target the translunar injection maneuver to put the spacecraft on an Apollo 11 type trajectory with the pericynthian altitude determined by performance optimization (but generally greater than 110 kilometers) rather than being constrained to be near 110 kilometers. About one day after translunar injection, following transposition, docking and extraction of the LM, a small transfer maneuver (Fig. 15) was performed to place the spacecraft on a trajectory having a pericynthian near 110 kilometers and constrained such that, in case the lunar orbit insertion were not performed, two hours or more after pericynthian passage the LM descent engine could produce sufficient energy to place the spacecraft on a safe return trajectory. The rationale for this approach was that at least one backup abort system would always be available should the SPS fail. During the initial period after translunar injection, while on the Apollo 11 type trajectory, the reaction (attitude) control engines would be sufficient to return the spacecraft to Earth via a circumlunar flight. After the LM was docked to the CSM and the transfer maneuver performed, the LM descent propulsion system could return the spacecraft to Earth if necessary.

A further reduction in the performance cost of the SPS maneuvers was effected for the J missions (Apollo 15, 16, and 17). For the J-mission translunar trajectories, the transfer maneuver was combined with the translunar injection burn made by the third stage (S-IVB) of the launch vehicle. The translunar injection was targeted to put the spacecraft directly onto a translunar trajectory from which a LM descent propulsion system maneuver, performed two hours or more after pericynthian, could return the spacecraft to Earth. However, the trajectory was constrained so that the spacecraft reaction control system was able to transfer the spacecraft to an Earth return trajectory during the first five hours following translunar injection to provide a backup abort capability, should LM docking or extraction not be executed. This latter requirement did not, in general, constrain the translunar trajectory design, since reaction control system abort capability typically existed for 30 to 60 hours after translunar injection on such trajectories.

The reduction in spacecraft propulsion requirements resulting from

the above evolution provided greater overall flexibility in the trajectory targeting by allowing a greater range of translunar trajectory planes and greater plane-change capability by the spacecraft at the Moon. All of these factors expanded the region of the Moon which could be reached on a given mission. Translunar flight times were constrained principally by safety (abortability) considerations and by SPS capabilities. The flight time for an Apollo 11 type trajectory was controlled by the reaction control system abort requirement; 66 to 76 hours were typical values for the normal range of Earth-Moon geometrical relationships. Flight times for later missions generally ranged from 72 to 90 hours.

(ii) *Transearth Trajectories.* Transearth flight time was constrained by ground rule to be less than 110 hours. Little would have been saved in SPS ΔV^* requirements by lengthening the transit time beyond 110 hours, while two other considerations influenced the selection of flight times: shorter flight times decreased the probability of some spacecraft system failure, and sensitivities to small errors were less for the faster trajectories. Shortening the transearth flight time required an increase in the transearth injection velocity, thereby increasing the SPS requirements. In addition, transearth flight time was in a sense "quantized" by the necessity of arriving at the desired Earth landing point when it was in the proper spatial position relative to the transearth trajectory; thus, arrival was possible only at times roughly 24 hours apart.

Entry problems were initially believed to be very serious, and entry speed was felt to be a strong constraint. However, heat-shield test flights showed that normally attainable entry speeds (around 10,000 meters/second) posed no problems. Since the speed of the Earth (including the atmosphere) at the equator is about 450 meters/second, an entry from east to west could have had as much as 900 meters/second added to its relative velocity compared with a west-to-east entry. Entry was therefore constrained to be posigrade, i.e., having a west-to-east component. Entry inclination was further constrained in order to limit the extremes of possible landing latitudes under off-nominal conditions. In early Apollo missions the entry inclination was not permitted to exceed 40 degrees with respect to the equator; thus, the latitude of the landing could not be greater than 40° North or South. This constraint

* ΔV , or delta velocity, was essentially the change in spacecraft velocity required for a given maneuver or contingency sequence. The corresponding amount of fuel required to complete the maneuver depended not only on the ΔV requirement, but also on the spacecraft mass at the time and the particular engine being used.

was later relaxed, however, and inclinations up to 70 degrees were permitted.

(iii) *Lunar Orbit Requirements.* As originally planned, the Apollo mission had a circular lunar parking orbit at 170 kilometers altitude. The altitude was soon lowered to 150 kilometers, a compromise based on requirements for maintaining direct CSM-LM communications throughout LM powered descent to touchdown, minimizing ΔV requirements, and maintaining acceptable abort capabilities. The LM launch window for lift-off from the lunar surface decreased with decreasing CSM altitude, as did the differential angular rate between the LM in a low orbit and the CSM in its higher orbit, so that phasing time for off-nominal LM launches was increased by lowering the orbit altitude.

With the accumulation of experience, these constraints were changed. Launch time, launch window, and phasing problems were eased and standardized by the development of the "coelliptic" or concentric rendezvous plan.¹³ Beginning with Apollo 12, the lunar parking orbit altitude was reduced to 110 kilometers, in keeping with the general tendency to relieve the LM's mass-performance problems by shifting some of the burden to the CSM. While the lower orbit increased the demands on the Service Propulsion System (SPS) for lunar orbit insertion and transearth injection, it reduced the requirements on the LM descent and ascent propulsion systems and the reaction control system. The lower CSM orbit altitude also assured that, if the LM launch was nominal or nearly so, the range between the two vehicles remained within the 740-kilometer rendezvous radar range capability.

It was highly desirable to track the LM both before powered descent initiation and after ascent orbit insertion, to receive data for processing and to transmit to the LM an update of its estimated position and velocity vectors. The time available for tracking was limited by the time from acquisition of signal (end of occultation of the LM by the Moon) to powered descent initiation in the descent pass, and by the time from orbit insertion to loss of signal (occultation of the LM by the Moon) on the ascent pass. This obviously imposed a constraint on the closeness of the landing site to the point of acquisition of signal or loss of signal and, therefore, on the magnitude of the landing site longitude.¹⁴

(iv) *LM Descent and Ascent Requirements.* The LM powered descent was initiated some 15 degrees in lunar longitude from the lunar landing site, and lasted some 10 to 12 minutes. The Manned Space Flight Network was sized to provide continuous coverage of the LM powered descent. The normal communications mode was to maintain tracking,

voice, and high-rate telemetry via the LM steerable antenna to the 26-meter antennas of the network. The same information was available from the LM omni antennas, but a 64-meter ground antenna was required to recover a usable signal. For mission planning, the trajectory was required to have 64-meter antenna coverage during LM powered descent to provide for possible loss of the LM steerable antenna lock or other malfunctions. This additional requirement was constraining in that there were only two stations with a 64-meter antenna available, Parkes (Australia) and Goldstone (California); consequently, complete coverage of all launch opportunities was not available without modifying other trajectory parameters. The mission parameter which most directly determined the availability of 64-meter antenna coverage was the Sun elevation angle at landing, since this fixed the time of landing. Figure 17 illustrates the ranges of Sun elevation angle for which coverage was possible for six feasible launch months for a mission to the Descartes site. It is evident that satisfying the 64-meter antenna requirement

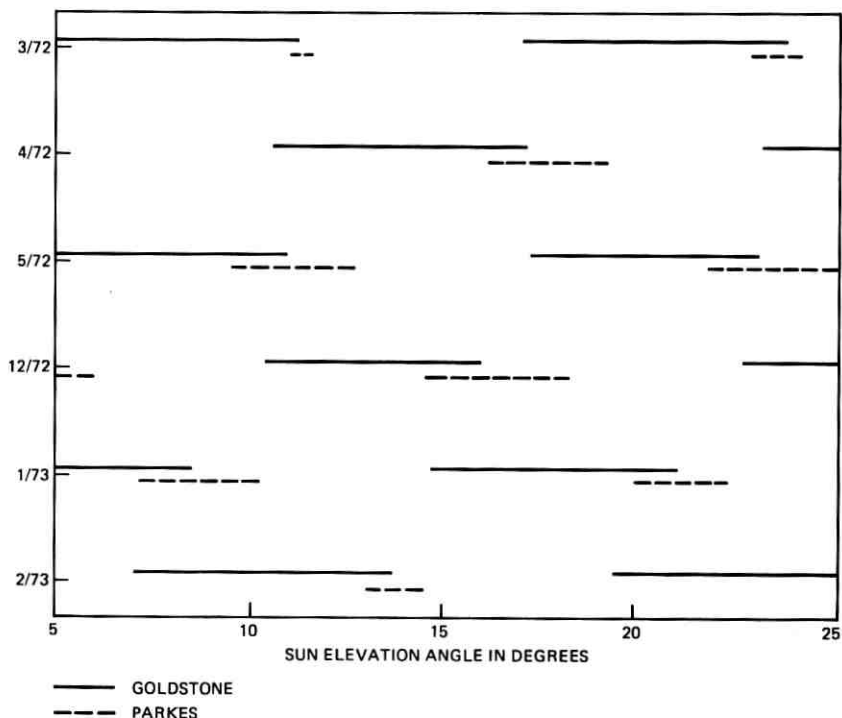


Fig. 17—Powered descent initiation antenna coverage for Descartes.

could lead to conflicts with the desired Sun elevation angle at landing, which in turn could require a change in the time of LM landing. The landing time directly affected the translunar flight time (for a given pre-LM descent lunar orbit timeline) thereby affecting lunar orbit insertion requirements and SPS propellant consumption.

The lighting required at lunar landing was the principal constraint defining the monthly period during which lunar landings could be accomplished. As the Apollo program planning developed, the lunar lighting requirement was soon reduced from any Sun-lighted condition to a restrictive range of 5 to 13 degrees Sun elevation angle at landing. Even landing in Earth-reflected light was considered at one time, but was subsequently rejected as not providing sufficient illumination. The lowest finally acceptable Sun elevation angle was that required to provide visibility of the landing terrain without excessive shadowing. This limit was generally higher for the landing sites with rougher terrain. The constraint varied between 5 and 10 degrees, depending on the site. The upper Sun-elevation limit was determined by contrast, which for the LM crew was a function of both the Sun elevation angle and the LM approach trajectory. Contrast depends on local slope variations and/or shadows. When the view line is below the Sun line, shadows are not visible to the observer and hence the contrast available is due only to slope variations. The lunar surface is retroreflective; that is, luminance reaches a maximum, and zero contrast occurs, when the view line is coincident with the Sun line (zero phase). Hence, in order to provide sufficient contrast for landing visibility, an elevation or azimuthal difference of more than 2 degrees was necessary between the view line and the Sun line to avoid zero phase lighting.

For the earlier Apollo missions, the LM flight path angle relative to the lunar surface was nominally 16 degrees during the final minutes of the descent; and the desired upper Sun elevation limit was 13 to 14 degrees. Sun elevation angles greater than 2 degrees above the view line were less desirable, but acceptable up to a nominal limit of 20 degrees (excluding 14 to 18 degrees). After Apollo 14, the LM descent elevation angle for the J missions (Apollo 15 through Apollo 17) was nominally 25 degrees, and the desirable Sun elevation range was approximately 7 to 23 degrees for a fairly smooth site with a LM approach differing in azimuth from the Sun direction.

A more complete analysis of lunar lighting appears in Appendix A.

(v) *Multiple Launch Opportunities.* Launch opportunities for lunar missions were continuous in time except for space vehicle limitations and certain launch constraints. Imposition of these constraints resulted in

two daily launch windows of a few hours each. Practical considerations further limited these opportunities to one per day; and only a few days per month were usable due to constraints on landing conditions at the Moon. The factors influencing the daily windows are discussed in further detail in Sections 3.2.3 and 3.2.4. Once the spacecraft propulsion systems were exposed to the hypergolic propellants about two weeks prior to launch, the clock began to run on the lifetime of the spacecraft. The limitation on the life of the propulsion subsystems after propellant loading was about 110 days, which meant that, at best, only three monthly launch periods were available once the initial launch commitment was made. Recognizing that even relatively minor hardware problems or adverse weather could cause a launch to be delayed beyond the launch window on a given day,* the program endeavored to provide as many launch opportunities as possible to insure that the hardware was flown during the systems lifetime. This had a significant impact on the site selection process.

For the initial lunar landing mission, multiple launch opportunities in a given monthly launch window were provided by using several possible landing sites distributed across the accessible area of the Moon from east to west. The first launch of the month was targeted for the most easterly site, when the rising Sun would be at the desired elevation at landing. Analysis showed that at least 44 hours would be required for reservicing the vehicle following a scrubbed launch attempt; consequently, a second launch was planned two days after the first and targeted for a site about 25 degrees further west on the Moon where the Sun would then be at the desired elevation at landing. Similarly, a third site further west was available for a launch on the fifth day of the monthly window. The exact location of the sites, while generally dictated by spacing to obtain suitable solar illumination, was further determined by vehicle performance capability, surface smoothness, available photography, etc. If the launch were not accomplished in the prime month, the whole cycle could be repeated the following month, or finally, in the third month.

Following the successful Apollo 11 lunar landing, the philosophy regarding multiple launch opportunities had to change in order to increase the scientific return. Mission planning and crew training emphasized one prime landing site, precluding the use of an array of sites across the Moon. The Apollo 12 site was selected in Oceanus Procellarum on the western portion of the Moon. Flamsteed, which is

* Planned "holds", or waiting periods, were included in the pre-launch count-down in order to partially offset this problem.

further to the west, was selected as a backup site to be used if the initial launch attempt to the prime site was scrubbed. This plan would also have been used in the second month if necessary. While not a perfect solution, this plan placed greater emphasis on the prime site and on the timely launching of the vehicle, but did include a mission to a less desirable backup site so as not to waste the vehicle.

The strong desire to concentrate planning and training for just one site per mission led to a further evolution of the multiple-launch strategy. A scheme was developed whereby, in the first month, one launch attempt was to be made on the optimum day (called T-O) to the prime site. In the succeeding two months, launch attempts could be made on two out of three possible days per month: the T-O day; the day before T-O, called T-24; and the day after T-O, called T+24. If the launch were made on T-24, the mission duration would be increased by spending an extra day in lunar orbit prior to landing, waiting for the Sun to reach the desired elevation at the landing site. If the T+24 mission were flown, the landing would have to be made at a higher Sun elevation than optimum, using special techniques during landing to enhance visibility. Launch vehicle and spacecraft servicing and turnaround procedures precluded the use of all three launch days in a given month.

The actual combination of launch opportunities planned for a specific mission also depended on the landing site characteristics and performance margins of the spacecraft propulsion systems. For the J missions, the visibility for T+24 landings was usually acceptable because of steeper LM descent trajectories and the generally higher-latitude sites, which have a larger component of side illumination by the Sun during landing. On the other hand, because of the longer J-mission duration, there was reluctance to add yet another day by using the T-24 launch opportunity. Therefore, the choice of launch opportunities for each month was specific for the selected site and launch date.

(vi) *Orbital Photographic and Scientific Requirements.* Each mission could have unique photographic objectives. If these objectives were of high priority, the mission was designed to make either a special orbital plane change maneuver or to select an approach azimuth that allowed the orbit to pass over the desired target. Either choice increased the required SPS propellant to fly the mission. In several cases, a prime mission objective was high resolution photography of areas being considered as future landing sites.

The J missions flew a set of scientific instruments in the Service Module. The requirements for the use of these instruments affected the mission design through altitude and timeline constraints. They also had some influence on site and approach azimuth selection because more

highly inclined orbits around the Moon meant that more of the Moon would be covered by these instruments.

3.2.2.2 *Contingency Requirements.* In the process of developing detailed plans for a mission, every conceivable contingency was investigated, and procedures were developed to cope with each contingency should it arise. However, from the standpoint of the impact on site selection, mission planning experience indicated that, although the majority of the contingency situations were site independent, three principal contingencies, LM rescue by the CSM, avoidance of adverse weather in the splashdown area, and post-pericyinthian abort following lunar orbit insertion failure, did have a strong influence on site selection. The major effect of the requirement to handle these contingencies was generally a decrease in the planned amount of SPS propellant available for nominal mission maneuvers, which, in turn, reduced the accessible region of the Moon.

(i) *LM Rescue.* The LM performed all maneuvers for rendezvous with the CSM in the nominal mission. However, if the LM became nonpropulsive, but in a safe orbit, at any time after separation from the CSM, the CSM was capable of performing the rendezvous maneuvers. Rendezvous was basically a problem of performing propulsive maneuvers with minimum propellant requirements to reduce the phase angle and differential height between the two vehicles to zero. A longer rendezvous time generally required less propellant (Fig. 18). Thus, the SPS propellant required for LM rescue could be decreased by increasing the lifetime of the LM ascent stage.

A generalized contingency rendezvous sequence put the active vehicle into a phasing orbit, circularized the orbit if necessary, and took the vehicle out of the phasing orbit (Fig. 19). The final rendezvous sequence used for a contingency rendezvous was the standard coelliptic rendezvous (Fig. 20), rather than the shortened nominal rendezvous used in the later Apollo missions.

If the LM aborted and was able to achieve its correct insertion orbit, but a subsequent failure occurred causing the LM to become nonpropulsive, the CSM was to be the active vehicle in rendezvous. A different type of double failure was the failure of both automatic guidance systems, requiring a manual LM ascent, in which case the LM ascent stage propellant would have been burned to depletion, and the CSM would have then performed the rendezvous. SPS propellant was reserved for a plane change in addition to that allotted for LM rescue, so that the CSM could reach the same orbital plane as the one achieved by the manual LM insertion.

The least probable class of aborts considered was the occurrence of

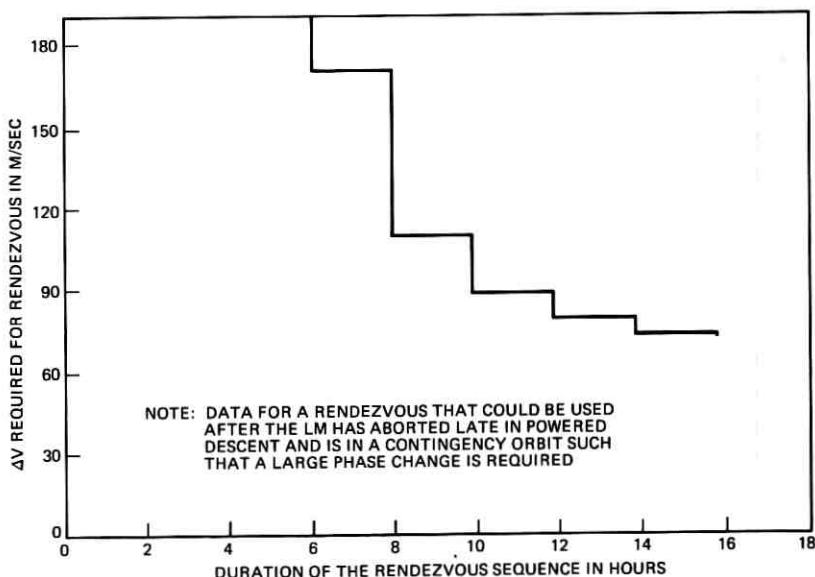


Fig. 18—Tradeoff of ΔV versus time required for rendezvous.

three or more failures. If the LM aborted before or during powered descent and was able to achieve a safe orbit, but not the desired one, a special CSM rescue technique was required. In most cases, the CSM went into a phasing orbit to increase or decrease the phase angle and then did a coelliptic rendezvous. However, there were possible cases where the CSM had to go high enough to lose up to a full 360 degrees with respect to the LM.

Further information on the planned rendezvous and rescue procedures for Apollo 11, Apollo 12, and Apollo 13 can be found in Ref. 15. Rescue plans for these missions included the improbable triple failures, and the CSM ΔV requirement for rescue was 240 meters/second. On later Apollo missions this requirement was reduced to 180 meters/second, covering all conceivable double failures.

(ii) *Weather Avoidance.* The spacecraft splashdown point upon return to Earth was chosen with care, in order to facilitate a safe and rapid recovery of the crew and spacecraft. Such a recovery could best be accomplished in an area which is free of large land masses, has generally favorable weather patterns throughout the year, and is reasonably accessible to the recovery fleet. For these reasons, an area in the Pacific bounded by 150°W and 170°W longitude and ± 35 degrees latitude was chosen as the Apollo Earth landing zone.

It was desirable to be able to move the planned optimum splashdown point, even within this landing zone, in order to avoid land masses, improve recovery fleet deployment characteristics, or avoid any highly predictable, unfavorable, annual weather patterns.

The additional fuel required to relocate the nominal splashdown point for weather avoidance or other landing and recovery considera-

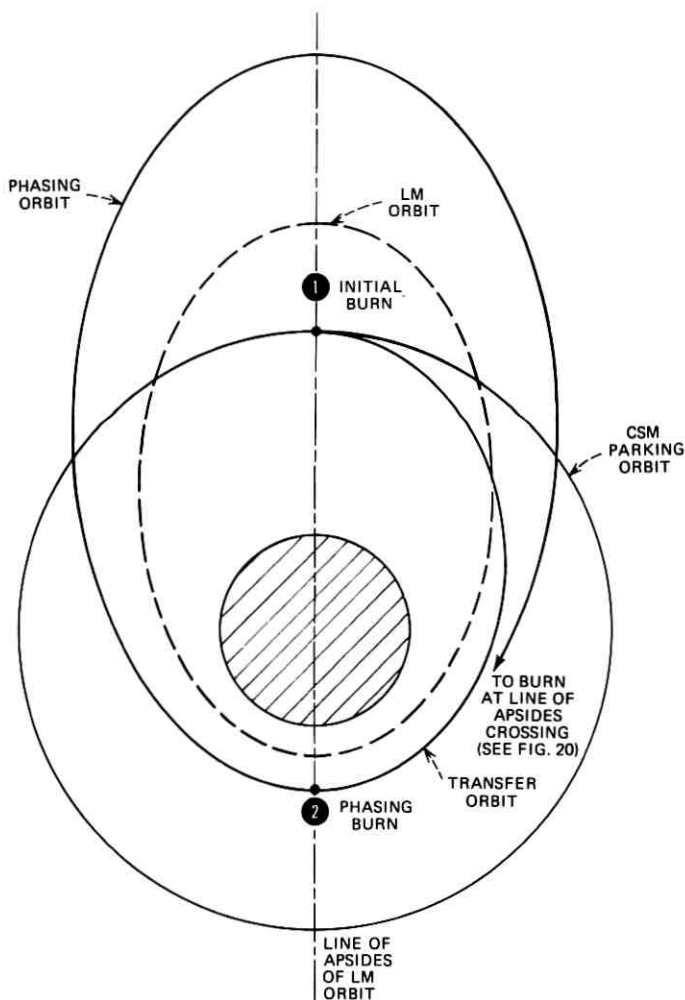


Fig. 19—First two burns of the CSM rescue rendezvous sequence used after abort from powered descent.

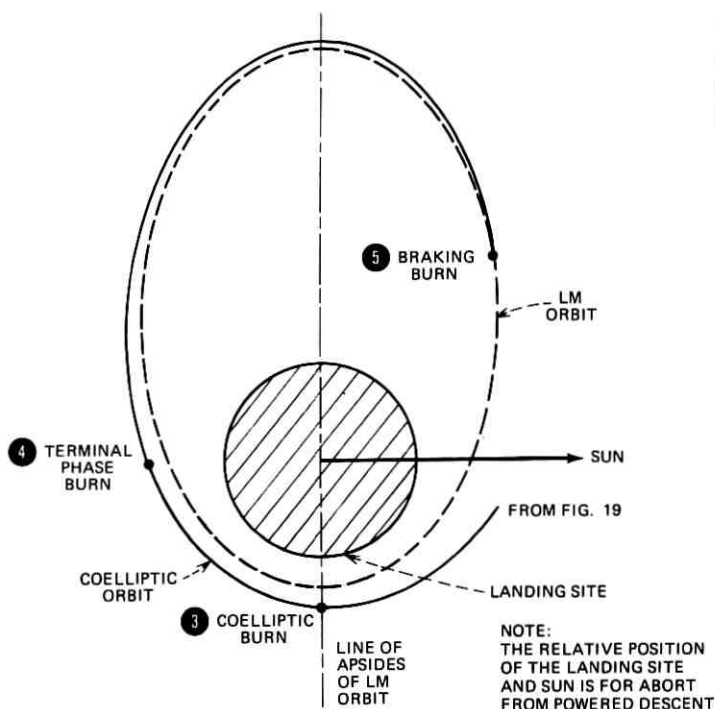


Fig. 20—The final rendezvous sequence.

tions was very much mission dependent,¹⁰ with ΔV costs at transearth injection ranging from 0 meters/second to as much as 75 meters/second.

A capability of moving the splashdown point in real time, if bad weather arose in the prime recovery area during the mission, was also highly desirable. Three main types of unpredictable weather occur that could force the movement of the splashdown point: thunderstorms, squalls, and hurricanes or tropical cyclones.

Based on the size and rate of movement of storms in the Apollo landing zone, it was concluded that a capability of changing the splashdown point by 900 kilometers would provide the maneuverability required to avoid any major weather system that might arise in the prime recovery area.

Three major constraints determined the point in the mission timeline at which splashdown point changes could be made for the purpose of weather avoidance: (a) flight controllers opposed any midcourse corrections for weather avoidance later than 24 hours before entry, (b) weather

predictions made more than 24 hours in advance were not sufficiently reliable, and (c) the recovery fleet could travel at a maximum speed of only about 20 knots; therefore, a splashdown point change of 900 kilometers would require at least 24 hours advance notice so that the fleet could reach the new splashdown point in time. For these reasons, it was necessary to perform any weather avoidance maneuvers approximately 24 hours before entry interface.

Fuel costs for an east-west change of the splashdown point at 24 hours before reentry were nearly independent of return time and return inclination; thus, the ΔV required to move the splashdown 900 kilometers was about 75 meters/second for all missions. A reasonable mission-independent SPS requirement for weather avoidance and other landing and recovery considerations, then, was 150 meters/second:¹⁶ 75 meters/second to provide for east-west movement of the splashdown point, and 75 meters/second for placing the nominal splashdown point somewhere other than the point of minimum SPS propellant usage in order to improve landing and recovery conditions.

(iii) *Aborts.* The safety of the crew was of paramount concern throughout the Apollo Program, and considerable effort was expended in defining those situations which might require a mission to be aborted and in providing the means for returning the crew safely to Earth. Appendix G contains a discussion of the various abort situations considered in the translunar and lunar orbit phases of the Apollo missions. As stated above, these aborts were generally site independent. The post-pericynthian abort requirement did, however, constrain the site selection in many cases. This requirement assured redundant return-to-Earth capability should the lunar orbit insertion burn, for any reason, not have been executed. The influence of the post-pericynthian abort requirement on the translunar trajectory design and hence on lunar accessibility has already been discussed in Section 3.2.2.1.

3.2.2.3 *The Effect of Mission Design Requirements and Constraints on SPS Propellant Consumption.* In order for a lunar mission to be feasible, it was necessary for the spacecraft SPS to be able to perform all required propulsive maneuvers. This, of course, implied that the propellant available for use was greater than that required for the specified maneuvers in both nominal and contingency situations.

The effects of all the requirements and constraints discussed above on the consumption of SPS propellant were complex because of their interdependence. Figure 21 represents these relationships in a schematic form, designed to show how the mission requirements affected each of the major maneuvers accomplished with the SPS.

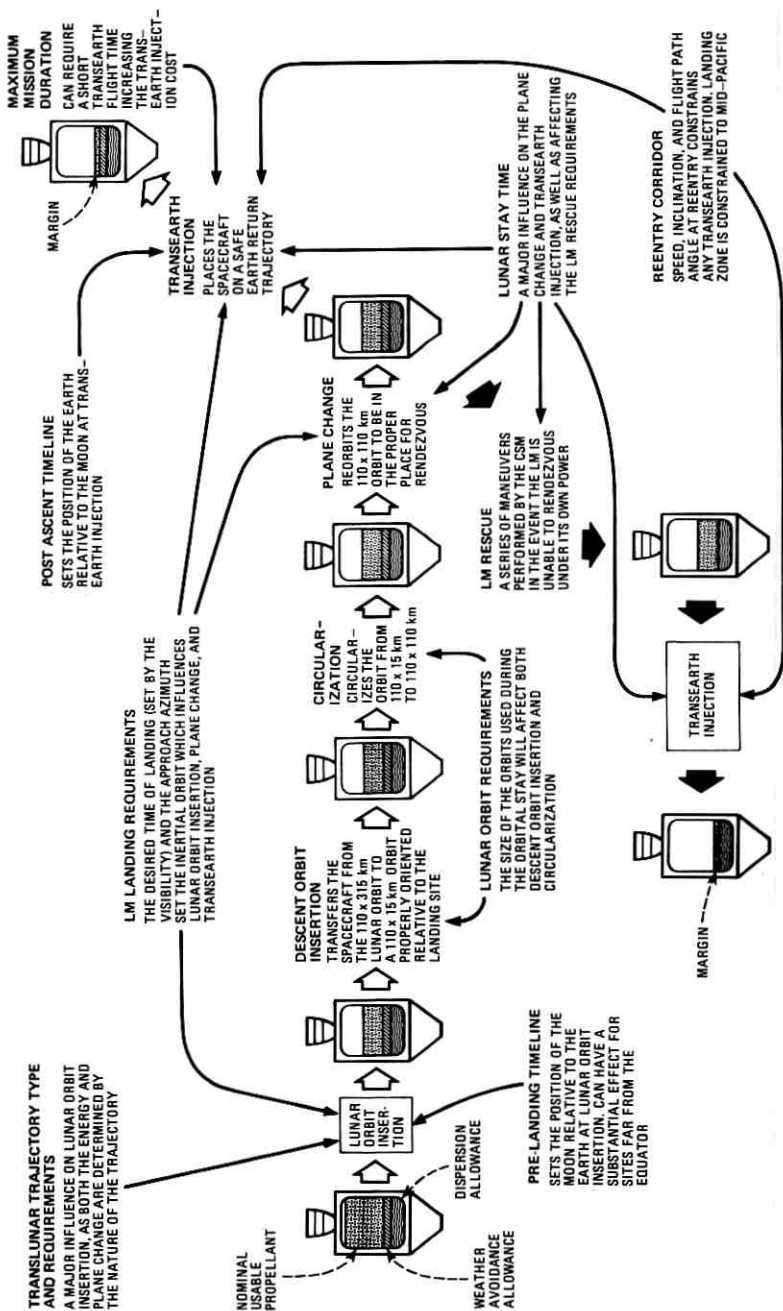


Fig. 21—Effect of requirements and constraints on SPS propellant.

In the schematic, the major nominal SPS maneuvers are lunar orbit insertion, descent orbit insertion, circularization, plane change and transearth injection. One contingency branch path which would be followed in the case of a LM rescue is also indicated. The propellant consumption during a maneuver is indicated by the schematic propellant tank. Although nearly 18,500 kilograms of SPS propellant were loaded into the spacecraft, not all of it was available for propulsion. Approximately 90 kilograms were trapped in the piping outside the tank and about 110 kilograms remained as residuals inside the tank. The uncertainties in vehicle mass, engine performance, and propellant loading were statistically combined, and resulted in over 270 kilograms of propellant being set aside. These uncertainties varied from mission to mission, resulting in some fluctuation of the amount of available propellant. Usually about 18,000 kilograms of propellant were available for propulsion. The available propellant for the nominal SPS maneuvers (nominal usable propellant) was the remainder after setting aside an allowance for possible post-transearth injection weather avoidance (Section 3.2.2.2) and an allowance for dispersions. The dispersion allowance was derived from a statistical analysis of SPS propellant consumption due to various error sources, including navigation uncertainties, guidance errors, and initial position and velocity vector errors.

Lunar orbit insertion consumed over two-thirds of the SPS propellant. The spacecraft was at its heaviest at this point with a nearly full load of consumables and the LM. Descent orbit insertion, circularization, and plane change consumed relatively small amounts of propellant, with transearth injection consuming the balance.

The contingency branch, required in case the LM could not perform the rendezvous, contains an added series of maneuvers¹⁷ which the CSM would have had to perform to rendezvous with the disabled LM.

It was assumed that, should CSM rescue of the LM become necessary, the remaining mission maneuvers would be modified to reduce the nominal SPS propellant consumption by optimizing the time of transearth injection (usually a few hours after rendezvous instead of the nominal two days later) and increasing the transearth coast time. In addition, no end-of-mission weather avoidance reserve was required in the LM rescue case. If, under these conditions, there was a ΔV capability with the SPS of 180 meters/second or more for the LM rescue, then this contingency requirement was satisfied.

Thus, for a mission to a given site to be considered feasible, the available SPS propellant had to be able to satisfy the performance require-

ments of both the nominal mission and the LM rescue mission, each considered separately.

3.2.3 *Launch Vehicle Considerations*

Lunar site accessibility depended not only upon the capability of the spacecraft to perform its required maneuvers, but also upon the Saturn V launch vehicle to inject the spacecraft onto the specified translunar trajectory. In retrospect, accessibility was usually limited by the spacecraft rather than by the launch vehicle. However, this condition was not always evident *a priori*, and the launch vehicle was always considered in the determination of lunar site accessibility. Launch vehicle performance considerations are discussed below, with attention being focused on those areas directly affecting lunar accessibility.

3.2.3.1 *Launch Vehicle Performance.* Standard launch vehicle performance was characterized by the mass which could be injected onto an Apollo 11 type translunar trajectory with sufficient propellant in reserve to make up for -2σ (-3σ on Apollo 11) performance dispersions. (The Apollo 11 trajectory represented close to a worst case for other trajectory types.) In order to determine the launch vehicle performance for a particular mission and site, the mission-specific translunar injection energy was computed and an adjustment to the launch vehicle payload (here, payload refers to the spacecraft, whereas it may have other meanings elsewhere) capability was determined. In addition, the payload capability was corrected for the wind and temperature effects expected during the launch month. There was about a 270-kilogram difference in allowable payload mass between a flight in the worst month (March) and the best month (July) due to these launch environmental effects.

For H missions (Apollo 12, 13, and 14), the total spacecraft masses were on the order of 46,000 kilograms while the launch vehicle capability was several thousand kilograms greater, even with 3σ performance reserves. However, the J-mission (Apollo 15 and subsequent) spacecraft mass was about 48,700 kilograms due to the extra consumables required for the longer-duration missions and the significant increase in the scientific and lunar exploration equipment carried. In order to accommodate the heavier spacecraft, several changes were made to the launch vehicle hardware, propellant budgeting, and trajectory. These changes were incorporated as system maturity and flight experience proved their acceptability.

The F-1 engines on the launch vehicle first stage were adjusted after acceptance firing to their pre-firing, high-thrust performance level, and

various engine cutoff timers on the first stage were adjusted to reduce the unburned propellant residuals left in the tanks at cutoff. On the second stage, modifications were made to the pressurization system which reduced propellant residuals on the stage. These and other hardware modifications increased the launch vehicle payload injection capability by more than 700 kilograms.

The most significant single change in terms of launch vehicle payload capability improvement was the decision to require that the launch vehicle reserves on J missions be sufficient to handle -2σ vehicle performance rather than -3σ performance as on earlier missions. The flight performance reserve was determined by statistically combining the propellant quantities required to overcome the effects of low engine thrust or specific impulse, uncertainties in actual vehicle mass, winds, propellant density, propellant quantities onboard, etc. The decision to reduce the flight performance reserve was taken after consideration of many factors and tradeoffs. The flight performance reserve quantity, ideally, did not affect crew safety but it could influence mission success. In particular, given a completed flight-ready spacecraft, the most practical way to reduce its mass, should it be beyond the launch vehicle capability, was to offload SPS propellant. This, of course, reduced the lunar accessibility and spacecraft performance margins. However, it was determined that the spacecraft could compensate for some launch vehicle underperformance. Thus, it seemed advantageous to reduce the launch vehicle reserves and load up the spacecraft, with the plan that the spacecraft reserves could be used to make up deficient launch vehicle performance if necessary, or be available should subsequent spacecraft contingencies arise. Furthermore, because of nonlinear effects, rather elaborate strategies were possible in order to gain maximum protection against performance uncertainties with the least propellant mass. The change in flight performance reserve, along with other propellant budgeting changes, added almost 700 kilograms to the launch vehicle payload capability.

In the area of trajectory changes, the translunar trajectory redesign from the Apollo 11 type trajectory reduced the translunar injection energy requirement and thereby improved the launch vehicle capability by an amount varying with landing site location and time of launch. Two other significant trajectory changes were the lowering of the Earth parking orbit from 185 to 167 kilometers and the optimizing of the launch azimuth range for each mission.

The original Earth parking orbit altitude was a compromise involving several factors. The desire for good tracking coverage, lower heating

of the vehicle during boost, and less in-orbit perturbation due to atmospheric drag tended to drive the nominal orbit higher. On the opposite side of the balance was payload capability. The matter was reconsidered after Apollo 14, and it was concluded on the basis of flight experience and increasing confidence in the system's overall performance that a modest increase in vehicle heating and about a 10 percent reduction in tracking coverage were acceptable costs to pay for an increase of 320 kilograms in capability.

In order to improve the chances of launching on a given day, the space vehicle hardware, software, and mission planning provided for a daily launch window of several hours, allowing holds to permit adverse weather conditions to improve or for the correction of minor malfunctions encountered during the countdown. The desired launch window duration was achieved by continuously varying the launch azimuth to be used as time elapsed so that, when the launch actually occurred, the vehicle was inserted into an Earth parking orbit with the desired inertial orientation with respect to the plane of the translunar trajectory.

Several parameters affected the selection of the usable launch azimuth range. A 4-hour launch window was the planning standard early in the program, with 2-1/2 hours set as an operational minimum. The allowable launch azimuth range was controlled by requirements in range safety, tracking, and launch vehicle performance. Range safety rules precluded trajectories which caused potential suborbital overflight or stage impacts on inhabited land areas. As a result, the launch azimuth variation was restricted to lie between 72 and 108 degrees (measured east of north) in order to avoid Bermuda and the West Indies, respectively. Tracking considerations reduced the allowable sector to a maximum of 26 degrees, so that one insertion tracking ship could be assured of obtaining the requisite 3 minutes of tracking following insertion. Closing of the Antigua tracking station forced the azimuths toward the north to assure continuous tracking during the Saturn V powered flight. Consequently, a launch azimuth range of 72 to 96 degrees was used for missions prior to Apollo 15.

With the substantial increase in spacecraft mass and the concomitant demands on launch vehicle performance for the J missions, the launch azimuth range was again re-examined for Apollo 15.¹⁸ It was found that by taking advantage of the nonlinearity in the relationship between launch window duration and launch azimuth range (Fig. 22), it was possible to maintain the launch window duration while shifting the azimuths toward the south and reducing the azimuth range. Optimum launch vehicle performance was achieved with a launch azimuth of

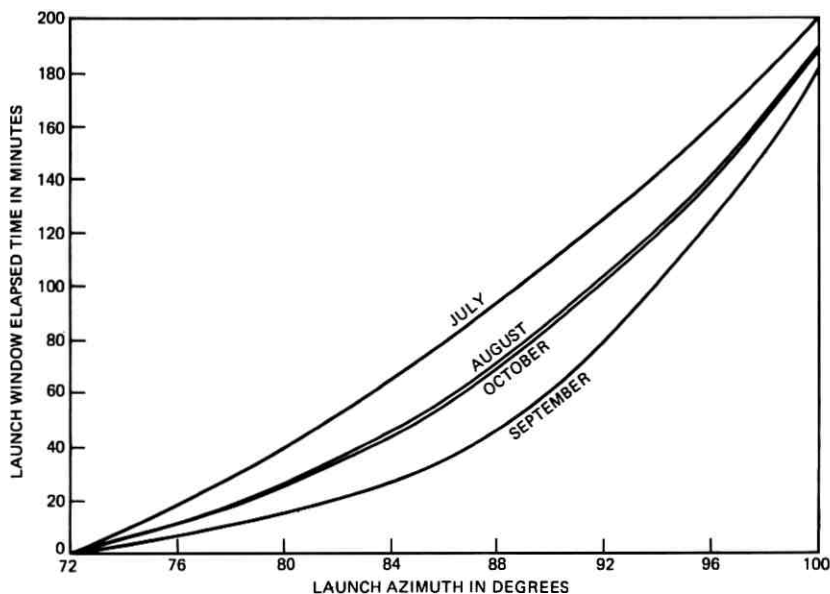


Fig. 22—Relationship between launch window range and duration (Apollo 15).

90 degrees, so that the Earth's rotational velocity added directly to the launch vehicle velocity. For a finite launch window, launch performance was best with a launch azimuth range symmetrical about the 90-degree azimuth. Thus, by shifting the launch azimuth range from 72 to 96 degrees, to 80 to 100 degrees on Apollo 15, a 2-hour and 40-minute launch window was maintained, while increasing the payload capability by more than 200 kilograms. Since the relationship between launch window duration and azimuth range was dependent on the landing site location on the Moon, Earth-Moon geometry, and trajectory injection type, the launch azimuth range had to be optimized on a mission-specific basis, thereby becoming an accessibility and site selection factor.

3.2.4 Launch Operational Considerations

The Apollo launches were subject to a number of operational, as well as performance, requirements. Perhaps the second most important operational requirement (choice of translunar trajectory type was first) related to lunar accessibility was the choice of injection opportunity.

Two translunar injection opportunities (and thus two launch opportunities) occurred during any given day for a given launch azimuth and time of month (lunar declination). One opportunity resulted in a

generally southeast translunar injection in the Atlantic Ocean region, while the other resulted in a generally northeast injection in the Pacific Ocean region. When the Moon was near its maximum or minimum declination, the injection points were close together; when the Moon was near the equator, the injection points were almost 180 degrees apart in Earth longitude. The injection points for each daily launch window moved with the launch date due to the angular movement of the Moon in its orbit of about 13 degrees per day. The inclination of the translunar trajectory with respect to the Earth-Moon plane for a typical lunar period is shown in Fig. 23 as a function of lunar declination and launch azimuth. During half of the month, Atlantic injections resulted in translunar trajectories which had relatively low inclinations to the Earth-Moon plane, while Pacific injections resulted in relatively high inclinations during the same period. The converse was true during the other half of the month.¹¹

Operationally, the ground support function was simplified by the use

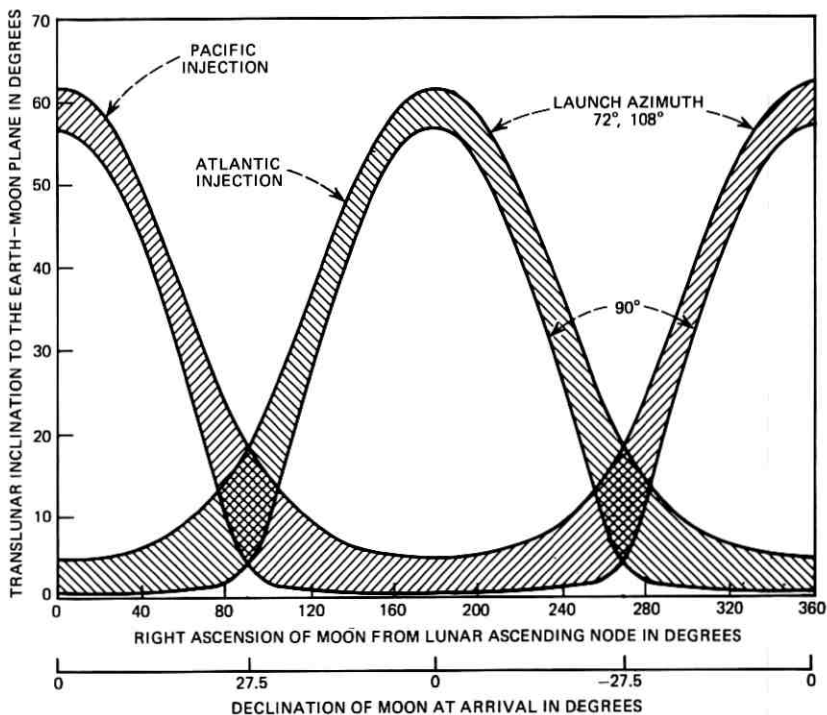


Fig. 23—Typical translunar trajectory plane inclination versus declination.

of only one of the two injection opportunities (and its associated launch window). Use of both opportunities would have created a logistics problem of switching the communications support aircraft from one part of the world to another between injection opportunities. Use of both windows on the same day would also have added additional complications to the onboard and ground guidance targeting for the injection maneuver.

The choice of injection opportunity was dictated, in most cases, by operational considerations rather than propellant economy. The Pacific injection opportunity during the spacecraft's second revolution (an operational choice) in Earth orbit was usually chosen as the prime injection opportunity. This opportunity allowed standard Earth parking orbit crew procedures and time sequence of tasks, as well as providing sufficient spacecraft checkout time prior to the injection maneuver. Because of the geographical location of the ground support stations, better ground station tracking and command coverage were provided both for the Earth orbit checkout requirements and for post-injection tracking requirements.

The geometry of the Earth-Moon-Sun system determined the Earth launch lighting conditions. In general, minimum propellant Pacific injection opportunities with daylight Earth launch occurred in the spring and summer* of the year. In the fall and winter, daylight launch windows for Pacific injection were usually available, but the Atlantic injection opportunities with night Earth launch windows were best from the standpoint of performance. This shift in better performance months for Pacific and Atlantic injections is illustrated in Fig. 24 for the landing site Copernicus. *The LM rescue ΔV available was a measure of SPS propellant consumption: the higher the ΔV available, the lower the propellant consumed for the nominal mission.* An Earth daylight launch was preferred when at all possible.

For these operational reasons, it was decided early in the program to use Pacific injection opportunities as a constraint in the site selection process, even though from a fuel performance point-of-view the Atlantic opportunity was preferable for certain cases. For later missions, use of the Atlantic opportunity for those landing sites which were not accessible from the Pacific opportunity within the existing performance capability was considered, although the restriction to only one injection

* This generality holds only if the lighting requirement at LM landing is accepted. Lunar trajectories respond principally to the monthly cycle in Earth-Moon geometry, but this is changed to a yearly cycle by the stroboscopic-like action of imposing the lighting requirement.

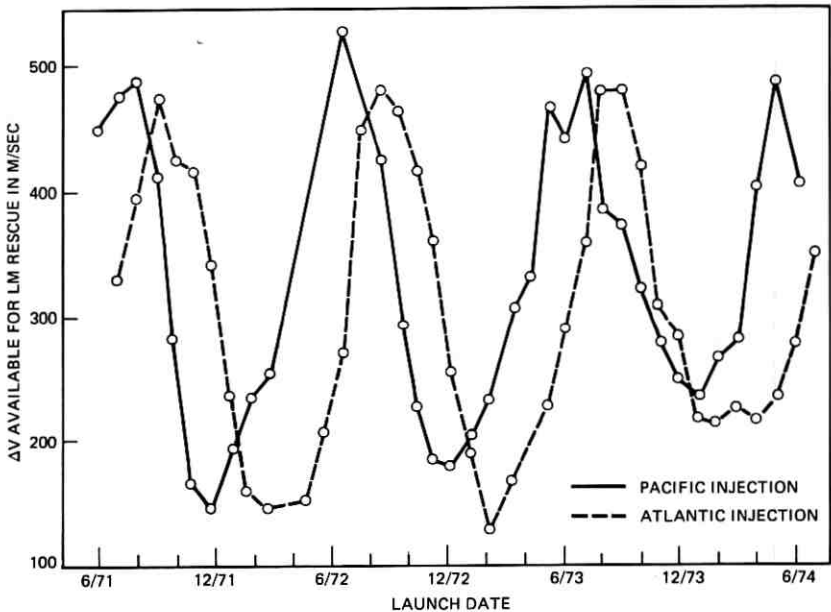


Fig. 24—Spacecraft performance as function of launch date and injection opportunity (Copernicus landing site).

opportunity was maintained for each day and the same type (Atlantic or Pacific) during any one month. An Atlantic injection was planned for the Apollo 17 mission.

3.2.5 Methods of Determining Accessibility

The major requirements and constraints of Apollo missions with regard to lunar accessibility have been discussed. It has been shown that lunar accessibility was ultimately determined by the SPS propellant required for the mission, as compared with the SPS propellant available, with due consideration given to launch vehicle performance. The application of those concepts to specific questions of lunar accessibility is now considered.

As previously mentioned, two general methods were used to describe lunar accessibility. The first considered a particular lunar site, usually chosen because of its scientific interest, and defined when and under what conditions that particular site would be accessible. The second method started with a particular launch month window, usually specified from launch scheduling considerations, and defined the lunar surface

area that would be accessible at that time. The first method was generally more appropriate when the site selection process had been narrowed to a choice of one of several candidate sites, while the second method was more useful early in the process, when broader areas of the Moon were being considered for possible lunar landing sites.

3.2.5.1 *Site Specific Accessibility.* Given an assumed lunar landing site location and the performance characteristics of the space vehicle, the ability to reach the site was examined as a function of time. This process frequently proceeded in successive stages of refinement, with the first step being one of determining whether a mission was at least feasible within all of the normal mission requirements, ground rules, and constraints. Assuming continuing interest or a decision to use the site, there were additional studies to consider available mission flexibility. Possible refinements included changes to make the landing site approach azimuth identical for each of the several launch opportunities; changes to improve the coverage of the lunar surface by instruments in lunar orbit; or changes to improve television coverage of lunar surface activities as constrained by Earth-based antenna locations. Site specific accessibility thus started out as an evaluation of minimum performance needed with a set of rigid mission requirements, and ended with the synthesis of new constraints* to refine the mission within the spirit, but perhaps not the letter, of the original requirements. Reviewing briefly, these mission requirements† included SPS propellant reserves for contingency purposes, descent propulsion system translunar abort capability, suitable lighting at LM landing, and the assurance of sufficient launch vehicle capability for successful translunar injection.

Prior to the adoption of steeper LM descents and an increased Sun elevation range at LM landing, accessibility of a particular lunar site was generally possible only for a single launch day each month. Subject to the mission ΔV requirements, including a contingency ΔV allowance, the feasibility of a mission was determined by a comparison of performance requirements with the capability of both the SPS and the launch vehicle. Sample results of a particular site-specific accessibility study¹⁹ are illustrated in Figs. 25 and 26. In this case, the LM approach azimuth and Sun elevation angle were optimized within the specified limits to

* It was frequently useful to constrain all but a few parameters and then to investigate all possible combinations of those remaining, thereby providing a basis for negotiating decisions on operational constraints such as lighting and approach azimuth.

† These are the major items, but there were many more lower-level requirements or constraints on each mission.

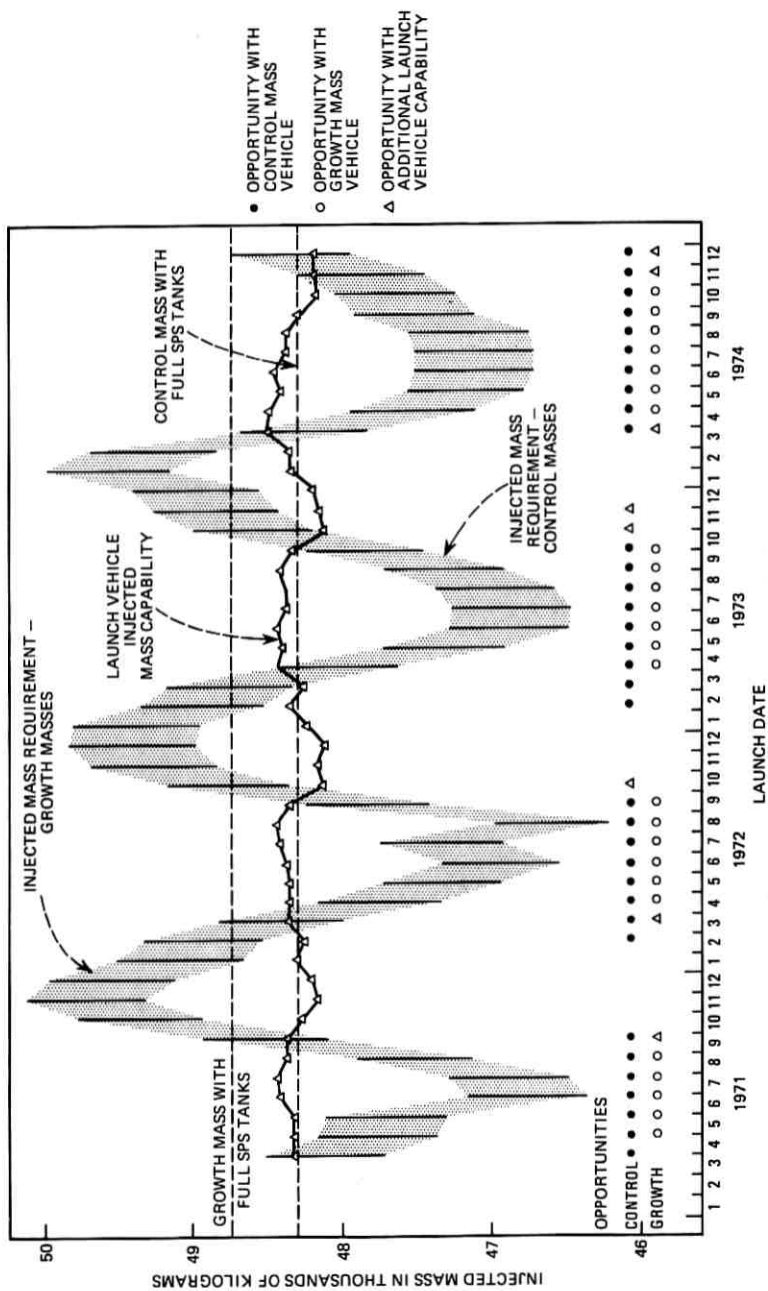
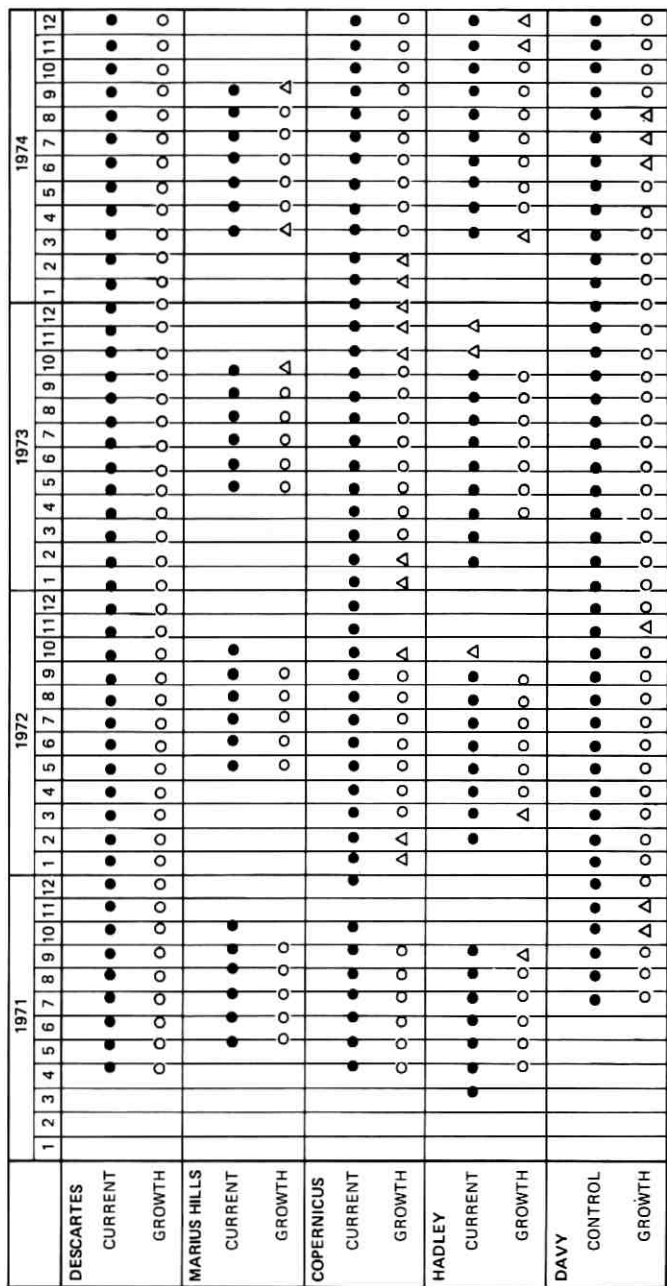


Fig. 25—J-mission opportunities to Hadley (Pacific injection).



● OPPORTUNITY WITH CONTROL MASS VEHICLE

○ OPPORTUNITY WITH GROWTH MASS VEHICLE

△ OPPORTUNITY WITH ADDITIONAL LAUNCH VEHICLE CAPABILITY

Fig. 26—Summary of J-mission opportunities.

maximize the contingency ΔV available. Similar accessibility studies for various lunar sites are described in Refs. 20 and 21.

The injected mass shown in Fig. 25 for a specific opportunity was derived by first determining the propellant required to accomplish the required propulsive maneuvers with a particular spacecraft mass model subject to all mission requirements. The two mass models considered corresponded to a control mass spacecraft at that time and a heavier model which allowed for possible growth beyond the identified limits. The required propellant was added to the inert mass of the CSM, the LM total mass, and the spacecraft-LM adapter mass to arrive at the injected mass requirement. If the SPS propellant required exceeded the tank capacity of the Service Module, the mission was not feasible. In addition, if the required injected mass exceeded the launch vehicle capability for that opportunity, the mission was not feasible. The determination of launch vehicle capability is described in Section 3.2.3. Briefly stated, launch vehicle capability represented the mass that could be injected by the launch vehicle within a specified high probability of success.

The injected mass in Fig. 25 provides comparisons among launch vehicle capabilities and maximum spacecraft masses at injection with full SPS propellant tanks. Two spacecraft limits are shown, one for each mass model with full SPS propellant tanks. The vertical bars indicate the range of injected mass requirements for both mass models, the lower value corresponding to the control mass model, the upper for the growth mass model. The shaded areas are shown in order to emphasize the time dependence of the performance requirements. The circles and triangles at the bottom of Fig. 25 denote the existence of launch opportunities based on the data plotted in the figure. In some cases, acceptable opportunities are shown for months that require propellant exceeding the tank capacity of the vehicle. In these cases, an early return to Earth from lunar orbit in the event of a LM rescue was investigated and found to result in a feasible mission where it was not feasible otherwise. The opportunities designated by a small triangle indicate that a mission could be flown if additional launch vehicle capability were made available, possibly by limiting the allowable launch azimuth range. It should be noted that significant increases in launch vehicle performance took place after the generation of the data described here. This led to a situation in which site accessibility was usually determined by SPS limits rather than by launch vehicle capability. A summary of mission opportunities for various sites is presented in Fig. 26. This type of chart was extremely useful in the site selection

process, reflecting as it did the net accessibility of specific sites and the sensitivity to changes in performance (mass).

Once a candidate lunar site was found to be accessible, it was desirable to consider the mission flexibility available for that site. This included a determination of the time available for CSM science after LM rendezvous and the determination of feasible shorter mission durations utilizing faster transearth return times. Another consideration arose from the adoption of the multiple launch day strategy for the J-series missions. For this strategy, a common LM approach azimuth was desired for all launch opportunities during the given time frame (three-month launch period) in order to simplify mission planning and crew training procedures.

The selection of approach azimuth and Sun elevation to satisfy the mission requirements and enhance mission flexibility could be accomplished in several ways. As a first step, the SPS propellant reserve available for contingency purposes was maximized with respect to these parameters for each launch date considered.²² Often, however, it was found that the selection of a common approach azimuth and Sun elevation angle at landing, to satisfy mission preferences, involved tradeoffs of SPS performance. Therefore, SPS performance scans with respect to approach azimuth, as described in Refs. 23 and 24, were often useful. A more comprehensive approach to this problem was described in Ref. 25, where contours of available end-of-mission ΔV (for weather avoidance) and LM rescue ΔV were presented as functions of approach azimuth and Sun elevation for several values of CSM science and total mission duration. A sample contour of end-of-mission ΔV reserve is presented in Fig. 27. Similar contours existed for LM rescue ΔV . This form of presentation essentially indicated the SPS propellant available over and above that required for the nominal mission. Those areas within which the end-of-mission reserve was greater than the required allotment, as derived in Section 3.2.2.2, corresponded to the values of approach azimuth and Sun elevation for which the mission was feasible. Therefore, with the ΔV reserve data in contour form, feasible ranges of Sun elevation angle could be found, potentially difficult or infeasible missions could be identified, and the necessary tradeoffs in the selection of a common approach azimuth became evident.

The highest Sun elevation that could be achieved for a given launch date was, in many cases, determined by the descent propulsion system abort requirement. This limitation was identified in the contour and provided for a safe Earth entry to an unspecified landing area.

3.2.5.2 Time-Specific Accessibility. When broad areas of the Moon

were under consideration for selecting landing sites, time-specific accessibility studies were usually performed. Given a specific launch opportunity, the surface of the Moon accessible for that opportunity was determined. The opportunity could be limited to a day, a month, or longer.²⁶⁻³¹ The accessible region defined for a monthly opportunity, where the Sun elevation at landing was limited to a specific range such as 5 to 25 degrees, was found to be particularly useful.

The accessible regions were determined by examining the possible trajectory configurations in a manner that allowed an orderly imposition of the mission design constraints.* The post-pericyinthian abort constraint was imposed first, since it limited only the translunar flight geometry. The desired time of arrival at the Moon set the energy of the translunar trajectory for a given launch day. The family of incoming trajectories to the Moon possible with this energy was examined to define the subset that met the descent propulsion system post-pericyinthian abort constraint. Each trajectory of the abortable subset was propagated through lunar orbit insertion, selecting those extremals in yaw angle (plane change) at lunar orbit insertion which allowed a lunar landing at least at one site under the lunar orbit and which resulted in the use of all the SPS propellant available for the lunar orbit insertion and transearth injection maneuvers. These two yaw angle extremals generally defined two points on the lunar surface where landing was possible such that the subsequent ascent and rendezvous required no plane change. Yaw angles between these extremals resulted in lunar orbits under which additional accessible sites lay, since part of the propellant used for lunar orbit insertion at an extremal yaw angle was now available for CSM plane change prior to rendezvous. Scanning through all yaw angles between the extremals and computing the allowable plane changes generated an accessible region. Superimposing the areas obtained from each abortable approach trajectory defined the region of the lunar surface which was accessible for a given arrival time and launch day. A rising Sun with an elevation between 5 and 25 degrees illuminated a portion of the front side of the Moon between 60 degrees west and 60 degrees east during only about one-third of a month. This period of acceptable lighting was broken up into specific arrival times, usually hours apart, and the accessible region determined for each of these arrival times. Superimposing those portions of each arrival time

* Although various parameters are treated as if they were independent variables, it should be recognized that they were always constrained implicitly to allow satisfactory completion of the transearth trajectory in a near optimum sense. Some ingenious computer programs were developed to handle this complexity and to permit efficient consideration of broader questions.

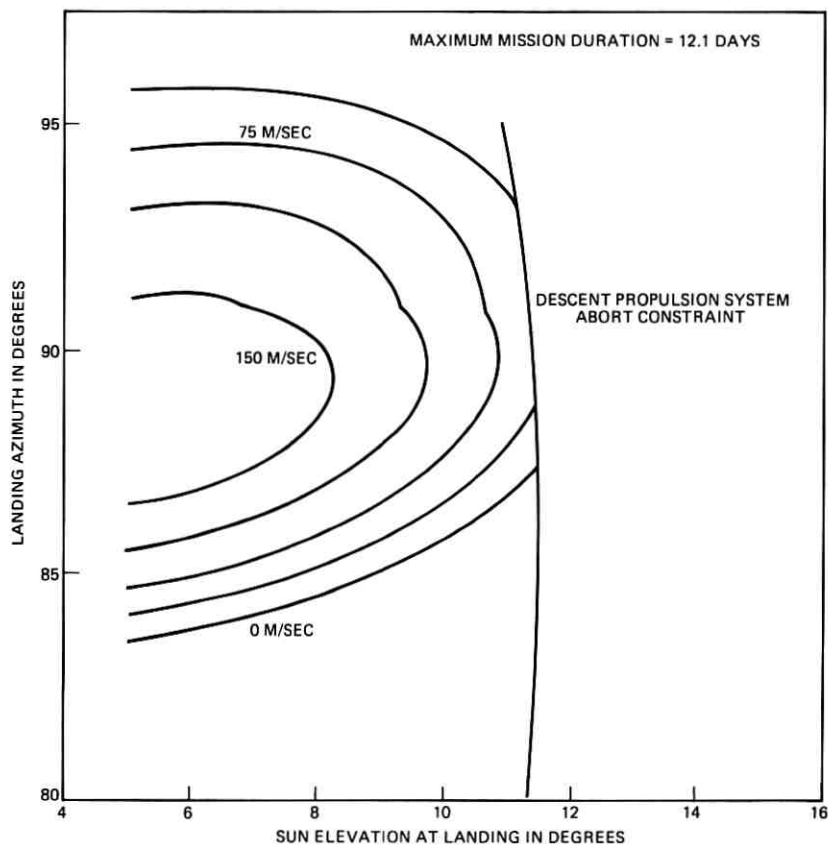


Fig. 27—End-of-mission ΔV reserve (Descartes—March 17, 1972).

accessible region, where the Sun elevation was within the desired range, defined the total accessible area that was feasible during the month.

Figure 28 shows typical accessible regions for four arrival times spaced about 4 hours apart, along with the portion of each region where the lighting was between 5 and 20 degrees elevation. The union of these subregions was the area accessible throughout this particular 16-hour period. Using the same method, the accessibility for March of 1972 with a Sun elevation at landing between 5 and 25 degrees was generated (Fig. 29). An alternative presentation indicates the launch days associated with each point of the accessible region (Fig. 30).

Figure 31 illustrates one way in which this information was used in site selection. Here the data were pointed toward site selection for

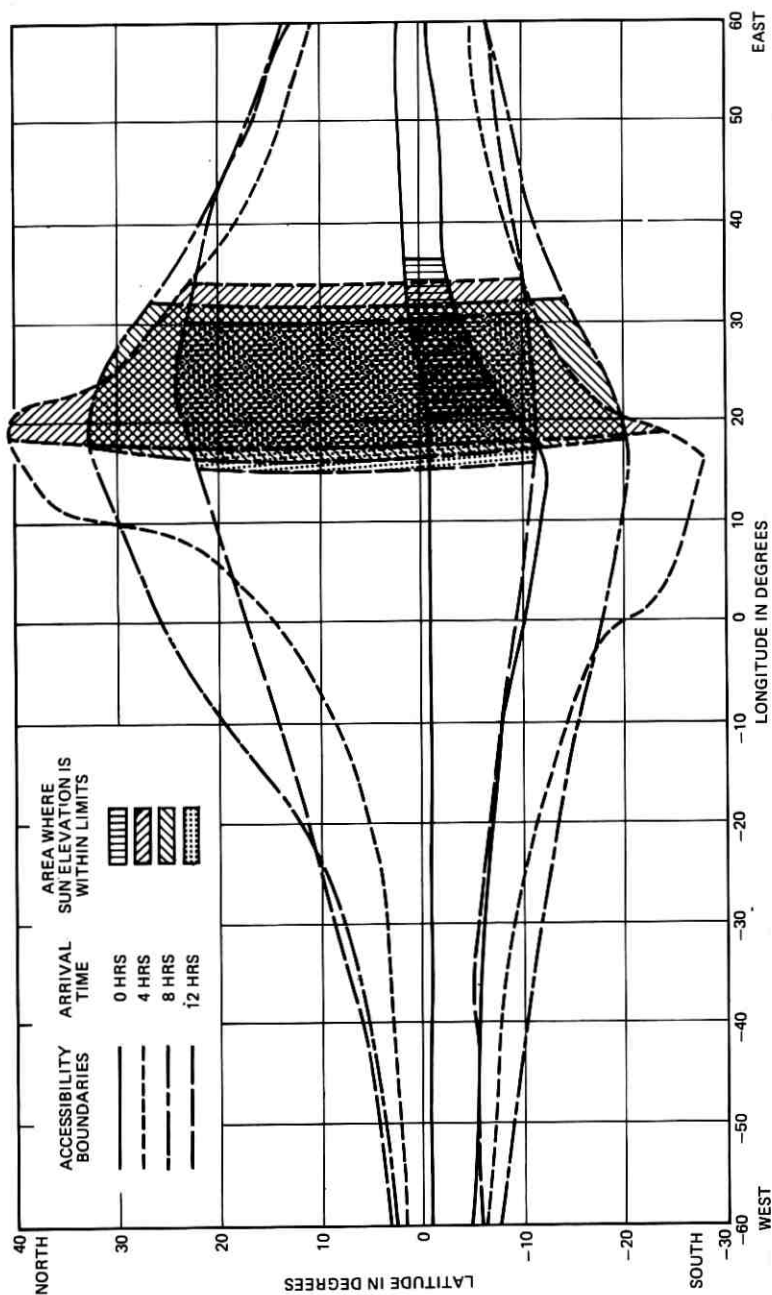


Fig. 28—Typical accessible regions.

Apollo 17. The accessible region for a December 1972 launch with a Pacific injection was compared with the locations of some of the sites under consideration. Also indicated is how the accessible region shifted when Atlantic injection was used. The overlap between photographic coverage from Apollo 15 and the accessible region for Apollo 17 indicated where additional candidate sites might be located.

3.3 Lunar Module Descent Considerations

The process of selecting Apollo landing sites has been described as evolving from the selection of a very large, smooth area for maximum landing safety to the selection of scientifically more interesting individual sites that required the landing to be more precise. The LM descent trajectory will be discussed in terms of the basic constraints which shaped the trajectory, and the restrictions placed on the selection of

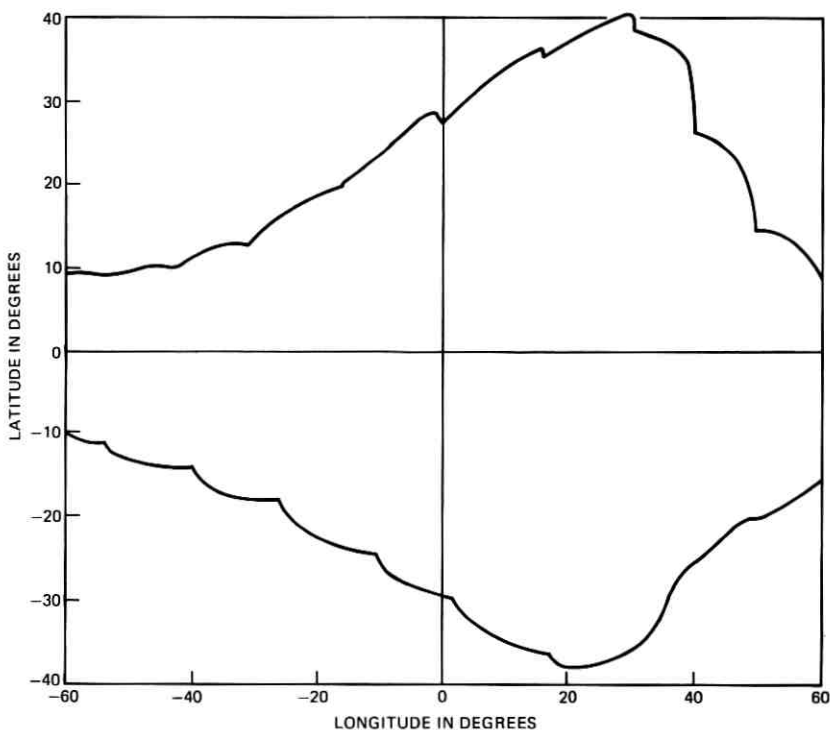


Fig. 29—Lunar surface accessible in March 1972.

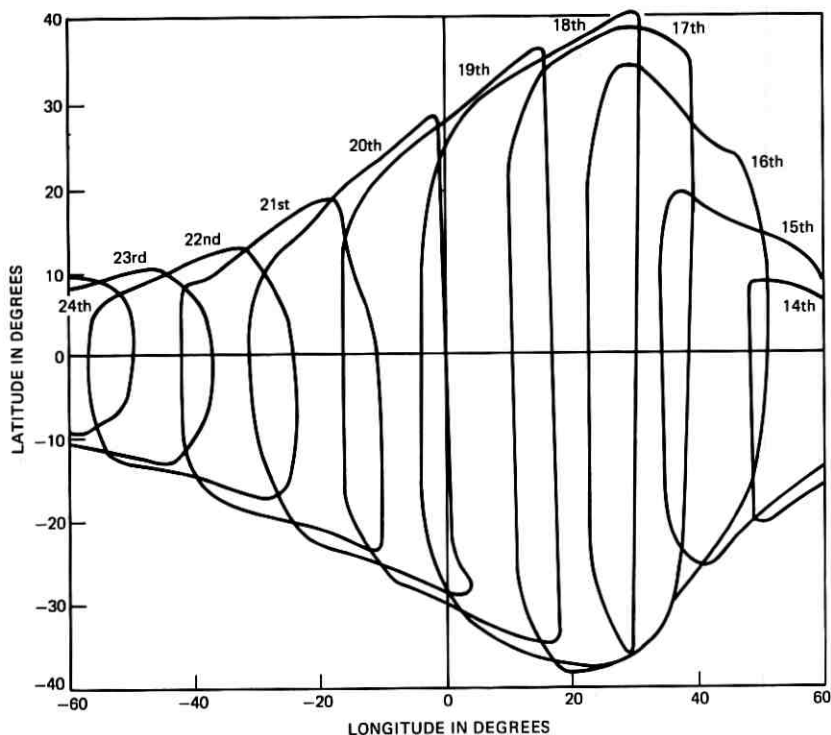


Fig. 30—Accessible area by launch date in March 1972.

sites by the LM descent trajectory. The descent guidance equations and certain aspects of the LM hardware are discussed in Appendix B.

3.3.1 Basic Shaping and Constraints

With the decision to design for the lunar orbit rendezvous type mission, the role of the Lunar Module became clear: it was to deliver the Commander and the Lunar Module Pilot from lunar orbit to the lunar surface safely and accurately with maximum scientific payload. After the stay on the lunar surface, the LM was to lift the crew and the lunar samples (and other returnable payload) into lunar orbit for the rendezvous with the CSM.

Figure 32 shows the basic shape of the LM descent trajectory, the characteristics of which depended on a number of factors. For optimum use of LM descent stage propellants, the CSM placed the LM in an orbit which passed over the chosen landing site at the expected time of

landing. This permitted the LM to descend in its orbit plane to the landing site. The powered descent initiation altitude was chosen to provide sufficient lunar terrain clearance while the LM was still in lunar orbit, before powered descent initiation. Since lunar terrain features 6 to 9 kilometers in altitude exist, and since guidance and navigation errors could contribute dispersions in altitude as well as horizontal position, a conservative nominal powered descent initiation altitude of 15 kilometers (relative to the lunar radius at the landing site) was used. This altitude also assured that the highest lunar terrain would be cleared during the early phases of powered descent.

The proper range to the landing site at ignition was determined primarily by the thrust-to-mass ratio of the vehicle. With an initial

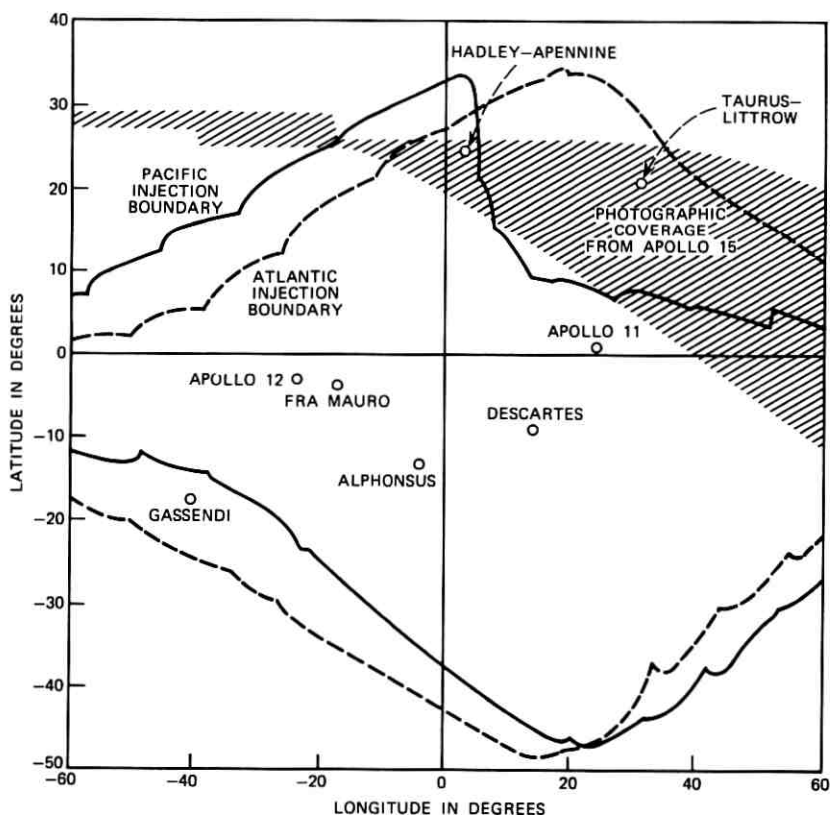


Fig. 31—Lunar surface accessible in December 1972.

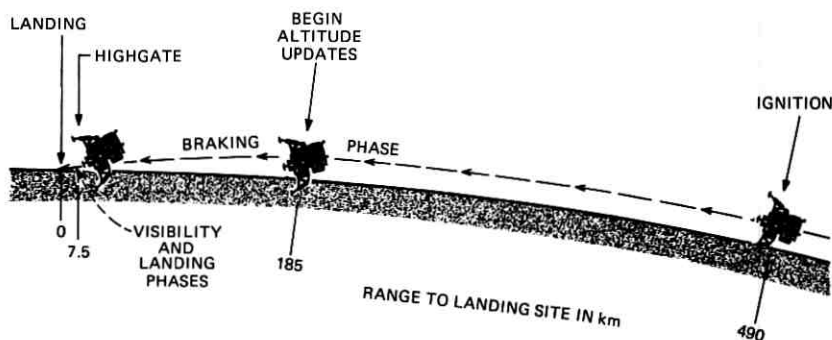


Fig. 32—The LM descent trajectory.

mass of about 15,000 kilograms, a maximum thrust of about 43,800 newtons, and an initial velocity of about 1690 meters/second relative to the surface, powered descent initiation was placed about 480 kilometers uprange of the site.

The propellant optimum trajectory from powered descent initiation to touchdown would have used the throttleable descent engine at full thrust for the entire descent. This would have involved a ΔV expenditure of slightly over 1770 meters/second, some 240 meters/second less than that required for the actual descent. The primary factor which compromised the optimum trajectory was the requirement to give the crew the ability to view the landing region and, if necessary, redirect the LM to another landing site up to several thousand meters from the original site. This redirection of the LM to a new site was termed landing site redesignation. In order to achieve an efficient trajectory, yet one which provided visibility of the surface and site redesignation capability, a three-phase trajectory was designed. It consisted of a braking phase, a visibility phase, and a landing phase as shown in Fig. 32.

The braking phase was designed to efficiently decelerate the LM from orbital velocity to about 150 meters/second. The braking phase carried the LM from the 15-kilometer powered descent initiation altitude, at a range of 480 kilometers, to an altitude of about 2300 meters, approximately 7.6 kilometers from the site.

During the visibility phase, the LM decelerated to near-zero velocity; however, the vehicle attitude during this phase was such that the crew could see and assess the landing area through the LM forward window and redesignate the landing site if desired. For Apollo missions 11 through 14, the elevation angle of the LM relative to the local horizontal plane at the landing site during the visibility phase was about 16 degrees.

For a given amount of visibility time, steeper descents tended to use more propellant, while shallower descents provided less terrain clearance. The 16-degree trajectory was chosen as a compromise between these two effects. Figure 33 shows the visibility phase of the trajectory used on the Apollo 14 mission.

Even though the basic 16-degree glide slope angle remained fixed for Apollo missions 11 through 14, the trajectory was continually modified as experience accumulated and as different landing sites were chosen for the missions. For Apollo 11, the visibility phase was designed so as to cause the LM to descend to the surface rather slowly. This intentionally slow trajectory was chosen because of the many unknowns involved in the first lunar landing. A study³² carried out just before Apollo 11 showed that a slightly more rapid descent could be made in order to save propellant and to allow more efficient redesignation of the landing site during the visibility phase. With the experience gained on Apollo 11, it was decided that the Apollo 12 mission was appropriate for such a descent. The aborted Apollo 13 mission and the Apollo 14 mission were targeted to the Fra Mauro region where the terrain uprange of the landing site had elevations several hundred meters higher than that of the landing site. For this reason, the latter portions of the visibility phase were steepened to give better terrain clearance.

Studies and simulations at the Manned Spacecraft Center, the Massachusetts Institute of Technology, and Bellcomm during 1970 showed that visibility phase elevation angles above 16 degrees offered several advantages over the shallower trajectories used on earlier missions. The steeper descents provided increased terrain clearance during descent and thus gave added flexibility in selecting landing sites

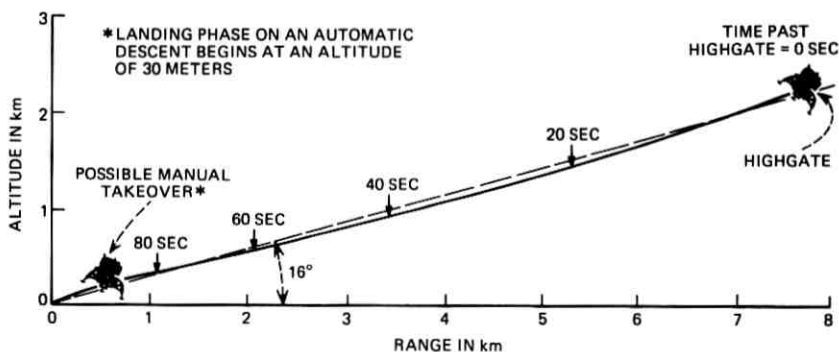


Fig. 33—The visibility and landing phases.

in rough areas. The more nearly vertical view of the landing area afforded by the steeper descent was also preferred by the flight crews. However, in order to minimize the increase in propellant required for landing with these steeper trajectories, it was necessary to decrease the amount of time that the landing site was visible to the crew during descent.

Computer studies^{33,34} considered the many tradeoffs involving visibility time, viewing conditions, propellant cost, and landing site redesignations. After many such studies at the Manned Spacecraft Center and various NASA contractors, and after many flight simulations at the Manned Spacecraft Center and the Grumman Aerospace Corporation, it was concluded that the additional terrain clearance and better view of the landing site outweighed the decrease in visibility time, and a descent trajectory with an elevation angle of 25 degrees was chosen.

The landing phase during any of the Apollo descents could consist of an automatically controlled or a manually controlled touchdown. The onboard computer was capable of landing the LM automatically (the crew only had to shut down the descent engine at the time of touchdown). However, the crews normally took over manual control of the LM at an altitude between 90 and 150 meters to select a specific touchdown spot free of rocks and small craters.

A final consideration in designing the descent trajectory was the requirement for abortability; that is, the LM had to be capable of achieving a safe orbit from any point on the descent trajectory. This abortability constraint meant that the vertical velocity of the LM at a given altitude had to be less than a limiting value in order to insure that the ascent engine could arrest the LM's descent before lunar impact if the descent engine failed.

3.3.2 *Navigation*

Navigation involved the determination of where the space vehicle was at a given instant and the prediction of where it would be at some later time. As mentioned previously, navigation directly influenced the choice of powered descent initiation altitude. It also influenced the choice of a landing site, since good navigation gave high confidence that the LM would be able to land quite close to the desired site, avoiding rough or uninteresting terrain, and making possible preplanned traverses on the lunar surface. If navigation were poor, it would have been necessary to select a site surrounded by large, smooth areas.

Data from Earth-based Doppler radar stations were used for the

estimation and prediction of the CSM and LM state (position and velocity) vectors in lunar orbit. Lunar orbit navigation is dealt with in more detail in Appendix C.

The state vector estimate of the LM one orbit before powered descent initiation was propagated forward to determine the powered descent initiation ignition point. Except for a downrange (along the trajectory) position update 2 minutes after powered descent initiation, LM navigation during descent was done using onboard sensors.

Any crossrange navigation errors which existed at powered descent initiation and any downrange errors which existed after the position update shortly after powered descent initiation resulted in a position error at touchdown unless the crew redesignated the landing site, based on visual observations of surface features.

Navigation errors in LM altitude existed at powered descent initiation, but were largely removed before the landing phase in order to eliminate the possibility of a lunar impact or a much longer than normal descent to the surface in the landing phase. Altitude and velocity navigation was done using an onboard radar array which measured the altitude and three velocity components of the LM relative to the surface. These data were used by the onboard computer from an altitude of about 12,000 meters on down to touchdown.

One of the problems associated with the use of landing radar data was that it measured the altitude of the LM relative to the local terrain, not relative to the landing site. As the LM flew over lunar hills and valleys, this could be interpreted by the computer as an undesired change in LM altitude. Since the LM steering commands were based on the LM's estimated position relative to the estimated position of the landing site, and since the terrain under the LM was assumed to be at the same altitude as the site, terrain variations could result in undesirable guidance perturbations from the nominal trajectory. Thus, it was helpful to have premission knowledge of the approach terrain, both to predict terrain clearance and to estimate the effect of the terrain on the descent trajectory. As mission complexity increased, so did that of the approach terrains, until it became necessary to introduce terrain models into the guidance computer in order to mitigate this problem. By including a premission estimate of the elevation of the approach terrain in the guidance logic, it was possible to reduce the perturbing effects of the terrain on the trajectory. On Apollo 14, the onboard computer used a simple five-straight-line-segment approximation of the approach terrain for the first time.

3.3.3 *Landing Site Redesignation*

As previously mentioned, the LM guidance system could land the LM on the Moon completely automatically. However, on the Apollo landings, the crew's ability to assess the landing area and redesignate the landing site was used to increase the chances for a safe and accurate landing. As discussed earlier, considerable effort went into determining the optimum lighting conditions at the time of LM descent (see Section 3.2.2.1 and Appendix A).

Essential to the process of assessing the landing area and redesignating the landing site was a method of informing the crew where on the lunar surface the automatic system was guiding the LM. The LM computer produced an estimate of its position relative to the landing site. This estimate was used to determine where the line-of-sight to the site should be. The display panel for the onboard computer gave this information to the crew, and the Commander looked through the prescribed spot on the specially scribed LM window to the appropriate spot on the lunar surface. Figure 34 shows a typical view from the LM window during the visibility phase. If the automatically targeted landing site was not acceptable, the Commander actuated his hand controller to redesignate

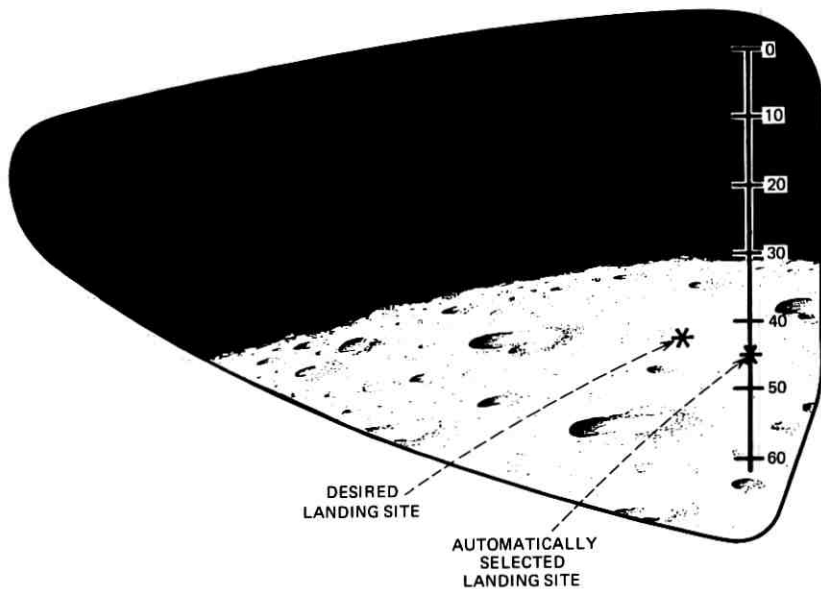


Fig. 34—View from the Commander's window.

the landing site in discrete increments in the uprange-downrange or crossrange direction.

The computer estimate of the landing site location was determined using current estimates of altitude, range, and attitude, and the calculation assumed that the terrain had constant altitude to the site. If the site elevation differed from the elevation of the terrain measured by the landing radar, then the apparent site was not precisely where the LM would eventually land (without manual intervention); thus, rough terrain complicated the crew's task of assessing whether or not the LM was approaching the desired landing site.*

If necessary, the process of assessment and redesignation could continue from the beginning of the visibility phase down to an altitude of about 90 meters, at which point the site was no longer visible in the window. Uprange redesignations saved descent propellant by shortening the time required to reach the site, but downrange and crossrange redesignations increased propellant consumption. Figure 35 shows contours of constant ΔV cost for landing site redesignations away from the automatically targeted landing site, with the redesignation being made at an altitude of 1200 meters. As the LM approached the landing site, the cost in propellant of moving the landing site a given distance increased, so the crews were trained to redesignate as soon as possible after the beginning of the visibility phase. The descent was designed with a propellant allotment for site redesignations. However, each kilogram of propellant allotted for redesignation reduced the potential payload capacity of the LM by about 2 kilograms.

Redesignation could cause the LM to undergo large attitude transients as the thrust vector was reoriented to guide to the new touchdown spot. This made further assessment of the landing site more difficult. Figure 35 also shows contours of maximum bank angle changes resulting from crossrange redesignations.

Final selection of a touchdown spot was made during the landing phase. Because of the low velocities during this portion of the trajectory, large relocations of the touchdown spot required relatively long maneuver times and were, therefore, quite inefficient in terms of propellant use. Thus, early and continuous use of the site redesignation capability was advantageous in removing large errors early and progressing toward the desired touchdown spot by successive stages of assessment and correction.

* The terrain approximation added to the onboard computer on Apollo 14 eased this problem, but did not entirely eliminate it.

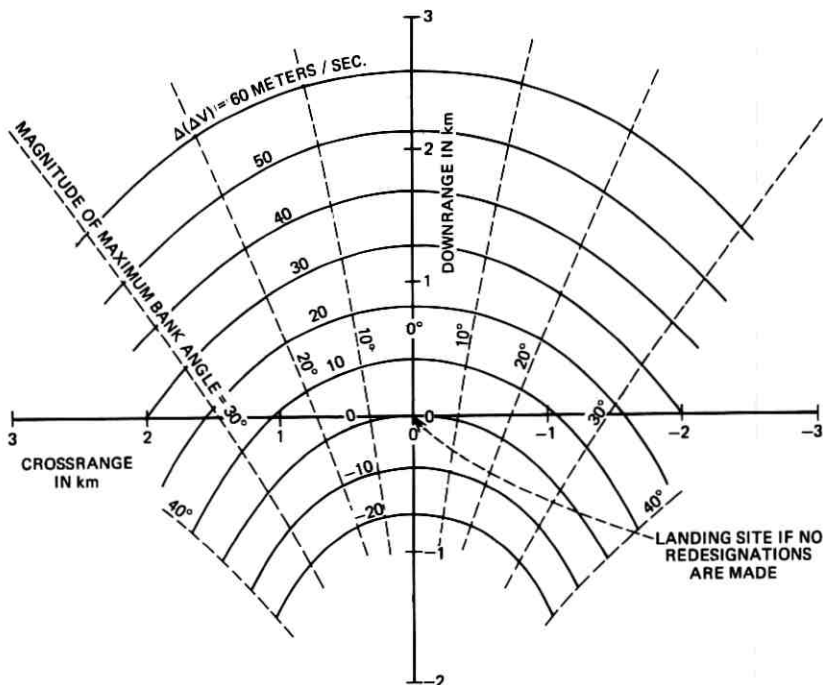


Fig. 35—Contours of constant ΔV penalty for landing site redesignations (LM altitude = 1200 meters).

In summary, the process of landing at or near a preselected landing site on the Moon consisted of:

- (i) Accurate navigation to the powered descent initiation point and throughout the descent.
- (ii) Redesignation of the landing site if necessary to avoid an unacceptable landing area (either too rough or not the preselected site).
- (iii) Final selection of the actual touchdown spot by manually maneuvering the LM during the landing phase.

3.3.4 Landability

A landing site with a wide variety of features was attractive from a scientific standpoint. Such surface features as craters, ridges, rilles, and scarps made a site scientifically interesting, but these very features also made landing more difficult.

In selecting a site, an analysis of the site's landability was made. That is, the descent trajectory was analyzed for its ability to clear the approach terrain, and the area around the landing site was studied in terms of its ability to provide suitable primary and secondary touchdown spots.

In choosing Apollo landing sites, one of the major factors used in judging the acceptability of a site was the ratio (called the site "n" number) of landable area to the total area within a 1-kilometer radius circle around the landing site.

One of the major issues in calculating "n" numbers was the definition of landable and unlandable terrain. A number of experimental and theoretical studies were carried out to determine the touchdown stability boundaries of the LM. Since the LM could land with forward, lateral, and vertical velocities as well as angular velocities about all axes; since the vehicle attitude at touchdown was not entirely predictable; since the four LM legs could be compressed inelastically; and since the lunar surface soil characteristics were not entirely predictable, much analysis was required to determine a maximum acceptable surface slope. Although the LM is statically stable on slopes somewhat greater than 45 degrees, a maximum surface slope of 7 degrees was used for premission site selection purposes because of the variability of touchdown conditions. Thus, certain areas within the 1-kilometer circle were rejected on the basis of slope. Areas which were presumed rocky, such as crater floors, were also rejected because of the possibility of damage to the lower portion of the LM.

The primary goal on Apollo 11 was to achieve a lunar landing and return to Earth. Since this was the first lunar landing and any lunar samples would greatly increase our knowledge of the Moon, the site was selected on the basis of its smooth terrain ("n" number of 0.8, which is quite high) for several kilometers and its relatively smooth approach terrain.

3.3.5 *Evolution of LM Descent Requirements*

The Apollo 11 landing demonstrated the capability of landing safely on the Moon. Navigation accuracy was only fair, with the LM landing about 7 kilometers downrange and 2 kilometers crossrange of the targeted site, but the smooth mare provided a safe touchdown spot. On this mission, the powered descent initiation state vector (position and velocity) was based on navigation data from the orbit before powered descent initiation. By the Apollo 12 mission, additional procedures, described in Appendix C, were available for improved

downrange navigation accuracy. In addition, operational procedures were modified to reduce the propulsive perturbing forces on the CSM and LM in order to make orbit determination and prediction more accurate. On Apollo 12 it was decided to attempt a pinpoint landing at the site of Surveyor III, which landed in Oceanus Procellarum in 1967. From a landing standpoint this site was acceptable, since the approach terrain was relatively smooth and the site was in an essentially mare area having an "n" number of about 0.7. The revised navigation techniques were successful and the LM touched down about 200 meters northwest of the Surveyor spacecraft.

The Fra Mauro site was chosen for Apollo 13. With an "n" number of about 0.6 and somewhat higher and rougher approach terrain, navigation and landing requirements were more exacting, but the experience of Apollo 12 and the desire to reach the scientific features of the region were sufficient reasons to choose the site.

After the Apollo 13 mission was forced to abort, the same general Fra Mauro site was chosen for the Apollo 14 mission. However, in the time between Apollo 13 and Apollo 14, the visibility phase of the descent trajectory was steepened slightly. This steepening gave additional terrain clearance, which allowed the landing site to be moved closer to the ridge east of the site. This shortened the distance the crew had to traverse back to Cone Crater during their lunar exploration. The Apollo 14 landing was made within about 30 meters of the preselected landing site.

For Apollo 15, the Hadley-Apennine landing site was chosen. The steep (25 degree) descent trajectory, used for the first time on this mission, gave additional clearance over the 4000-meter-high mountain range east of the site. The Apollo 15 Lunar Module made a successful landing within 700 meters of the preselected landing site on the plain at Hadley. Here the limiting factor was the ability to recognize the exact location of the desired touchdown point, a problem that has not been previously mentioned. Unfortunately, smooth landing areas tend not to have distinctively marked points corresponding to desired touchdown spots.

Experience was gained mission by mission, and changes were made which allowed landings to be made at increasingly more difficult sites. This provided added flexibility in selecting scientifically interesting sites, and increased the total scientific return from the Apollo program.

IV. SUMMARY

A multitude of objectives, requirements, and constraints had to be taken into account in the process of selecting Apollo lunar landing sites.

Among the significant parameters identified as affecting the site selection process were lunar lighting, landing site approach terrain, landing site smoothness, science requirements and objectives, trajectory mechanics, navigation, mass and performance, safety, and scheduling. The site selection process was a very real systems engineering problem, standing as it did at the interface between the science and engineering interests of the Apollo program, and involving not only all the pertinent technical considerations, but also the realities of hardware and software development and production, the vagaries of the budget process (forcing the cancellation first of Apollo 20, and later of Apollo 18 and 19), the sometimes conflicting desires of the scientific community, the real-time mission successes and failures, and evolving mission priorities.

Early in the Apollo program, Bellcomm recognized the pivotal significance that site selection would have, and took a leading role in defining the scope of the problem and carried out independent analyses in problem areas related to site selection. Of crucial importance was the recognition that, for maximum scientific return from the Apollo program, it was necessary to develop the ability to go to *specific selected* sites on the later missions, as contrasted with the more general objective of the first landing mission, where a landing at any of several suitable sites was perfectly acceptable.

Site selection was more than just a necessary systems engineering problem; it was also an important program management mechanism which was useful for achieving program goals, particularly as it helped force the evolution of the system capability to achieve science objectives. Within this framework, the concept of lunar accessibility was a major management tool, as it focused the impact of the principal factors affecting site selection.

The site selection process itself evolved from mission to mission, as hardware, software, experience, knowledge, constraints, requirements, and objectives changed and matured. The progressive increase in mission capability and site complexity, along with the concerted data analyses, has enabled scientists to reach, in about four years, an understanding of lunar evolution and properties comparable in many respects to that which took hundreds of years to acquire for the Earth.

APPENDIX A

Lunar Lighting

A.1 *Introduction*

Those singular characteristics of lighting and vision on the Moon which constrained the design of lunar missions have been known, at

least in broad outline, since the time of the first telescopic observations of the Moon. The past decade has seen both the application of our general knowledge of the Moon's photometric behavior to the specific problems of lunar descent and an attempt to relax the constraints so imposed in order to broaden the lunar landing "window." The need to ensure good visibility during LM descent to the surface remained the biggest single factor in limiting the number of opportunities per month for landings at a given site on the Moon. This appendix discusses the photometric properties of the lunar surface, some of the psychophysics of human vision, and the way in which they were combined in attempts to predict the astronaut's ability to detect landmarks and landing hazards during the final portion of the descent to the lunar surface.

A.2 Photometric Quantities

Since the photometric variables are not usually encountered by workers in other branches of science and engineering, a short review of the basic quantities used in lunar photometry is appropriate.

Photometric quantities parallel those used in radiometry, the difference being that the basic unit, the luminous flux, expressed in lumens (lm), is a function of the radiant flux, weighted by the spectral response characteristics of the visual system. Although luminous flux is the logical starting point in defining the photometric units, the quantity actually defined directly in terms of a physical standard is the luminous intensity, I , which is the luminous flux per unit solid angle. The unit of intensity, the new candle or candela (cd), is defined as one sixtieth of the luminous intensity of one square centimeter of the surface of a black body at the temperature of freezing platinum (2042°K).

The two remaining photometric quantities of interest, illuminance and luminance, are confusingly similar in sound. However, illuminance (or illumination) is a measure of the amount of light striking an extended surface, while luminance is a measure of the amount of light leaving the surface in a particular direction; illuminance is the photometric analog of the radiometric term, irradiance, and luminance is the analog of radiance. Thus, if dF is the total luminous flux from whatever source or combination of sources falling on a surface element ds , then the illuminance, E , is given by

$$E = \frac{dF}{ds} \quad (1)$$

and is measured in lumens/meter².

Luminance is the intensity per unit area of an extended source, which

may be self-luminous or merely a reflecting surface. That is, if dS is a surface element of the source, θ is the angle between the surface normal and the observer's line of sight, and dI is the intensity of the source in a given direction, then the luminance of the surface element in the given direction will be

$$B = \frac{dI}{dS \cos \theta} = \frac{dI}{d\sigma}, \quad (2)$$

where

$$d\sigma = dS \cos \theta$$

is the projected area of the surface visible to the observer.

Algebraic manipulation results in an alternative and operationally more useful definition of luminance in terms of variables measurable at the observer's position:

$$B = \frac{dE_n}{d\omega} \quad (3)$$

Thus, the luminance of a source in a given direction is equal to the illuminance it produces normal to an elementary surface at the observer's position, dE_n , divided by the solid angle $d\omega$ subtended by the source as seen by the observer. The units for luminance in both definitions are candles/meter².

The luminance of a surface depends not only on how well it is illuminated, but also on the manner in which it reflects, transmits, and absorbs light, and generally also depends on the direction from which it is viewed. There is one very useful, if imaginary, surface which has the same luminance no matter what the viewing direction, called the lambert, or perfectly diffusing, surface. The luminance of a lambert surface under a given illumination is given by the expression

$$B_l \text{ (cd/area)} = \frac{R}{\pi} E \text{ (lm/area)}, \quad (4)$$

where B_l is the luminance of the surface, E is the illumination it receives, and R is the fraction of light reflected. If the lambert surface reflects all the light incident upon it ($R = 1$) then, for example, under an illuminance of one lumen/meter² it will have a luminance of $1/\pi$ candle/meter² in all directions. The lambert surface has no physical justification, but it does provide a reasonable approximation to the reflection characteristics of "diffuse" surfaces, especially for angles near the normal; and its mathematical simplicity makes it useful in many applications. The Moon, however, is far from being a lambert surface.

Luminance, like the other photometric quantities listed, is a mathematically defined function which can be calculated exactly. It is important to realize, however, that all these psychophysical quantities are only attempts to quantify psychological sensations which will vary from person to person and from time to time in a complicated fashion. This is especially true in the case of luminance. For convenience, luminance is often equated simply with the perceived brightness of an object, but, in reality, the brightness (a psychological sensation) depends not only on the luminance of the object observed (a psychophysical quantity), but on the luminance of the background as well. The experience of the Apollo 11 astronauts illustrates this fact very well. Neil Armstrong described the appearance of the lunar surface as seen from within the LM cabin as follows:

It's a peculiar thing, but the surface looked very warm and inviting. It looked as if it would be a nice place to take a sunbath . . . From the cockpit the surface seemed to be tan. It's hard to account for that, because later when I held this material in my hand, it wasn't tan at all. It was black, grey and so on.³⁵

Seen from within the comparatively dim cabin, the intensely illuminated surface appeared almost white, but when compared with the truly white Beta cloth covering of the space suit it was perceived as being very dark. The complex dependence of visual perception upon many variables was a major cause of uncertainty in lunar visibility predictions.

The key parameter employed in these visibility predictions was the luminance contrast, defined in standard fashion as

$$C = \frac{B_T - B_B}{B_B}, \quad (5)$$

where B_T is the target luminance and B_B is the luminance of its background. According to this formula, a star seen against a perfectly dark sky has an infinite contrast, while at the other extreme a perfectly black object has a contrast of -1 . Since it has been found that otherwise equivalent objects which differ only in the sign of their contrast are equally visible, the absolute value of the contrast is usually taken. On Earth, the color contrast of an object with its surroundings is, if anything, even more important than its luminance contrast for providing the necessary visual recognition cues. On the Moon, where everything appears a uniform shade of tan or grey depending on the direction of the

illumination, brightness differences are all-important in distinguishing one object from another.

A.3 Visual Psychophysics

An object's luminance contrast, while important, is not the only characteristic which influences its visibility. Prior to the Apollo program, a great deal of laboratory data on factors influencing human vision had been gathered which were later used to analyze the lunar lighting constraints. Only a brief discussion of the most pertinent of these experiments is included here; Ref. 36 should be consulted for additional data.

An extensive study of the variation of visibility with contrast, angular size, and background brightness was carried out at the Tiffany Foundation during World War II, and the results reported by Blackwell in Ref. 37 are often referred to as the Tiffany data. Other studies supplemented the Tiffany data, but it has remained the standard source for many later visibility studies. Two separate experiments comprised the Tiffany work, differing primarily in the observing technique. In the forced-choice approach, the observers were forced to choose among several possible areas in which the just-visible target might be shown; using the yes-no method, the observers were forced to make a yes-no judgment on the visibility of the target. Figure 36 shows the results of

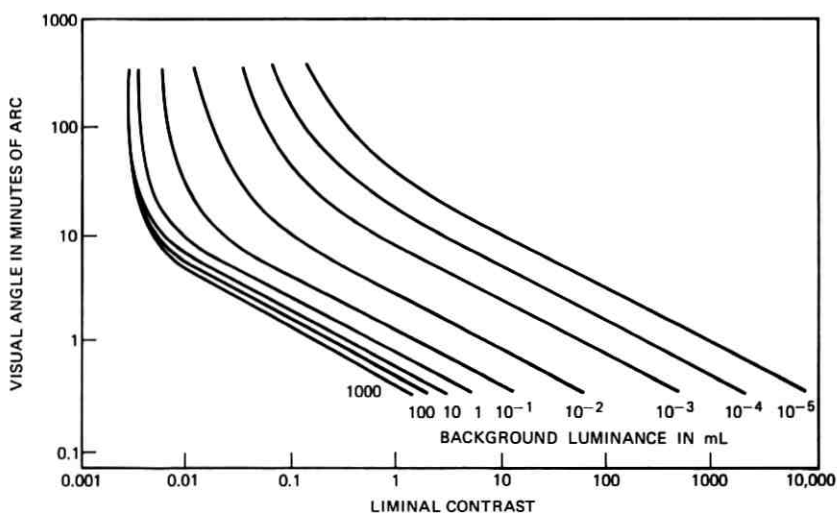


Fig. 36—Threshold visibility as a function of angular diameter and contrast with background luminance as parameter (from Tiffany data).

the 90,000 observations made with the yes-no method. Threshold visibility is plotted as a function of target contrast and angular subtense, with background luminance as the parameter. The curves indicate the visual threshold for a 50-percent probability of detection of a uniform circular target on a uniformly illuminated background.

Three important relationships can be seen in the figure: (i) the detection threshold is nearly independent of the background luminance over the range of light levels—ten to several hundred millilamberts—encountered in a lunar landing; (ii) the detectability of small target elements, those of about 5 minutes of arc and smaller, varies as the *product* of their contrast and angular area, i.e., as the contrast decreases, the size must increase to preserve the same detectability; and (iii) the detectability of large targets, on the order of a degree in diameter, is almost independent of target size; targets with a contrast less than about 0.003 cannot be detected regardless of their size.

Conditions during the lunar landings (as for any in-the-field situation) were generally quite different from the ideal laboratory environment exemplified by the Tiffany studies. Furthermore, the visual task was different and more taxing. Detection of a uniform target on a featureless background, where the time of occurrence and location are known and essentially unlimited viewing time is allowed, is the simplest visual task with the lowest threshold contrast. If less information is available about the target and a visual search is required, the threshold will be higher. If one is required not merely to *detect* the target, but also to *recognize* it or to abstract a pattern from a complex visual field, the threshold will be generally higher yet. Also, in a real-life task, a higher detection probability is desired than the 50-percent probability of the laboratory data. Further, the observer's detection strategy under field conditions will not be as efficient as that of the highly trained laboratory observer's.

All of these factors, as well as differences due to such variables as training, vigilance level, glare, acceleration, vibration, psychological pressures, and other special conditions must be allowed for in estimating visibility conditions in the field. One method of doing this is to simulate all the pertinent viewing conditions as exactly as possible in the laboratory. Unfortunately, sufficient fidelity in all the parameters is often difficult to achieve, especially in the simulation of a lunar landing. A more general, if less precise, method is to apply the basic visual performance data to the particular visual task through the use of so-called "field factors" which account for differences in the mode of data collection and the relative lack of knowledge of the field observer about the visual target's characteristics. The laboratory contrast value

is multiplied by the field factor to produce a final field threshold contrast value, which is then compared with the calculated or measured target contrast to predict the field performance capability. Both of these methods were followed in the various lunar visibility studies discussed below.

Table I, based on data from Refs. 38 and 39, presents field factors to be applied to the Tiffany data. For example, assume that a 1-meter-diameter target must be detected with a probability of 1.0 at a slant range of 1000 meters against a surface of 100 millilamberts background luminance. With an angular diameter of 3.5 arc minutes, the target has a threshold contrast from Fig. 36 of 0.019. If the untrained observer in the field has then to scan over a 4-degree field of view (a typical value), the threshold contrast for the target would become

$$2.0(p = 1.0) \times 2.0 \text{ (training)} \times 4.0 \text{ (4° field)} \times 0.019 = 0.3,$$

a 16-fold increase in threshold.

The approximate nature of such contrast calculations must be emphasized. There are several sources of uncertainty in the final threshold values. Individual variations from the forced-choice Tiffany data were found to be ± 12 percent in the original experiment, with occasional deviations of 40 percent. Variation from the yes-no data is expected to be somewhat greater. Definition of the significant components of the visual task (search strategy, size of visual field, salient

TABLE I—SOME FIELD FACTORS FOR VISIBILITY DATA

Visibility Data	Field Factor
<i>Probability Conversion</i>	
From $P = 0.5$ to 0.90	1.50
0.99	1.91
1.00	~2.50 (forced choice)
1.00	2.00 (yes-no)
<i>Knowledge of Target Properties</i>	
Time of occurrence unknown	1.40
Time and duration unknown	1.60
Time and size unknown	1.50
Time, size, and duration unknown	1.45
Location (± 4 degrees or more) unknown	1.31
<i>Other Conditions</i>	
Lack of visibility training	2.00
Vigilance	1.19
Forced choice to yes-no	1.20
4-degree visual field	4.00

target characteristics, etc.) is difficult. The corresponding field factors (except the probability correction), in the absence of knowledge derived from exact simulations, may be in error by a factor of two or more, with a general tendency to be conservative. Nor is it clear to what extent it is allowable to concatenate field factors, as was done in the example given above. The effects of some aspects of the visual task, such as fixation time, target shape, edge gradient, and background nonuniformities, do not lend themselves to the field factor approach and must generally be introduced separately where appropriate. Uncertainty in the lunar surface luminance values, discussed below, further complicates the analysis.

A.4 Lunar Photometry

On Earth, natural objects possess either specular or reasonably diffusely reflecting surfaces, and contrast values can be easily calculated. On the Moon, however, there is no evidence of any specular surface, and two simple naked-eye observations demonstrate at once that the lunar surface cannot be a diffuse reflector. First, all, or almost all, features on the lunar surface reach their maximum brightness at full Moon, and second, there is no evidence of limb-darkening. If the lunar surface were lambertian, the brightness at any point on the full lunar disk would vary as the cosine of its angular distance from the center; that is,

$$B = \frac{\rho_n}{\pi} E_n \cos i, \quad (6)$$

where B is the surface luminance and ρ_n is the normal albedo, defined as the brightness of a surface element viewed and illuminated normally relative to a perfectly reflecting lambert surface with the same orientation. E_n is the normal solar illumination at the lunar surface, and i is the angle of incidence, which at full Moon is (approximately) equal to 0 degrees at the center of the disk and 90 degrees at the limb. As the limb is clearly not dark, the variation of lunar brightness must be described by a more complicated photometric function than the cosine law.

In the general case, this photometric function, Φ , will be a function of three angles which serve to completely define the relative orientation in space of the Sun, the observer, and the surface normal: the angle of incidence i , the angle of emittance ϵ , and the phase angle g . Alternatively, instead of i and ϵ , the luminance longitude α and the luminance latitude β may be used. These angles are illustrated in Fig. 37. Angles i and ϵ

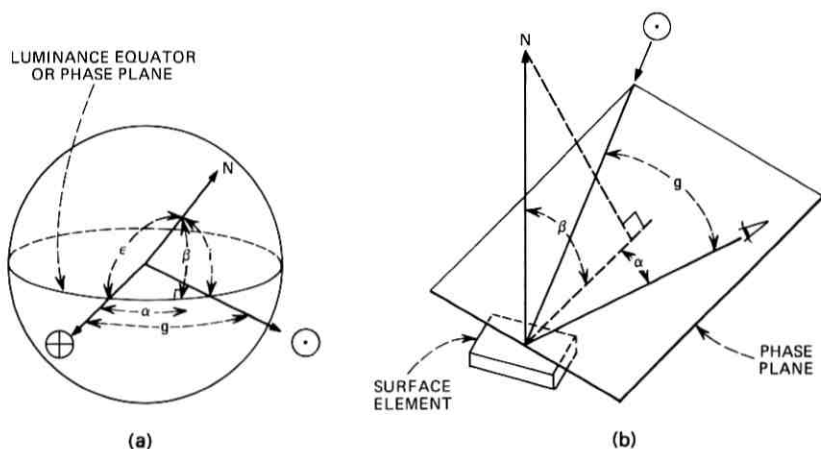


Fig. 37—Lunar photometric geometry: (a) as viewed from the Earth, and (b) as viewed on the lunar surface. Symbols: \odot , Sun; \oplus , Earth; \times , line of sight; g , phase angle; i , angle of incidence; N , surface normal; α , luminance longitude (negative toward normal in the Sun direction); ϵ , angle of emittance; β , luminance latitude.

are measured between the surface normal and the Sun line and between the surface normal and the observer's line of sight, respectively. The Sun and observer vectors define a plane called the phase plane. The luminance longitude is the angle between the projection of the surface normal in this plane and the line of sight to the observer. It varies between -90 and $+90$ degrees, the sign convention being such that the angle is positive when the line of sight is between the projected normal and the Sun. The luminance latitude is the angle of projection between the surface normal and the phase plane. Seen from the Earth, the phase plane is nearly parallel to the lunar equator, so that the selenographic latitude and longitude of a point are approximately equal to the luminance latitude and longitude; hence, the names.

Of greatest significance in lunar photometry is the angle in the phase plane between the Sun and the observer, which is called the phase angle (g). If the observer is on the Earth, the phase angle remains essentially constant over the entire lunar disk, not varying by more than half a degree. The phase angle derives its name from the lunar phases: from nearly 0 degrees at full Moon, it increases to nearly 180 degrees at new Moon. It becomes exactly 0 or 180 degrees only during a lunar or solar eclipse.

The first accurate measurements of the variation in lunar brightness

with phase angle were carried out by Rougier by means of photoelectric photometry in 1933. His curve for the integrated radiation of the Moon over the course of a lunation is reproduced in Fig. 38 (based on data from Ref. 40). Although this is an averaged curve over all portions of the visible sunlit hemisphere, detailed photometry shows that smaller areas exhibit a similar steep rise to a sharp maximum at zero phase. The value of the maximum, the albedo, varies from feature to feature. Maria generally possess an albedo of about 7 percent while the lunar highlands are somewhat brighter, with an albedo of 10 percent. These values are much lower than for most terrestrial substances—solid granite, for instance, has an albedo of 24 percent—and the variation between the darkest and lightest areas is much less.

The Moon, even at highest resolution, is remarkably uniform. It is almost neutral in color, only slightly reddening the incident sunlight. It polarizes the incident light to only a small extent. The surface exhibits one salient characteristic: everywhere it tends to reflect light back toward its source regardless of what the local surface slope may be.

This retroreflective property of the lunar surface is both global in character and unique in the sharpness of its maximum. Accordingly, it has inspired a great number of observational and theoretical studies on the part of astronomers interested in deciphering the structure and composition of the lunar surface material from the scattered radiation.

Two observational programs which deserve special mention in view of their importance to the American lunar space program are those of the Russian astronomers Fedorets, Sytinskaya, and Sharonov. In

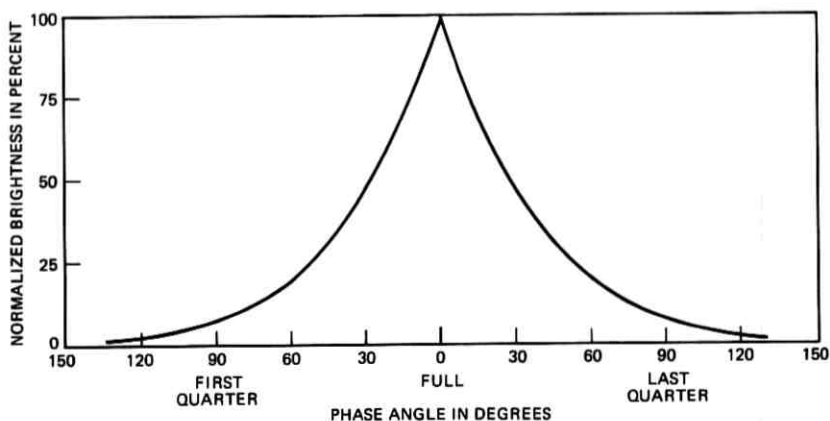


Fig. 38—Integrated lunar surface brightness, due to Rougier.

1948 to 1949, Fedorets photographed 172 lunar regions at 40 different phases and measured the relative brightness of the features as functions of i , ϵ , and g . By observing just before a lunar eclipse, she was able to obtain data for phase angles as low as 1.5 degrees. In 1962 Herriman, Washburn, and Willingham, at the Jet Propulsion Laboratory (JPL), handfit smooth curves to the Fedorets data for selected points in the lunar maria in order to produce a photometric function which was used in the Ranger program and afterwards.⁴¹ Due to the large scatter noticed in Fedorets' data and uncertainty in the assignment of absolute luminance values, another photometric function was developed at JPL in 1964 called the Lunar Reflectivity Model. It used as a data base observations of mare areas made by Sytinskaya and Sharonov in 1939 by means of direct visual photometry. Again large data scatter was evident, but the Lunar Reflectivity Model was felt to be a definite improvement over the Fedorets function.⁴² The two functions are shown in Figure 39. The vertical axis is the relative brightness, Φ , normalized so that at zero phase, Φ is equal to 1.0; the horizontal axis represents the luminance longitude α ; and the phase angle g is the parameter. In this figure, it was possible to represent Φ as a function of just two variables, g and α , since it was found that the lunar isophotes roughly follow the luminance meridians, so that the effect of varying β can be disregarded.

Several interesting properties of the photometric function can be seen. Note first that, for zero phase angle ($g = 0$), Φ is a constant. For a fixed phase angle, a difference in luminance longitude is equivalent to a difference in slope between the surface elements. At zero phase, the curve predicts that all surface elements of equal albedo will appear equally bright regardless of slope; slope contrast is zero, in accord with observations, resulting in what is called zero phase washout. Away from zero phase, contrast is proportional to the slope of the lines of constant phase in the photometric function; in the realm of negative α , contrast remains low even at large phase angles (especially as measured by the Lunar Reflectivity Model, while for positive α , it becomes large at phase angles only slightly greater than zero. As α increases, the contrast increases and the surface darkens, going to zero brightness when $g + \alpha$ (and angle of incidence i) equals 90 degrees.

Succeeding lunar photometric studies have corroborated the general form of the photometric function, although data scatter and a restricted variable range have precluded much improvement in detail. In order to gain insight into the physical processes responsible for the lunar photometric function, many attempts were made to match the observed

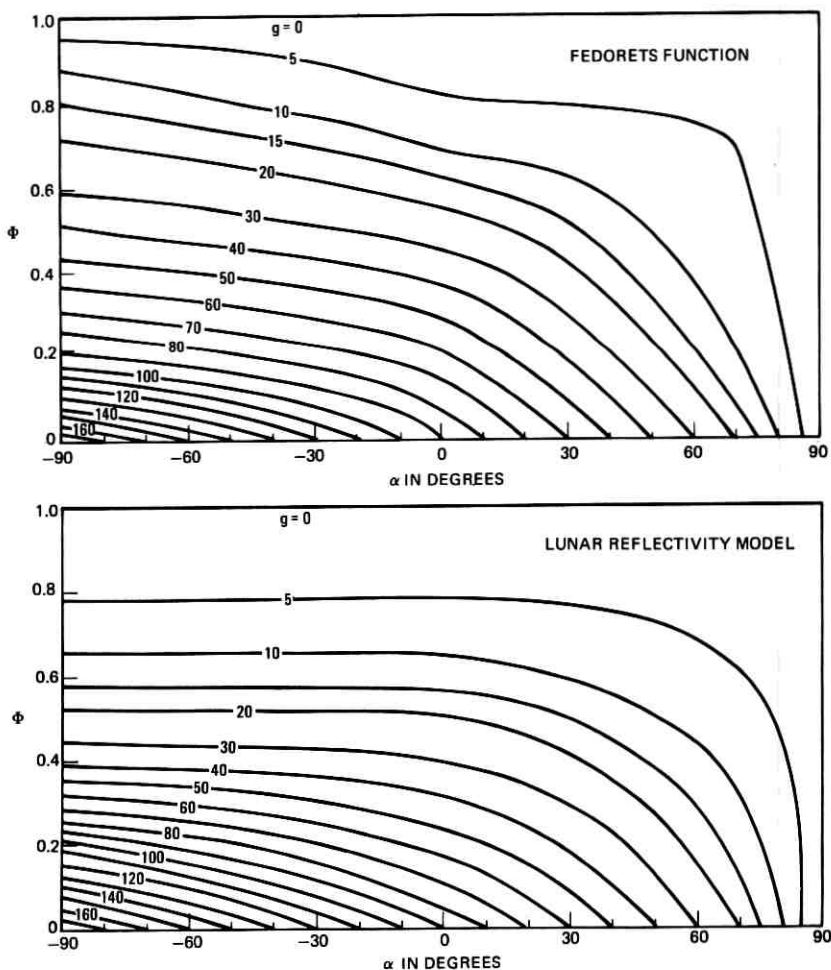


Fig. 39—Lunar photometric functions.

function using terrestrial substances or to construct simplified geometrical models with similar reflective properties. Extensive comparisons with terrestrial substances were carried out by van Diggelen⁴³ and Hapke and Van Horn.⁴⁴ Van Diggelen found that reindeer moss, with its intricately branching structure, best matched the lunar photometric function, while Hapke and Van Horn suggested that, on the lunar surface, finely pulverized rock dust could build up an elaborate, dendritic "fairy castle" structure, which would then retroreflect light in the

observed fashion. Hapke⁴⁵ developed the most successful analytical formula to simulate the lunar photometric function. In his model, each soil particle was assumed to be at the bottom of a tube which was aligned toward the light source; any light not reflected directly back toward the source was attenuated in the wall of the tube. By adjusting the model parameters, a good fit to the data could be had and some estimate of the surface properties could be derived. Although the Hapke function was not employed in visibility studies to the extent that the tabulated photometric functions were, it still remained of interest where an approximate analytical expression was desired.

The flight of Apollo 8 in December, 1968, offered the first opportunity to carry out a detailed photometric reduction at zero phase from the original film.⁴⁶ A sudden brightness surge for phase angles less than 5 degrees, which had been noted earlier by Gehrels in Earth-based observations,⁴⁷ was confirmed by densitometric analysis of the film, but was found to be less than expected. Apollo 8 was also the first opportunity for visual observations from lunar orbit. In general, the visibility from orbit was reported to be better than had been expected: there were many high albedo craters which could be distinguished even at zero phase and details could be seen in shadows due to reflected light from the surrounding bright areas. The rapid movement of zero phase along the surface resulting from the spacecraft's high orbital velocity permitted tracing details into the washout region which had first been detected outside it. The crew of Apollo 10 in May, 1969, confirmed the Apollo 8 observations, but noted during the descent of the Lunar Module to 15 kilometers altitude that the washout area was noticeably larger than in high orbit.⁴⁸ When Apollo 11 landed on the Moon on July 20, 1969, the optimum visibility conditions for the descent had been analyzed over the preceding six years in a series of studies combining both visual psychophysics and lunar photometry.

A.5 *Visibility Analyses*

At the beginning of the Apollo program, it seemed as if poor visibility conditions should hamper a landing on the Moon less than on the Earth; since without an atmosphere, there could be no clouds or haze to block vision of the surface. On the other hand, that same lack of atmosphere implied glaring sunlight, 30 percent higher than on Earth, and deep shadow; without the usual atmospheric haze, distance and size would be hard to judge on a crater-spattered landscape which offered no familiar objects with which to calibrate the eye. In addition, only a short time would be available in the descent trajectory for visually assessing

the landing area, and there would be no possibility of circling around and trying again should the first landing spot prove unsuitable.

The visibility phase of the descent trajectory began at highgate when the LM pitched up and the landing site came into view for the first time, and it ended at lowgate about 2 minutes later. During this period, the touchdown point could be seen at a constant but rather shallow angle, the viewing angle, which was about 16 degrees for Apollo missions 11 through 14 and about 25 degrees for Apollo 15 and after. Although the landing area remained visible even after lowgate until the LM began the final vertical descent, the most critical period was the initial few seconds of the visibility phase. At this time, the Commander had to orient himself by means of some large-scale features distinctive enough to act as landmarks and began evaluating the touchdown spot for smoothness and lack of landing hazards. If he had to redesignate to a different point a large distance away from his current target, he needed to do so as soon as possible in order to conserve propellant. Highgate occurred at about 2100 meters, but within 20 seconds the LM dropped below 1200 meters and the Commander's view of off-track landmarks was considerably restricted. One of his concurrent visual tasks, landmark recognition, had to be fairly well completed by this time. His other task, which might be called obstacle avoidance, continued during the descent as smaller and smaller details became visible. The Commander's ultimate goal was to pick an area at least 10 meters in diameter, level in slope, and free of boulders or craters large enough to tilt the LM to the point of instability.

The first lunar landing was planned for the relatively featureless mare; consequently, the initial emphasis in lighting analyses before Apollo 11 was in the detection of landing hazards rather than in landmark recognition. Later, with the requirement for a pinpoint landing in order to investigate specific geological objectives, landmarks were studied more intensively. To improve surface visibility, only one parameter, the elevation of the Sun from the horizon, was generally modifiable, since the viewing angle and the flight path azimuth were to some extent fixed by the trajectory and propellant budget. Near the lunar equator (at most of the Apollo sites), the Sun changes in elevation by about 13 degrees per day; any restriction on Sun elevation restricted the number of opportunities and the length of the landing window. The history of lunar visibility studies can be viewed as a gradual reduction in the allowable Sun elevation range for the first lunar landing mission, followed by a search for ways of expanding the landing window for later landings.

The initial restriction for a landing in sunlight was simply that the Sun be behind the LM in order to avoid the effects of glare. When the lunar photometric function was developed in 1963 by JPL for the Ranger program, it was applied to Orbiter and Apollo as well.⁴⁹ It was found that contrast at high Sun elevations was very poor, while at low Sun, shadows covered a large percentage of the surface so that visibility was again poor. In 1965, Sun elevation limits of 3 to 45 degrees were accepted, but because landmark tracking was required two revolutions (4 hours) before landing, when the Sun would be lower than at landing, and because the average surface slope was uncertain, a lower elevation limit of 7 degrees was set. The resulting range of 38 degrees permitted a landing window duration of three days to any specific landing site on the Moon.

Analyses performed early in the Apollo program showed that very few shadows are visible at high Sun elevations. The majority of craters are shadowless at Sun elevations above 20 degrees, and at 35 degrees, only the freshest of craters and boulders still possess any shadows. For any Sun elevation greater than the viewing angle, shadows directly down-Sun are hidden by the objects casting them, and some relative azimuth between the line of sight and the Sun direction is then necessary to bring the shadows into view. The loss of shadows, with their very high contrast of -1 , drastically reduces the visibility of landing hazards at high Sun elevations.

In 1965, Hamza and Radin⁵⁰ photographed a scale model of the lunar surface and compared its general appearance under varying lighting conditions with the photometric function. The model was dusted with cupric oxide, a substance whose photometric function closely matches that of the Moon. Difficulty in collimating the light source tended to broaden the washout area in the photographs; nonetheless, they clearly showed the poor visibility at zero phase, as well as the improvement possible at high Sun elevations by employing a steep descent or a "dog-leg" or "buttonhook" trajectory. (In the dog-leg trajectory, the LM turned through a large angle cross-Sun during the visibility phase, while in the buttonhook the LM turned a full 180 degrees and flew up-Sun.)

In 1966 it was recommended that the upper Sun elevation limit be lowered to 20 degrees and that the lower limit be set at 7 degrees, based on the visibility studies then in progress. This change reduced the length of the landing window to one day per month and made the capability of launching to the same site on successive days doubtful. In order to investigate the suitability of these constraints, Anselmo

and Cavedo⁵¹ calculated scene contrast as a function of Sun angle, relative azimuth, and viewing angle over a very wide range of the parameters, choosing as a criterion the contrast of a 10-degree slope (10 degrees is roughly the median slope of an interior crater wall). They showed that visibility would be very poor in the upper end of the proposed 7 to 20 degree range when the Sun was above the viewing angle (16 to 20 degrees) unless at least 10 degrees relative azimuth were available. An azimuth difference at the lower end of the range brought no advantage.

At the NASA Manned Spacecraft Center, Saulietis developed an elaborate analytical model for lunar visibility.⁵² Since most small craters which might be landing hazards have about a 10:1 diameter:depth ratio and are roughly spherical in form, he calculated the brightness distribution across the visible portion of such a crater using the lunar photometric function. He then converted the luminance values to a detection range by means of the Tiffany data. Detection range was calculated using two techniques. For the first technique, three crater areas were defined: the visible shadow area (geometric shadow), the area of lower luminance than the average background (photometric shadow), and the area of greater luminance (bright side). Average contrast and equivalent circular areas were calculated and the threshold visual angle was found from the Tiffany data for each area. A field factor of 2.29 was included to convert from 50 percent to 99 percent threshold and from forced-choice to yes-no detection strategies. Since the range calculated by this method seemed too small when compared with visual observations of a model dusted with cupric oxide to match the lunar photometric function, a second method of specifying effective contrast was developed. The average contrast of each of the three areas was weighted by the fraction of the total projected area it occupied, and then all were summed; that is, each crater at its maximum detection range was assumed to appear as a small blurred disk with the separate area contrasts "smeared" over the entire disk. Generally, the detection ranges predicted were large and the angular subtense small (e.g., an 8-meter crater was visible at 8000 meters range at 10 degrees Sun elevation) so that the averaging assumption was valid. In the critical high-Sun and zero-phase regions, however, where detection range was less, the angular subtense was large. Where detail is large enough to be resolved, the proper method of combining areas of differing luminance is not well understood and the reliability of the detection range is in doubt. Because of the small field factor employed in this study, the predictions were considered to be optimistic and to apply more to a laboratory-like situation than to the hurried timeline of LM descent.

Hughes Aircraft Company, under contract to the Manned Spacecraft Center, continued development of the analytical model and carried out ambitious laboratory experiments on lunar surface visibility.⁵³ Both phases of the study generally confirmed the Sun elevation constraints.

The laboratory simulations, which might have resolved the question of field factors, unfortunately did not do so unequivocally. In the simulation, an observer was seated on a chair which traveled along a 2.5-meter track toward a screen on which was projected the image of a dusted model of a schematicized lunar surface. While in motion in the simulated LM trajectory, the observer operated a switch to indicate when he saw each of the four craters or protuberances which were included in the image for that particular run. A great deal of effort was expended in matching the brightness and contrast of the image to the lunar surface values, effort which was vitiated to some extent by the small size of the projected image, 5×5 centimeters, and by scratches and other flaws in the film. A very large detection range was generally recorded, which was roughly twice the analytically predicted range. This large difference was probably caused, in part at least, by the small field of view and the uniform background employed in the visual simulation.

The Sun elevation limits for landing were further reduced at that time as a result of concern over the poor visibility available around the zero-phase point, which for a 16-degree approach trajectory would cover the landing site at a Sun elevation of 16 degrees. The size of the zero-phase washout was estimated at 4 degrees, and Sun elevations from 14 to 18 degrees were deleted from the window. Effectively, the small isolated block from 18 to 20 degrees was deleted as well.

In 1968, the analytical visibility model was developed into its final form in a generalized landing hazard analysis by Ziedman of TRW Systems.⁵⁴ The Manned Spacecraft Center crater luminances were used, but the detection criterion was changed. For a crater to be detectable as a crater, both its bright side and either its geometric or photometric shadow areas had to be simultaneously detectable. Instead of the Tiffany data, Taylor's liminal contrast data³⁸ were used because they referred to a 1/3 second viewing time, which closely corresponds to the eye's dwell time during a visual scan such as would occur in a landing hazard search. The field factor was 4, 2 for converting to 99 percent probability and 2 for converting to a yes-no detection strategy. Principal detection targets were a 6-meter-diameter, 10:1 crater and a 3.5-meter-diameter, 6:1 crater, sizes which were determined to be the minimum that would represent a hazard to the LM on landing.

As in previous hazard detection analyses, it was assumed that the

LM might well land in an area without recognizable landmarks and where it would be necessary to detect small hazards at a relatively high altitude, such as 1000 meters, in order to make the largest redesignation at the lowest cost in propellant. This was a very conservative assumption, since at high altitude, a 6-meter crater subtends only a few minutes of arc, much less than the minimum LM redesignation granularity of one-half degree. Based on this stringent criterion, it was recommended that the Sun elevation be restricted to less than 13 degrees, unless a dog-leg maneuver could be incorporated into the trajectory.

Effectively, 13 degrees became the upper Sun elevation constraint for the prime launch opportunity in the Apollo program. The Sun elevation at landing (through Apollo 15) was never more than 12 degrees since it was always found possible to select a trajectory meeting the conservative lighting constraints.* For the first lunar landing mission in July, 1969, the Sun elevation limits were officially set as 5 to 13 degrees. The dog-leg maneuver was never favored, since to be effective it had to be large, and a large azimuth turn involved piloting problems, was costly in propellant, and could cause landing radar dropout.

In order to increase the number of launch opportunities per month, several alternative methods were investigated: landing in earthlight, landing in the lunar afternoon, steep descents, and T+24 (launch and landing one day later than nominal) landings. Only the latter two options were incorporated in the Apollo program. Earthlight landings were superficially quite attractive, and were even accepted as the prime method very early in the Apollo program. The Earth at full phase, while only 1/10000 as bright as the Sun, still casts 80 times more light on the lunar surface than the full Moon does on the Earth, and as the Earth is fixed in the lunar sky, lighting conditions are more uniform in earthlight than in sunlight. Helicopter landings at low light levels were carried out in 1963⁵⁵ to determine the illumination required for landing. It was found that, at least for sites in the western lunar hemisphere, light levels during a 3-1/2 day period around "full Earth" were sufficient for a safe landing. The problems attendant to planning for both sunlight and earthlight conditions on the same mission, not to mention the restricted range of applicable sites, prevented use of this option, however. A lunar afternoon landing (the Sun being in front of the LM in the lunar sky) was another option which would have provided excellent visibility but was precluded due to training problems. Glare was a

* On Apollo 16, due to a 6-hour delay in lunar orbit before landing, the Sun elevation angle reached 15 degrees. However, the craters chosen as landmarks were still partially shadowed and quite visible.

major consideration in an afternoon landing, but a study by Troester⁵⁶ showed that, in most cases, the afternoon landing window was three to five times longer than the dawn window, since the zero-phase washout area was out of the field of view. The appearance of the terrain was greatly altered, however, since the shadow direction was reversed, so that landmark recognition would have been difficult.

A.6 *Apollo Mission Launch Opportunities*

The requirement that the lunar landing take place only in the lunar morning at a Sun elevation range of 5 to 13 degrees allowed only one launch opportunity per month to a given site. For Apollo 11 and 12, this was sufficient because backup sites could be selected in case of a delayed launch and the mission objectives were not particularized to a specific location.

For Apollo 11, in order to permit the choice of three launch opportunities per month with Sun elevations in the 5- to 13-degree range, three alternative sites distributed in longitude were chosen, to be selected as necessary to provide the proper lighting. For Apollo 12, the same strategy was employed, except that only a prime and single backup site were selected. For Apollo 13, a prime and backup site were selected, but it was decided to plan for only one opportunity in the first month to the prime site (Fra Mauro) and to include the backup site only in the second and third months. In order to provide more than one opportunity per month for Apollo 14, at least for the second and third months, a different approach was taken. By launching a day early and waiting in lunar orbit, a second method of landing at the favored Sun angle was made available; the so-called T-24 opportunity. A detailed analysis⁵⁷ was made of the landmark visibility at Fra Mauro for a launch and landing one day later than nominal (the T+24 opportunity) and sufficient visibility was found to permit a landing mission. As long as sufficient landmarks were visible to indicate the nominal touchdown point, hazard detection could safely be delayed until late in the descent when the steepening view angle would lead to increasing visibility.

In the hope of reducing the uncertainty remaining in the analytical visibility analyses, a test of zero-phase visibility was carried out during Apollo 14. On previous missions, the astronauts, observing the zero-phase washout from orbit and on the surface, had maintained that visibility was much higher than calculated. On Apollo 14, the Command Module Pilot, while in orbit around the Moon, was asked to observe and photograph selected craters as they passed through zero phase. He

reported that some of the craters disappeared completely near zero phase, whereas others remained visible, possibly due to their higher intrinsic albedo. These data should lead to a better knowledge of both the average lunar photometric function and the detection field factor.

For the J-mission series, beginning with Apollo 15, the use of a steep descent trajectory greatly improved visibility of surface features both because of the steeper viewing angle (25 degrees vs 16 degrees) and the shorter range to the landing site. Due to this and the presence of a number of highly visible gross landmarks (Hadley Rille, Hadley Delta mountain), the T+24 opportunity was approved for the first month as well as the second and third months. Like the previous lunar missions, Apollo 15 was launched at the nominal time and the Sun elevation at lunar descent was only 12 degrees. However, the Commander had been misled into thinking that he was about 1 kilometer south of the desired track; consequently, even though the Sun lighting was good, he was unable to recognize the lead-in landmarks to the preplanned touchdown point and was forced to choose another landing point. (On Apollo 11, computer alarms occupied the Commander until near touchdown; on Apollo 12 and 14 the landmarks were instantly recognized at highgate.)

For the remaining Apollo missions, lunar trajectories continued to be constrained to ensure good visibility of landmarks and landing hazards during lunar descent.

APPENDIX B

LM Descent Hardware and Trajectory Details

The LM descent hardware system evolved from preliminary concepts in the early 1960's to hardware in the late 1960's. In a similar fashion, the software and trajectory design evolved over the years as additional knowledge was gained. The results of many of these early analyses are summarized in Ref. 58. The LM hardware and trajectory details are discussed in the following sections at their level of development during the period of the actual lunar landings. Section 3.3 of the main text should also be consulted in order to gain a broader understanding of LM descent.

B.1 Hardware Description

The major hardware components involved in LM descent were the descent engine, the attitude control system, the inertial measurement unit, and the onboard computer.

The descent engine was a liquid hypergolic propellant engine (nitrogen tetroxide and hydrazine) and had a maximum thrust of about 43,800 newtons. It could be run at its maximum thrust and was continuously throttleable between about 5300 newtons and 26,700 newtons thrust. It could also be run between 26,700 and 43,800 newtons, but excessive engine throat erosion made it advisable to minimize operation in this range.

For a steady state attitude, the thrust vector should pass through the center of gravity of the LM in order to minimize use of the attitude control system. This was accomplished by automatically trimming out the center of gravity offset with the descent engine, which could gimbal through a range of ± 6 degrees in two axes.

Rapid changes in LM attitude were accomplished by using the attitude control system, which consisted of two independent sets of eight 440-newton-thrust rockets. These jets could be used for rotational or translational motion.

The inertial measurement unit was used to measure the attitude and acceleration of the LM. A stable platform with gimbal angle sensors was used to measure the attitude changes, and accelerometers mounted on the platform measured velocity changes due to nongravitational forces. During descent, the onboard landing radar provided additional information for updating the altitude and velocity of the LM relative to the lunar surface. The landing radar consisted of a three-beam continuous-wave velocity sensor and a single-beam frequency-modulated continuous-wave altimeter. Without the landing radar, the LM altitude estimate would have been based on onboard inertial sensor readings and Earth-based tracking information, and altitude estimation accuracy would have been degraded. For this reason, landing radar operation was considered mandatory for lunar landings.

The onboard computer memory consisted of 2048 words which were erasable and 36,864 which were in fixed storage. The administration of the computer software development was an extremely complex task because of the limited storage capacity and the desire for accuracy and extreme reliability. LM software verification was carried out at the Massachusetts Institute of Technology Instrumentation Laboratory (now the Charles Stark Draper Laboratory) where it was programmed; Grumman Aerospace Corp. (the LM contractor); the Manned Spacecraft Center; the Kennedy Space Center; and TRW Systems Group.

The Apollo Spacecraft Software Configuration Control Board, with members from each of the above organizations and from Bellcomm, administered changes to the software programs. Software for both the

CSM and LM computers was handled by the same Board in order to keep the software of one spacecraft compatible with that of the other and to make operation of both computers as nearly identical as possible.

B.2 Guidance Equations

The LM guidance equations were used to calculate the thrust and attitude required to guide the LM from its estimated state (position and velocity) at a given instant to the desired position and velocity at the end of that phase of the descent.

It was assumed that the total vehicle acceleration was a quadratic function of time:

$$\mathbf{a} = \mathbf{c}_1 \frac{t^2}{2} + \mathbf{c}_2 t + \mathbf{c}_3, \quad (7)$$

where t progressed from negative values during the descent phase toward zero at the end of that phase. Integration of this equation yields

$$\mathbf{v} = \frac{\mathbf{c}_1 t^3}{6} + \frac{\mathbf{c}_2 t^2}{2} + \mathbf{c}_3 t + \mathbf{c}_4 \quad (8)$$

$$\mathbf{p} = \frac{\mathbf{c}_1 t^4}{24} + \frac{\mathbf{c}_2 t^3}{6} + \frac{\mathbf{c}_3 t^2}{2} + \mathbf{c}_4 t + \mathbf{c}_5. \quad (9)$$

These equations were expressed in a coordinate system (called the guidance coordinate system) having its origin at the desired landing site and rotating with the Moon. They expressed the desired position and velocity of the LM. If a landing site redesignation was made, the origin of the guidance coordinate frame was moved to the new landing site. New guidance commands were then computed by the quadratic guidance equations. These new commands could be significantly different from those just before the redesignation because of the changes in the location of the landing site relative to the LM.

In the vector equations (7), (8), and (9), the current velocity (\mathbf{v}) and the position (\mathbf{p}), which were assumed to equal the current desired values, were known from the navigation calculations, while the final velocity (\mathbf{c}_4) and position (\mathbf{c}_5) were specified to give the desired final state. By specifying the desired final acceleration (\mathbf{c}_3), it was possible to solve the three equations for \mathbf{a} . The final acceleration vector determined the final vehicle attitude. In addition, the downrange component of \mathbf{c}_2 , the time derivative of acceleration, was specified. This allowed the determination of a solution for t (time-to-go to the end of the phase), which was required in order to solve for the desired acceleration. Once

the desired acceleration vector was found, the acceleration due to lunar gravity was subtracted to obtain the required acceleration vector. This vector was converted into a thrust command for the descent engine and an attitude command for the attitude control system. Figure 40 summarizes the descent guidance logic flow.

The onboard computer recalculated the current position and velocity and the desired acceleration every 2 seconds during the descent and issued new thrust and attitude commands. In order to prevent large fluctuations in the commands as t approached zero, the trajectory was designed so that the desired state at the end of each phase (see Fig. 32) was reached before $t = 0$. The braking phase ended and the visibility phase began when $t \geq -62$ seconds. The switch to the landing phase was made when $t \geq -12$ seconds. Guidance in the landing phase was done by simple horizontal velocity nulling with a constant vertical velocity. Throttle control logic was added to prevent running the engine in the region between 26,700 and 43,800 newtons thrust.

The choice of constants to be used in eqs. (7), (8), and (9), as well as the choice of the vehicle position and velocity at the beginning of a phase, determined the shape of the trajectory which the LM followed. During the braking phase, the major trajectory constraints were that propellant be utilized with maximum efficiency and that the commanded thrust fall into the throttleable region (below 26,700 newtons) for 120 seconds before the end of the phase. The choice of guidance constants during the visibility phase involved a number of constraints. These constraints

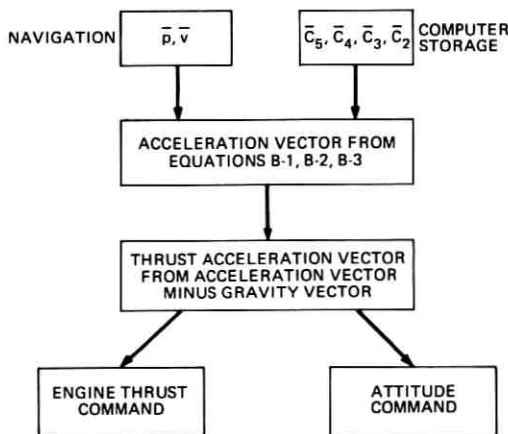


Fig. 40—Descent guidance logic.

principally involved shaping the trajectory to provide satisfactory conditions for viewing the lunar surface during the visibility phase and providing a vertical velocity-altitude profile from which it was possible to abort safely using the ascent stage engine if the descent engine failed. In addition, the final seconds of the visibility phase were required to have a velocity-position profile which provided comfortable conditions for manual takeover of LM control by the crew for final selection of a landing point. By carefully selecting guidance constants, it was possible to design a trajectory having more than 1-1/2 minutes of landing site visibility, a nearly constant location of the landing site in the LM window, abortability with the ascent engine, sufficient terrain clearance, and suitable crew takeover conditions.

Although the quadratic guidance scheme was used for LM descent throughout the Apollo program, several other schemes were considered at one time or another. Prior to the selection of quadratic guidance, a guidance technique was considered in which the acceleration was a linear function of time; however, the quadratic guidance technique was chosen because of the added flexibility it allowed in shaping the trajectory.

Late in 1969 and early in 1970 a proposal^{59,60} was made at NASA's Manned Spacecraft Center to use the so-called "delta" guidance technique for the descent to the Moon. This proposal involved two significant changes: (i) modifying the guidance equations so that the LM was constantly being guided back to a nominal trajectory throughout the descent, rather than just being guided toward specified end conditions, and (ii) throttling-down the descent engine into the throttleable region several times during the braking phase rather than just once at the end of the phase. Reference 61 pointed out a number of advantages of delta guidance, such as (i) the ability to fly a near-nominal trajectory even with engine performance variations and with landing site redesignations, (ii) a reduction of approximately 30 meters/second in the LM descent ΔV requirements, and (iii) a significant reduction in the cost of landing site redesignations. Among the disadvantages were: (i) terrain variations and landing site redesignations caused greater attitude variations using delta guidance as the LM attempted to rapidly return to a nominal trajectory path, (ii) the effects on the LM descent engine of the numerous thrust reductions during the braking phase were unknown, and (iii) it would have been necessary to completely reevaluate the effects of the new guidance equations on the LM control system stability. When all of the advantages and disadvantages of delta guidance were considered, it was concluded that the requalifica-

tion and reverification of the LM hardware and software would be too expensive and time consuming to be practical at that stage in the program.

Figure 41 shows the nominal thrust versus time history using quadratic guidance for the descent engine on Apollo 14. The descent engine was run at 4670 newtons thrust for the first 26 seconds after ignition in order to allow the engine gimbals to direct the thrust vector through the center of gravity. Following this, the desired thrust was well above the maximum engine thrust, so the engine delivered the maximum thrust of 43,800 newtons. As time passed, the quadratic thrust command decreased to a value below 43,800 newtons, but the engine thrust was not brought into the throttleable region (this action is called throttle down) until the command fell below 26,700 newtons. The nominal throttle down occurred 120 seconds before the beginning of the visibility phase so that the desired position and velocity could be reached at the end of the braking phase even if the descent engine thrust was as much as 1100 newtons below nominal.

Figure 42 shows the angle between the thrust axis and the normal to the lunar surface (this angle is called the pitch angle). During the visibility phase this angle had to be small enough that the landing site could be viewed by the crew.

On Apollo missions, the quadratic guidance scheme performed well: attitude and thrust behavior were both stable, and altitude, range, and

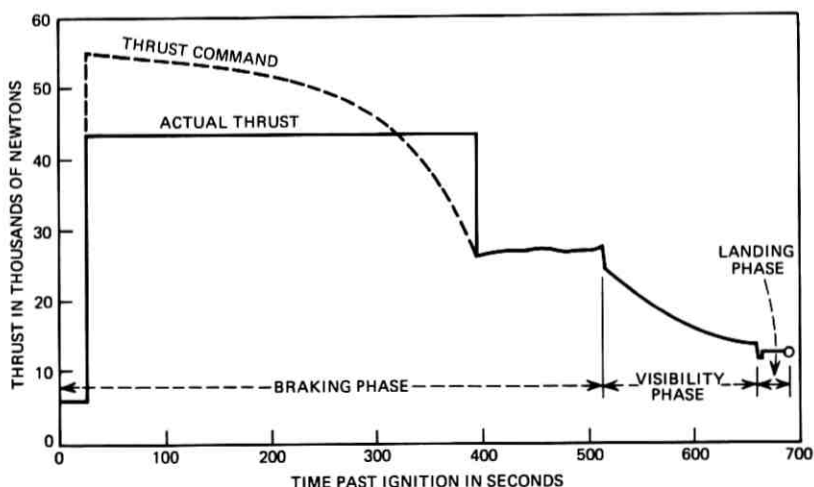


Fig. 41—LM descent thrust profile (automatic landing).

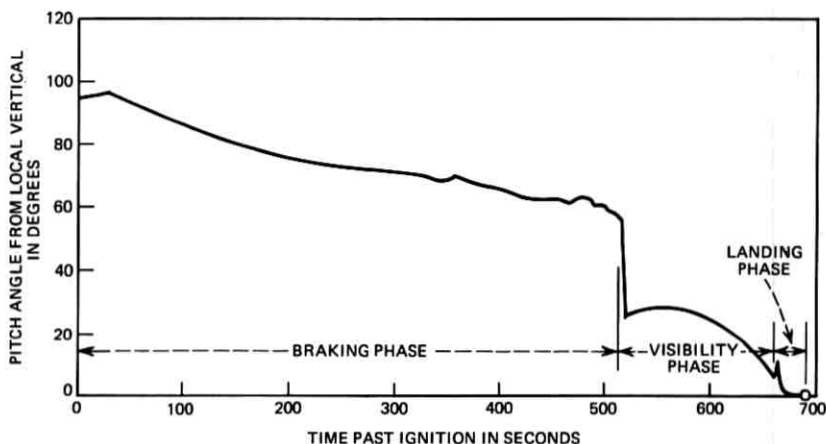


Fig. 42—Pitch angle versus time.

velocity were near nominal. The major perturbation on trajectory parameters was caused by incomplete knowledge of the approach terrain. Terrain variations entered the guidance equations through the landing radar data. If the approach terrain had different altitudes than expected, the trajectory was slightly different than expected; however, in no case did this cause any difficulty during descent.

APPENDIX C

Lunar Orbital Navigation

c.1 Introduction

The objectives of lunar orbital navigation were to provide accurate knowledge of current and future spacecraft position and velocity vectors to the primary guidance, navigation, and control systems. This information was necessary for achieving pinpoint (high-precision) landings on the lunar surface. Navigation data was used in conjunction with guidance laws to calculate the propulsive thrusts necessary to perform the proper descent orbit insertion and powered descent initiation maneuvers.

Navigation measurements were reduced using a minimization technique to provide a best estimate of the spacecraft state (position and velocity) at some epoch t_0 . Extrapolations of this state vector were made by numerically integrating the equations of motion to any desired time.

The two largest navigation error sources arose from an incomplete mathematical model of the lunar gravity field and from unmeasured spacecraft propulsive thrusts. Both of these error sources degraded the quality of navigation data extrapolations.

c.2 *Observational Data*

Two types of measurements were used for navigation in lunar orbit: Earth-based Doppler and onboard optical sightings. The Doppler data were used to refine the estimate of the spacecraft position and velocity in the orbit, while the optical measurements were used to improve the estimate of the position of the landing site relative to the spacecraft orbit.

The Doppler data were acquired using the world-wide facilities of the Manned Space Flight Network. This data type measured the average range rate (along the line of sight) of the spacecraft over a small increment of time. A transmitting station transmitted a signal of a fixed frequency to the spacecraft. This signal was received by the spacecraft, coherently frequency multiplied, and retransmitted to the Earth station. The number of signal cycles were counted over a 60-second interval. The retransmitted signal was received by both the transmitting station and any other operating tracking stations which could view the spacecraft. A typical tracking station configuration is shown in Fig. 43.

The onboard tracking data were obtained from crew-operated optical instruments, consisting of a 28-power sextant with a 1.8-degree field of view and a unity-power scanning telescope with a 60-degree field of view. These instruments were used to obtain angular measurements referenced to the inertial platform (and were also used to align the inertial platform relative to the stars). The two angular measurements taken for landing site updating were called shaft and trunnion angles. The physical orientation of these angles is shown in Fig. 44.

c.3 *Dynamical Formulation*

The largest gravitational acceleration experienced by the spacecraft was that arising from the lunar gravity field. The mass distribution of the Moon has some noncentral properties both in bulk and in localized mass concentrations (mascons); its gravitational potential was mathematically represented using the generalized spherical harmonic expansion:

$$U = \frac{\mu}{r} \left[1 + \sum_{n=2}^{\infty} \sum_{m=0}^n \left(\frac{R_M}{r} \right)^2 P_n^m(\sin \phi) \{ C_{nm} \cos m\lambda + S_{nm} \sin m\lambda \} \right]. \quad (10)$$

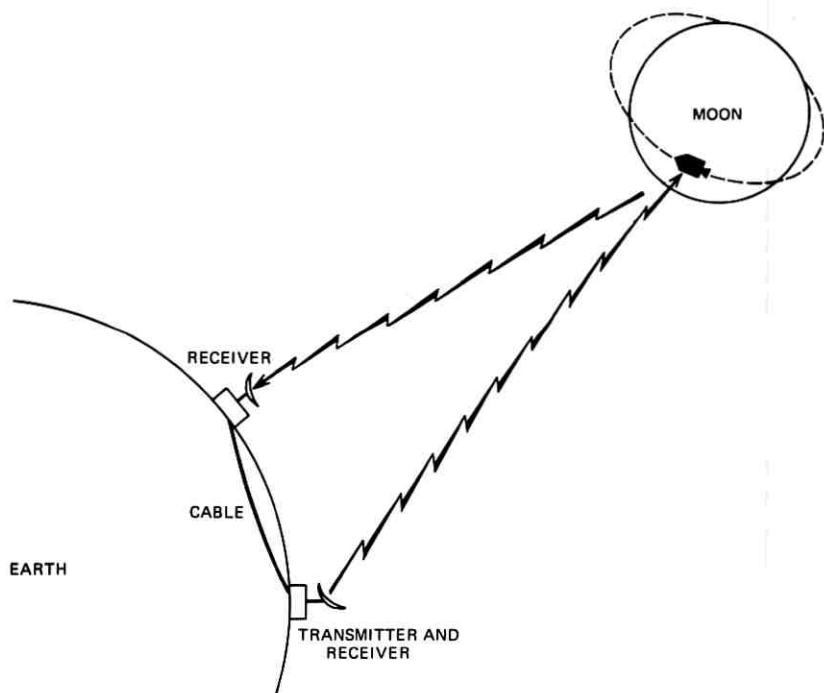


Fig. 43—Tracking configuration.

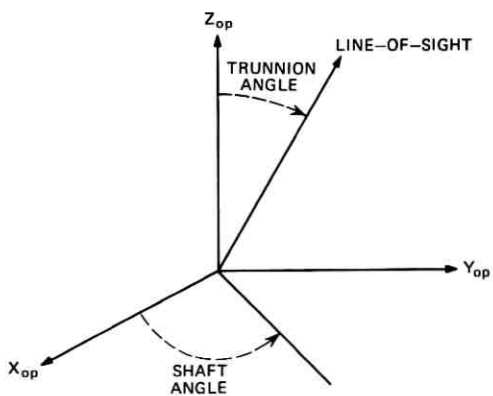


Fig. 44—Spacecraft onboard optical coordinate system.

In this expression μ is the product of the lunar mass and the universal gravitational constant; R_M is the mean radius of the Moon; P_n^m is the associated Legendre polynomial; r , ϕ , λ are the selenographic radius, latitude, and longitude, respectively; and C_{nm} and S_{nm} are the noncentral gravitational harmonics. The series begins with second-degree terms since it was assumed that the center of coordinates and the center of figure are coincident.

A simple gravitational model, the L1 field, was developed by NASA's Langley Research Center in support of the Apollo program. This model consisted of five harmonic coefficients determined from the Lunar Orbiter satellites and some of the early Apollo data. The coefficients comprising the L1 field are given in Table II.

In order to illustrate the noncentral gravitational features implied by the L1 field, equipotential surfaces are shown in Figs. 45 and 46, which demonstrate the variations from a spherical potential. These surfaces were determined by computing the radial deviations (in meters) of the L1 potential from a spherical potential based on the mean radius of the Moon.

The dynamical state of the spacecraft was found by numerically integrating the equations of motion. The coordinate system for this integration was defined by the mean celestial equator and vernal equinox at the beginning of the nearest Besselian year, with the origin translated to the center of mass of the Moon. The numerical integrator consisted of a Runge-Kutta integration combined with a Gauss-Jackson backward difference scheme.

The equations of motion for the spacecraft were as follows:

$$\frac{d^2 \mathbf{r}}{dt^2} = -\frac{\mu}{r^3} \mathbf{r} + \mathbf{a}_d \quad (11)$$

where \mathbf{a}_d is the sum of all perturbing accelerations: the noncentral gravity of the Moon and the perturbing effects of the Earth and Sun. Given the initial conditions $\mathbf{x}(t_0)$, the trajectory could then be numerically computed.

The state transition matrix (error partials), Φ , was found using ana-

TABLE II—COEFFICIENTS OF THE L1 FIELD

C_{20}	$=$	-2.07108×10^{-4}
C_{22}	$=$	0.20716×10^{-4}
C_{30}	$=$	0.21×10^{-4}
C_{31}	$=$	0.34×10^{-4}
C_{33}	$=$	0.02583×10^{-4}

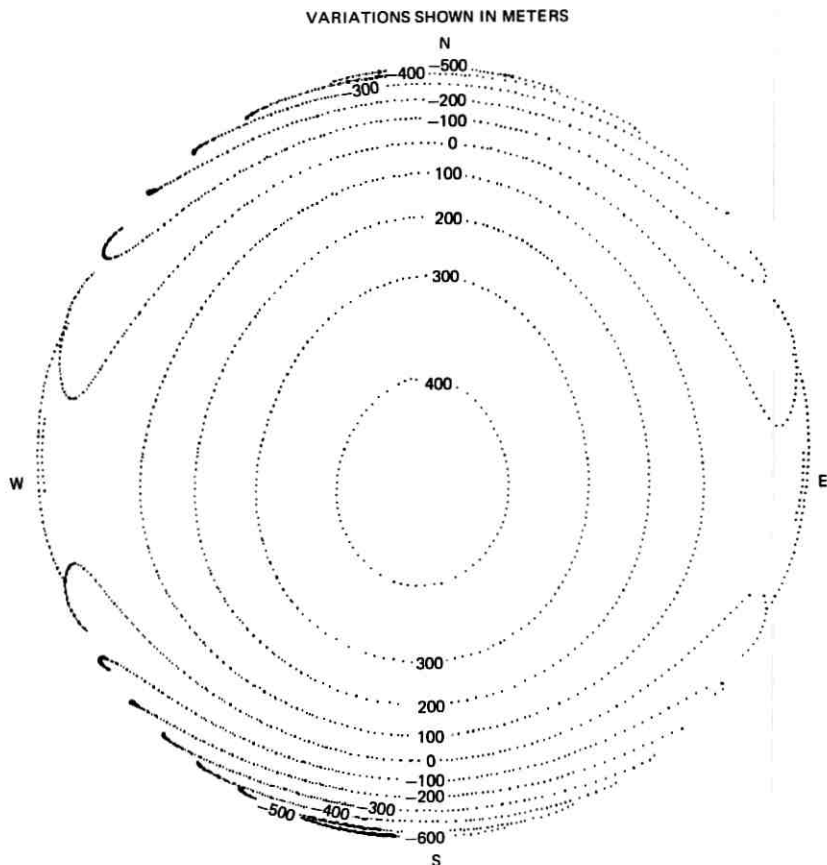


Fig. 45—L1 lunar gravity field equipotential surfaces (near side).

lytical partial derivatives for a conic orbit. Errors in the trajectory at time t were assumed to be related to errors in the initial conditions as follows:

$$\mathbf{x}(t) = \mathbf{x}'(t) + \frac{\partial \mathbf{x}'(t)}{\partial \mathbf{x}(t_0)} [\mathbf{x}(t_0) - \mathbf{x}'(t_0)], \quad (12)$$

where $\mathbf{x}(t)$ was the nominal trajectory and $\mathbf{x}'(t)$ was the perturbed trajectory. Hence, the propagation of trajectory errors had the following approximate linear form:

$$\Delta \mathbf{x}(t) = \frac{\partial \mathbf{x}'(t)}{\partial \mathbf{x}(t_0)} \Delta \mathbf{x}(t_0) \quad (13)$$

$$\Phi(t, t_0) = \frac{\partial \mathbf{x}'(t)}{\partial \mathbf{x}(t_0)}. \quad (14)$$

Closed solution formulas for the conic transition matrix were obtained.⁶² A method using a mean orbit and the conic formulas was developed by Goodyear⁶³ and was used in real-time data reduction; given the initial state $\mathbf{x}(t_0)$ and the final state $\mathbf{x}(t)$, an average or mean conic was generated which did not pass precisely through either $\mathbf{x}(t_0)$ or $\mathbf{x}(t)$.

c.4 Data Reduction

The philosophy used in lunar orbit determination was to gather batches of Doppler data over one front-side pass (one spacecraft crossing

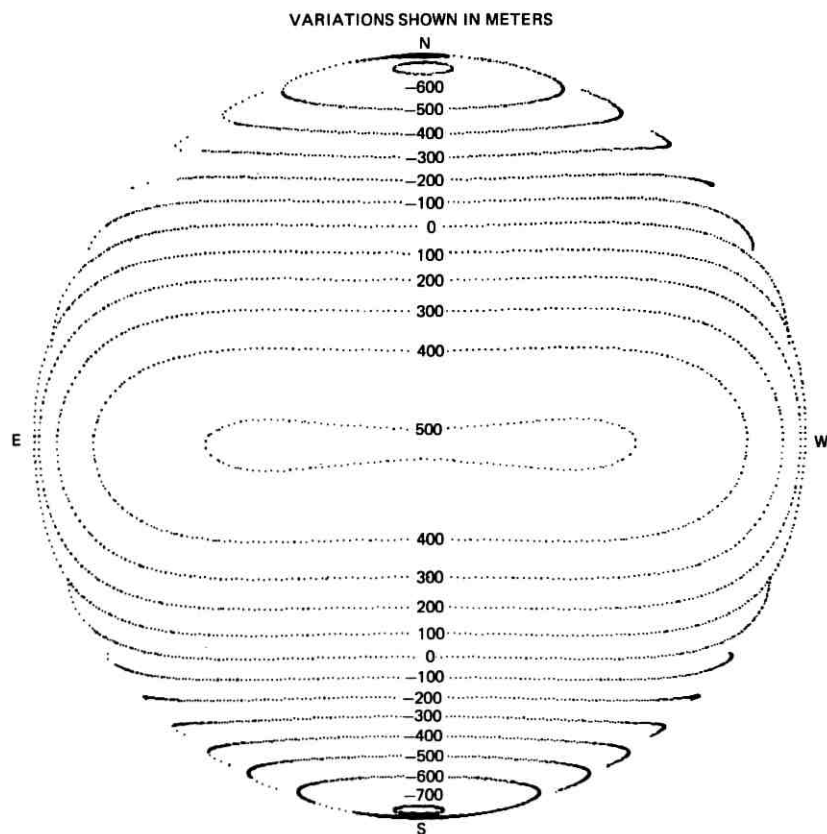


Fig. 46—L1 lunar gravity field equipotential surfaces (far side).

of the near side of the Moon in view of the Earth-based tracking radars) and use these data to improve the estimate of the spacecraft position and velocity at some epoch $\mathbf{x}(t_o)$. The Doppler tracking data \dot{R} was a scalar quantity that was a nonlinear function of the spacecraft position and velocity.⁶⁴

$$\dot{R}(t) = \dot{R}[\mathbf{x}(t)] + \eta, \quad (15)$$

where η is the random noise associated with the physical measurements. The errors in the measurements were assumed to have the following form:

$$E[\eta] = 0 \quad \text{and} \quad E[\eta^2] = \sigma^2,$$

where $E(\eta)$ is the expectation operator and σ^2 is the variance of the measurements.

Since the measurements were nonlinear functions of the state variables (position and velocity), the output equations, $\dot{R} = \dot{R}(\mathbf{x})$, had to be linearized for use in linear minimization methods. A Doppler measurement $\dot{R}[\mathbf{x}(t_i)]$ could be expanded in series form about some neighboring trajectory $\hat{\mathbf{x}}(t_i)$ as follows:

$$\dot{R}[\mathbf{x}(t_i)] = \dot{R}[\hat{\mathbf{x}}(t_i)] + \left. \frac{\partial \dot{R}}{\partial \mathbf{x}_o} \right|_{t_i} \Delta \mathbf{x}(t_o) + \dots, \quad (16)$$

where:

$$\hat{\mathbf{x}} = \hat{\mathbf{x}}[\hat{\mathbf{x}}_o, t_o]$$

$$\Delta \mathbf{x}(t_o) = \mathbf{x}(t_o) - \hat{\mathbf{x}}(t_o).$$

Now defining:

$$\Delta \dot{R}(t_i) = \dot{R}[\mathbf{x}(t_i)] - \dot{R}[\hat{\mathbf{x}}(t_i)] \quad (1 \times 1)$$

$$J(t_i) = \left. \frac{\partial \dot{R}}{\partial \hat{\mathbf{x}}_o} \right|_{t_i} \quad (1 \times 6).$$

Then, in general:

$$\Delta \dot{R}(t_k) = J(t_k) \Delta \mathbf{x}(t_o). \quad (17)$$

For n measurements taken over times t_1, t_2, \dots, t_n , the linear relationship between the variation in state and the variation in measurement was as follows:

$$\underbrace{\Delta \dot{R}}_{(n \times 1)} = \underbrace{[J]}_{(n \times 6)} \underbrace{\Delta \mathbf{x}}_{(6 \times 1)} \quad (18)$$

The objective in the data reduction was to obtain a best estimate

of $\hat{\mathbf{x}}(t_o)$ by minimizing the weighted sum of the squares of errors. An error function for n observations is:

$$\epsilon^2 = (\Delta\dot{\mathbf{R}} - [J] \Delta\mathbf{x}^T)W(\Delta\dot{\mathbf{R}} - [J] \Delta\mathbf{x}), \quad (19)$$

where $W = (1/\sigma\dot{R}^2)$. Forming $(\partial\epsilon^2/\partial\mathbf{x}_o)$ and solving yields the least squares solution

$$\underbrace{\Delta\mathbf{x}}_{6 \times 1} = \underbrace{[J^T W J]^{-1}}_{6 \times 6} \underbrace{J^T W \Delta\dot{\mathbf{R}}}_{6 \times 1}. \quad (20)$$

The sensitivity partials are

$$\left. \frac{\partial\dot{R}}{\partial\mathbf{x}_o} \right|_{t_i} = \left. \frac{\partial\dot{R}}{\partial\dot{\mathbf{x}}} \cdot \frac{\partial\dot{\mathbf{x}}}{\partial\dot{\mathbf{x}}_o} \right|_{t_i}, \quad (21)$$

where $(\partial\dot{R}/\partial\dot{\mathbf{x}})$ is the geometric sensitivity of the data to the orbit, and $(\partial\dot{\mathbf{x}}/\partial\dot{\mathbf{x}}_o)$ is the dynamic sensitivity to the epoch (state transition matrix for the orbit). Since the least squares equations are a linearization of a nonlinear system, they had to be solved iteratively. Convergence was achieved when

$$\frac{\sum_{n=1}^k [\Delta\dot{R}(t_n)]^2 \Big|_{(k-1)}}{\sum_{n=1}^k [\Delta\dot{R}(t_n)]^2 \Big|_{(k)}} - 1 < \delta,$$

where δ is a small positive number, and $(k-1)$ and (k) designate the $(k-1)$ and (k) computing iterations.

c.5 Real-Time Procedures

Analysis⁶⁵ showed that the L1 gravity model produced the most consistent navigation results when solutions were obtained using one front-side pass of tracking data. Data acquired during the revolutions prior to the landing were used to establish navigation consistency for solutions, but the last pass was used to establish the initial conditions for LM descent (Appendix B).

After spending two revolutions in the initial 105×315 -kilometer elliptical lunar orbit, the descent orbit insertion burn placed the spacecraft in a 130×15 -kilometer orbit, the low point of which was appropriate for initiation of the LM descent. Solutions obtained from revolutions three through eleven were used to determine the prediction quantity of the state vectors being obtained. Each solution was propagated forward one and two revolutions and compared with the local

(most recent single-pass) solution. The comparisons were made at the time of crossing the landing site longitude. Propagation errors caused by the inaccuracies in the lunar gravity model for the Apollo 12 mission are given in Table III.

During the twelfth revolution, a crew member used the onboard optics and made five sightings on the landing site or a nearby feature. The sighting sequence consisted of taking five measurements commencing when the spacecraft elevation angle was approximately 35 degrees with respect to the landing site. A typical landmark tracking sequence is shown in Fig. 47. Each sighting resulted in a shaft and a trunnion angle and an associated time. A solution was obtained from Doppler tracking data acquired during the twelfth revolution. Hence, the state of the spacecraft was assumed to be well known. The optical measurements were processed in the Manned Spacecraft Center Real Time Computing Center using a least-squares method to solve for the latitude, longitude, and radius of the landing site. Using this technique, the problem of inertial navigation was reduced to a relative one and the errors in spacecraft position relative to local terrain were reduced to a minimum.

The updated landing site position, together with the navigation error trends previously developed, were used in the LM descent targeting computations. The Lunar Module computer required the location of the LM relative to the landing site for targeting purposes. In order to account for known navigation errors in the LM position at powered descent initiation, the position of the landing site (RLS) was biased. The two biasing methods used were called RLS1 and RLS2.

The two-revolution error trends were used in RLS1. The altitude errors Δh and the crossrange errors ΔW were applied to the landmark solution obtained in the twelfth revolution. The downrange errors, although computed, were not applied to the landing site. These errors were extracted later (in the fourteenth revolution) using a more accurate method. The error trends obtained were rotated to the selenographic

TABLE III—PROPAGATION ERRORS

Propagation Interval	Position Errors, meters		
	Crossrange	Downrange	Radial
1 Revolution	500 \pm 450	150 \pm 300	600 \pm 60
2 Revolutions	600 \pm 500	100 \pm 500	400 \pm 60

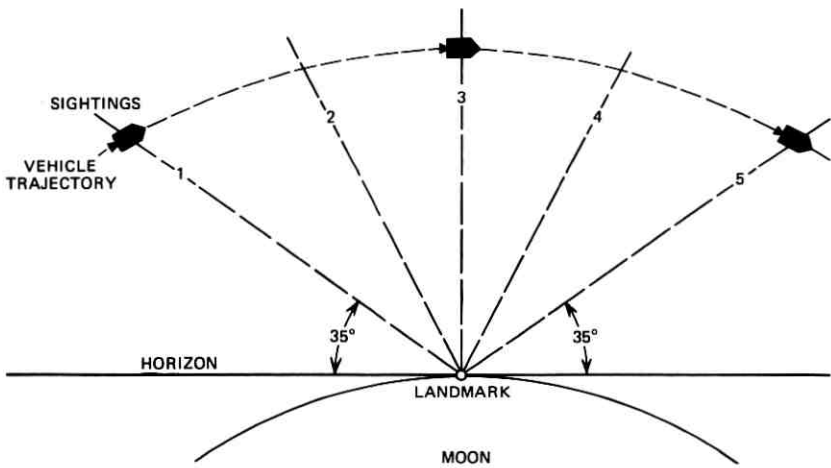


Fig. 47—Typical sighting sequence.

system. This rotation was accomplished in the following manner:

$$\begin{bmatrix} \Delta\phi \\ \Delta\lambda \\ \Delta r_{\text{Bias}} \end{bmatrix} = \begin{bmatrix} 10^{-5} & 0 & 0 \\ 0 & 10^{-5} & 0 \\ 0 & 0 & 1 \end{bmatrix} \begin{bmatrix} \cos \psi & \sin \psi & 0 \\ \sin \psi & -\cos \psi & 0 \\ 0 & 0 & 1 \end{bmatrix} \begin{bmatrix} 0 \\ \Delta W \\ \Delta h \end{bmatrix}, \quad (22)$$

where ψ is the azimuth measured from north, positive eastward. The actual landing site coordinates which the LM targeted to were:

$$\begin{bmatrix} \phi \\ \lambda \\ r_{\text{TARGET}} \end{bmatrix} = \begin{bmatrix} \phi \\ \lambda \\ r_{\text{REV 12}} \end{bmatrix} - \begin{bmatrix} \Delta\phi \\ \Delta\lambda \\ \Delta r_{\text{BIAS}} \end{bmatrix} \quad (23)$$

It should be noted that if the navigation offsets ΔW and Δh used in the procedure had confidence limits lower than certain predetermined values, no bias correction was used.

The RLS2 bias used a Manned Space Flight Network solution and optical tracking taken in the thirteenth revolution. Again, the optical data was used in conjunction with the Manned Space Flight Network solution to update the landing site. The same procedures were used as for RLS1 except that in this case one-pass propagation offsets Δh and ΔW were used.

The updated landing site from either RLS1 or RLS2 was entered into

the primary guidance, navigation, and control systems for powered descent initiation targeting. The RLS1 and RLS2 biasing methods were used when the landing site coordinates were not well known. If the landing site coordinates had been surveyed on a previous Apollo flight, only the RLS2 correction was used.

One last correction, called Δ RLS, was applied to the coordinates of the landing site at 2 minutes after powered descent initiation. The purpose of this correction was to eliminate the downrange error in the LM/landing site relative system. There were three methods for computing Δ RLS: the range rate residual $\Delta\dot{R}$, the Lear powered flight processor, and the range residual ΔR . Although all three of these methods were used in real time and yielded similar results, the range rate residual method was preferred.

In the range rate residual method, the LM state vector was used to estimate the range change per unit time that an Earth-based tracker should observe. A series of these values was differenced from the observed values every 2 seconds beginning at powered descent initiation minus 10 minutes and continuing to powered descent initiation. The value obtained was multiplied by the partial of the downtrack position with respect to the range rate to arrive at the downtrack error:

$$\Delta D = \frac{\partial D}{\partial \dot{R}} \Delta \dot{R}, \quad (24)$$

where the partial derivative was computed prior to the mission. This process was repeated about every half minute and an average ΔD was thus obtained. Hence, the total effect of the range rate residual was put in the most sensitive state component. This ΔD value was telemetered to the LM and manually inputted into the primary guidance, navigation, and control systems. The total effect of the Δ RLS update was to move the landing site along the downrange coordinate of the orbit. As an example, a Δ RLS of 850 meters was applied during the Apollo 14 mission. The remainder of the lunar landing trajectory was under the control of the primary guidance, navigation, and control systems and the crew.

APPENDIX D

The Bellcomm Apollo Simulation Program

D.1 Introduction

The Bellcomm Apollo Simulation Program (BCMASP) was developed for Bellcomm by Bell Telephone Laboratories, Incorporated, Whippany,

New Jersey, and was officially delivered to Bellcomm on January 1, 1965.^{66,67} Since then, there have been three documented updates of the program made by Bell Laboratories and three by Bellcomm.

The BCMASP was designed to generate precision trajectories for Apollo lunar missions. The program included an extensive group of general, multipurpose mathematical subroutines. Use of the program was aided by the provision of a problem-oriented language which simplified the programming tasks required of the user. A precompiler translated simple problem language trajectory descriptions and data processing specifications into FORTRAN IV subroutines. Input and control data were handled by similar straightforward techniques. The program required 34,535 words of memory during execution.

Targeting, the process of shaping the trajectory to meet design constraints and end conditions, was provided by a collection of routines that contained logic applicable to Apollo lunar missions. In a mission analysis mode, the family of trajectories satisfying the mission constraints was systematically studied using patched conic subroutines in order to select that trajectory which optimized the mission. The final targeting phase then employed the same subroutines and the precision simulator with an iterative mirror imaging method to generate the corresponding precision reference trajectory. In this technique, initial estimates for the precision simulator shaping parameters were obtained by matching the desired constraint with a patched conic trajectory. On succeeding iterations, the shaping parameters were then corrected by the differences between the patched conic shaping parameters which matched the desired trajectory and those which matched the precision trajectory generated on the previous iteration.⁶⁸

The patched conic approximation of lunar trajectories was first suggested by V. A. Egorov⁶⁹ and was widely used for lunar trajectory studies. This model divided Earth-Moon space into two domains of influence. Near the Earth, the attraction of the Moon was neglected and the gravitational field of the Earth was approximated by a central force field. Near the Moon, the attraction of the Earth was neglected and the gravitational field of the Moon was approximated by a central force field. The corresponding conic arcs were patched in position, velocity, and time at the point where the ratio of the perturbing force* to the central force in geocentric space was equal to the corresponding ratio in selenocentric space. The locus of all such points was approxi-

* In an Earth-centered system, the Moon represents the perturbing force, and vice versa.

mated by a sphere centered at the Moon called the Moon's sphere of influence.

The usefulness of the patched conic approximation derived primarily from these properties:

- (i) The speed of computation was several orders of magnitude faster than corresponding calculations using the precision simulator.
- (ii) Changes along the patched conic trajectory with respect to discrete changes in the initial conditions were nearly equal to those for the precision simulated trajectories.
- (iii) Since the conic arcs satisfied Kepler's equation of motion, the desired terminal conditions could often be related to initial conditions through closed form expressions.

Open and closed loop simulation modes afforded direct access to the precision simulator, with the closed loop mode providing additional facilities for accommodating guidance equations.

Printing and auxiliary computations were performed in the output data processing mode, as well as concurrently with targeting and simulation in the other modes, if required.

D.2 Structure

The BCMASP was basically a group of subroutines forming a consistent simulation and targeting package. These subroutines were structured to provide a suitable level of accuracy, to require a minimum amount of computer storage, and to allow considerable potential for future expansion. Although BCMASP was designed to simulate and target an Apollo manned lunar mission, the simulation portion was sufficiently general that it could be easily adapted to other powered flight simulations.

The main program and most of the subroutines were written in FORTRAN IV. Some of the more recent changes used some features of FORTRAN V, e.g., multiple entry points. Some routines were written in the UNIVAC 1108 EXEC VIII assembly language, but only in those cases where it was not possible to do the task with FORTRAN.

Communication between the subroutines of the BCMASP was normally via common. This greatly reduced the number of routines having calling parameters. All common variables were defined by mnemonic symbols and the use of these symbols was consistent among all subroutines. Areas of FORTRAN IV labeled common were identified with particular classes of variables, e.g., physical constants, shaping parameters, etc.

D.3 *The Simulator*

The center of BCMASP was its precision simulator, consisting basically of an integrator package and a differential equation evaluation package. In order to provide simulator flexibility, the packages were designed to operate under the control of user-supplied simulation programs. The remainder of the programs constituted mathematical support for the basic simulator, as well as additional mathematical and logical tools needed for targeting and data processing operations.

Construction of the user-supplied simulation programs was facilitated by writing them in a simple source language tailored to the simulation situation. The language enabled the user to describe the simulation as a list of "events" that were to occur in some predetermined logical sequence. Conversion of the events list description of the simulation to FORTRAN language was performed by a precompiler supplied with BCMASP.

In designing the events list language, the event concept was generalized so that an entire simulation could be described completely in terms of arbitrarily defined events. These events were linked logically, in that a given event could be made to inhibit or enable the execution of other events. Basic events ordinarily corresponded to discontinuities in the equations describing the simulation, e.g., shutting down an engine, or changes in boundary conditions, e.g., entering the Earth's atmosphere, while other events could be introduced as "markers" for data processing purposes.

A flexible printing and data reduction scheme was provided by a correspondingly simple "print list." Its structure was comparable to the events list, and a similar precompiler was furnished that generated a FORTRAN print control program from a print list deck of cards. The print list was used to extract, process, and print out information generated during the simulation program.

These lists, and their associated precompilers, relieved the user of the burdens of the highly routine programming operations required to generate a simulator. The user could specify his problem (simulation and/or processing) in FORTRAN IV language augmented by certain operators provided by the event and print list precompilers. The precompilers, in turn, did the mechanical work of constructing the simulator program.

D.4 *Modes of Operation*

The BCMASP was designed to have four basic modes of operation: (i) targeting, (ii) open loop simulation, (iii) closed loop simulation, and (iv) output data processing.

The *targeting mode* provided the logic necessary for selecting parameter values to provide trajectories for any of three different types of missions: (i) circumlunar* (nonlanding) missions, (ii) lunar orbital rendezvous missions with deboost to lunar orbit from a circumlunar trajectory, and (iii) lunar orbital rendezvous missions with optimum deboost to lunar orbit from the translunar trajectory.

Targeting logic provided the basis for finding a flight path and flight parameters that simultaneously satisfied all the requirements of the problem (including such parameters as liftoff date, landing sites on the Earth and Moon, etc.). Trajectory selection was accomplished in two phases. In the first phase, an approximation to the trajectory satisfying the given requirements was obtained using patched conic approximations. In the second phase, a precision trajectory was generated using the simulator and the conic approximations in a mirror imaging technique. For many studies, the first phase provided acceptable accuracy along with the capacity for economical wholesale generation of trajectories.

Once the flight path and parameters were established, further studies could be made using the *open loop mode*. It was intended that this mode be used for such activities as parameter studies, where the sensitivity of the trajectory to certain parameters was to be ascertained. The *closed loop mode* of operation was designed to extend the capabilities of the open loop mode to include guidance or similar closed loop operations in the trajectory simulation, and was primarily intended for guidance equation design and checkout.

When BCMASP was run in any of the above modes, certain simulation variables were recorded on an intermediate tape before and after the execution of an event and after each normal integration cycle. The intermediate tape produced was the input to the *output data processing mode* of operation, which was under control of the print list. This mode permitted further computations to be made using the data from the tape, and provided for the printing of specified data in a selected format.

D.5 Program Modifications

As confidence built up in the reliability and capability of the Apollo hardware, the ground rules and types of missions changed. However, it was not feasible to keep changing the standard version of BCMASP with every change in mission design. Thus, for each different mission

* As used here, circumlunar implies that the spacecraft is injected onto a translunar trajectory from Earth orbit, passes behind the Moon, and returns to reenter the Earth's atmosphere with given reentry conditions, all without additional propulsion following the initial translunar injection burn. This is a restricted subset of all possible lunar trajectories.

type, a separate program file was set up, consisting of those subroutines of BCMASP that had to be changed in order to simulate that particular kind of mission. Some of the more significant mission types will be discussed in this section. The level of detail is greater than in earlier sections in order to show the complexity of the internal program logic.

D.5.1 *Optimization of Hybrid Trajectories*⁷⁰

The hybrid mission differed from the Apollo 11 mission only in translunar flight. The spacecraft was injected from Earth orbit into a high (900 to 9000 kilometers) pericynthian circumlunar trajectory which could be aborted from, using only the reaction control system, followed by a later transfer using the SPS engine to a different trajectory whose pericynthian altitude was optimum for the chosen lunar parking orbit. The resulting trajectory was constrained by a requirement of abort capability by the LM descent propulsion system onto an Earth return trajectory a short time (usually 2 hours) after the time of predicted nominal lunar orbit insertion.

The objective was to minimize the total mission SPS propellant requirement. The optimization logic could be divided into two loops, or phases. The inner loop determined the optimum translunar trajectory that could be flown from the prehybrid maneuver point. The outer loop selected the optimum initial high pericynthian trajectory. An optimum translunar leg was developed for each circumlunar trajectory considered in the outer optimization loop.

The outer loop trajectories had two degrees of freedom: inclination of the transearth trajectory plane and pericynthian distance. Specification of both of these uniquely determined a circumlunar, reaction control system abortable, trajectory for a given launch azimuth and injection type.

The inner loop had to determine the best translunar trajectory starting from a specified position in space. Here, three parameters were available for optimization: the inclination of the lunar approach hyperbola, the time of flight from the hybrid maneuver to lunar orbit insertion, and the orientation of the lunar orbit. The values of these three independent variables were constrained such that the descent propulsion system abort ΔV required to return to Earth was less than a specified maximum and that the SPS propellant consumption for the mission was minimized. The coast time between translunar injection and the hybrid maneuver could also be added as an independent variable, but it was found that the sensitivity of propellant consumption to the time of the hybrid maneuver was low. A coast time of 5 hours was used for the hybrid simulator. Minimization of the SPS propellant consumption during the

mission was accomplished in the optimization program by maximizing the remaining spacecraft mass after transearth injection.

D.5.2 *Optimized Three-Impulse Transfer from a Hyperbolic Orbit to a Parking Orbit*⁷¹

The three-impulse transfer consisted of the following maneuvers: (i) transfer from the hyperbola to a first ellipse, (ii) transfer from the first ellipse to a second ellipse, and (iii) transfer from the second ellipse to a final circular parking orbit. The second and third maneuvers involved both an energy change and a plane change, while the first maneuver was constrained to occur in the plane of the hyperbola. If an initial hyperbola and a final parking orbit were assumed, there were eight parameters necessary to specify the three-impulse geometry completely:

- (i) apocynthian radius of the first ellipse, r_a
- (ii) true anomaly on the hyperbola at the first burn, f_{1A}
- (iii) true anomaly on the first ellipse at the first burn, f_{1B}
- (iv) plane change at the first burn, ρ_1
- (v) true anomaly on the first ellipse at the second burn, f_{2A}
- (vi) true anomaly on the second ellipse at the second burn, f_{2B}
- (vii) plane change at the second burn, ρ_2
- (viii) true anomaly on the second ellipse at the third burn, f_{3A} .

The three-impulse optimization used consisted of a three-dimensional linear search on f_{1A} , f_{1B} , and f_{2A} . The transfer from the hyperbola to the first ellipse was constrained to be coplanar, that is $\rho_1 = 0$, since it was found that optimizing ρ_1 yielded a negligible ΔV advantage. These parameters specified the first burn completely and determined the position and velocity prior to the second burn.

The optimum transfer trajectory from the state at the initiation of the second burn to the final burn was obtained by using a method developed in Ref. 72. The final state was specified by the angle θ measured from the projection of the radius vector at the second burn onto the circular orbit to the final radius vector. A linear walk optimization was performed on θ , internal to the linear search on f_{1A} , f_{1B} , and f_{2A} . The approach hyperbola was optimized external to the three-impulse optimization.

D.5.3 *Determination of Time Specific Lunar Surface Accessibility*^{30,73}

The accessible lunar regions at a given time were defined by examining the possible trajectory configurations in a manner that allowed an orderly imposition of the mission design constraints. The descent

propulsion system abort constraint was imposed first, since it limited only the translunar flight geometry. The desired time of arrival at the Moon determined the energy of the translunar trajectory for a given launch day.

The family of incoming trajectories to the Moon possible with this energy was examined, defining the subset that met the descent propulsion system abort constraint 8 hours past pericynthian. Each trajectory of the abortable subset was then propagated through lunar orbit insertion, selecting the extremals in yaw angle at lunar orbit insertion that allowed landing at the site under the lunar orbit where a CSM plane change prior to rendezvous was not required, and using all the SPS propellant available for the lunar orbit insertion and transearth injection maneuvers. These two yaw angle extremals defined two points on the lunar surface where landing was possible. Yaw angles between these extremals resulted in lunar orbits under which a line of accessible sites lay, since a portion of the propellant used in lunar orbit insertion at an extremal yaw was then available for CSM plane change prior to rendezvous. Scanning through all yaw angles between the extremals generated an accessible region. Superimposing the areas obtained from each abortable approach trajectory defined the region of the lunar surface which was accessible for a given arrival time and launch day.

In order to find the accessible area for a given month, it was first necessary to determine the arrival times that illuminated a portion of the front side of the Moon (60°W to 60°E). For later arrival times, the region of the lunar surface with the desired illumination moved westward. The accessible area on the Moon was determined for arrival times between that which illuminated 60°E and that which illuminated 60°W in increments of 4 hours. Superimposing the accessible region of the Moon and the properly illuminated region for a specific arrival time defined the accessible area that would have the specified Sun elevation range. The accessible region for the month was the superposition of the regions obtained for each arrival time.

Impulsive maneuvers and patched conics were used in generating the required trajectories. Allowance for the error between integrated and patched conic trajectories was made in the ΔV budget. The accuracy of the accessibility curves was estimated to be ± 0.5 degrees in both latitude and longitude.

D.5.4 *Determination of Optimum Moon-to-Earth Trajectories*⁷⁴

The nominal transearth injection maneuver placed the CSM on a trajectory from lunar parking orbit to a safe Earth landing. The transearth trajectory was constrained to provide a suitable entry into the

Earth's atmosphere and a landing within a specified geographic zone defined by latitude and longitude limits. The trajectory could not violate the maximum geographic return inclination. The transearth injection maneuver could be made at any time after LM-CSM rendezvous, as long as the resulting trajectory did not violate the specified maximum mission duration. The time spent in lunar parking orbit after rendezvous could be specified or it could be optimized to produce minimal transearth injection fuel requirements.

Subject to the above requirements, it was desirable to perform the transearth injection maneuver with minimum characteristic velocity (ΔV). The parameters that were available for optimization included longitude of Earth landing, velocity azimuth at exit from the Moon's sphere of influence, time of flight, and post-ascent time in lunar orbit.

The standard version of BCMASP provided for optimization with respect to exit velocity azimuth and Earth landing longitude within an allowable range. However, the optimization logic was based upon maximizing time of flight. While this criteria was generally valid for low inclination lunar orbits, it was not necessarily valid for higher latitude sites and higher inclination lunar parking orbits. A program modification described in Ref. 74 provided for optimization with respect to Earth landing longitude (within a specified longitude band) that was based on a selection criterion valid for any lunar parking orbit. It also provided the additional capability to optimize the transearth injection maneuver with respect to time of flight and time of departure from lunar orbit.

The order of optimization that was employed is as follows:

- (i) Optimization with respect to post-rendezvous time in lunar parking orbit
- (ii) Optimization with respect to time of flight
- (iii) Optimization with respect to Earth landing longitude
- (iv) Optimization with respect to azimuth of the Moon's sphere of influence exit velocity subject to limits determined from maximum inclination and maximum latitude constraints
- (v) Targeting transearth trajectory to given Earth landing longitude.

APPENDIX E

Mass and Performance Tradeoffs

E.1 *Introduction*

The mass of the Apollo space vehicle at liftoff from the launch pad was in excess of 2.7×10^6 kilograms. Less than 0.3 percent of this mass

actually landed on the Moon, and the first scientific payload returned from the Moon was less than 0.005 percent of the initial liftoff mass. Yet, in order to achieve even these small percentage yields, it was necessary to carefully balance the masses and performance capabilities of the six major propulsive stages of the vehicle. The process of evaluating the numerous tradeoffs available, and making adjustments to keep the system balanced when appropriate, continued from the inception of the program through the completion of each mission in succession. Some of the tradeoffs that were made are discussed in this appendix and examples are given of the tremendous leverage inherent in the system. There is also a discussion of limit masses, which formed the basis for a management tool which gave insight into the effects of some of these tradeoffs on the overall system.

E.2 Tradeoffs

There were numerous parameters that affected the balance of the system. Although there were no sharp boundaries, it was convenient to consider three categories: (i) the Apollo hardware, (ii) the physics of the Earth-Moon system, and (iii) operational procedures.

The original hardware design was basically an optimum match to the mission as understood at the time the hardware was built. As is the case in most development efforts, the tradeoffs available through changes in the Apollo hardware became more and more limited as the program matured. In fact, different stages reached maturity with differing levels of conformity to initial design performance, leading to imbalances in the overall vehicle. Although several major design changes were undertaken to save mass and improve performance during the early phases of development, the long lead times and expense required to produce man-rated hardware precluded most such alternatives in the later stages of the program. However, mass changes continued even into the latter phases of the program in areas such as stowed items that were not an integral part of the spacecraft, consumable liquids and gases (e.g., water, oxygen, and reaction control system propellant), and the amount of lunar samples returned. Some of the tradeoffs that could be made as a result of such changes are outlined below.

(i) *Stage Mass.* The propellant required to provide a given velocity change (ΔV) varied directly with the mass of each of the stages involved. For example, if the LM ascent stage mass were decreased by 10 kilograms, it would have been possible to load about 8.5 kilograms less ascent stage propellant and still provide the same flight performance. This, in turn, would have made it possible to decrease the descent stage propellant by 19.5 kilograms, and the Service Module propellant by

14 kilograms. Thus, the spacecraft (CSM/LM) could be made 52 kilograms lighter by a decrease in ascent stage mass of only 10 kilograms. In theory, this effect could have been reflected further back to the launch vehicle; for example, the 52-kilogram spacecraft reduction would have allowed a decrease in S-IVB propellant of over 500 kilograms. However, in practice, spacecraft and launch vehicle tradeoffs were generally considered separately since the two were under the cognizance of separate NASA centers. In order to keep the interface between the centers clean and simple, a single payload requirement for the launch vehicle was formally set and renegotiated only when necessitated by unexpected spacecraft mass growth or other problems.

Other options were also available. For example, in the above illustration, one might have preferred to maintain the same Service Module and descent stage propellant loadings and gain about 2.2 seconds of hover time just prior to LM landing, or the decrease due to ascent stage mass and propellant could have been offset by an 18.5-kilogram increase in landed payload. The actual choice depended on the relative margins for the various parameters and the particular ground rules that were in effect.

(ii) *Engine Efficiency.* Any improvement in the efficiency of an engine, indicated by a change in the specific impulse of the engine, resulted in using less propellant to do the same job. Thus, a 1-second increase in the specific impulse of the LM descent engine would have resulted in the ability to land an additional 38 kilograms, or, equivalently, increased the LM hover time by 4-1/2 seconds. Alternatively, if the total mass of the LM were of concern, the improved engine performance would have allowed the amount of descent propellant loaded to be decreased by 39 kilograms.

(iii) *Available Propellant.* The amount of propellant available to provide ΔV depended on (a) the size of the propellant tanks, (b) the ullage (empty volume needed for pressurant) requirement for the tanks, and (c) the amount of propellant loaded that had to be considered unusable. Increasing the amount of propellant that could be loaded on a given stage clearly increased the ΔV capability of that stage, but, by virtue of the increase in mass, may have decreased the capability of another stage. For example, a 10-kilogram increase in LM descent propellant loaded would have increased the LM descent stage ΔV capability by 1.7 meters per second. This would have had no effect on the ascent stage capability, but would have decreased the Service Module end-of-mission ΔV reserve by 0.5 meters per second.

The amount of propellant available could sometimes be increased by

decreasing the amount that had to be considered unusable. This included propellant that was trapped or that had to be set aside to make up for deficiencies that might result from statistical variations in various mass and performance parameters.^{75,76} Propellant made available in this manner was more effective than added propellant because it was achieved with no increase in the mass that had to be carried. In the case of the LM descent stage, it was twice as effective as added propellant.

Although it was not possible to exert control over the physical laws governing the flight of a space vehicle between the Earth and the Moon, a thorough understanding of these laws was obviously necessary so that they could be used to maximum advantage. In fact, improvements in knowledge of the Moon since the beginning of the Apollo program directly influenced mission design and some of the mass and performance tradeoffs. Perhaps the most notable example of this was the discovery of the lunar mascons (mass concentrations) and their effects on the accuracy of orbital navigation, and ultimately the accuracy of reaching a desired landing site. Many of the tradeoffs available were a direct result of the principles of trajectory mechanics.⁷⁷ Most of these were also influenced by operational requirements and procedures that evolved. Some of these tradeoffs had the desirable characteristic that they could be invoked very late in the mission planning process. Typical examples are outlined below.

- (i) The amount of payload that the Saturn V could place on a translunar trajectory was a function of the altitude of the Earth parking orbit. Since a change in this parameter influenced the planning in many areas, it needed to be set fairly early during the design of a mission. The first lunar landing missions utilized a 185-kilometer Earth parking orbit, but this was decreased to 170 kilometers for the J missions in order to increase the payload capability by about 360 kilograms.
- (ii) Additional launch vehicle payload capability could be gained by narrowing the range of acceptable launch azimuths; however, this resulted in a decrease in the duration of the launch window. This type of change could be made shortly before launch.
- (iii) For a given set of vehicle masses and performance, the accessible area on the Moon could be increased by accepting both Atlantic and Pacific type injection opportunities. This had to be traded off against the tracking and recovery requirements imposed.
- (iv) The flight time between the Earth and the Moon could be traded

off for increased Service Module ΔV reserves or allowable spacecraft mass. Generally, a longer flight time improved the ΔV and/or mass margins.

- (v) The Service Module ΔV reserves could sometimes be improved by relaxing the constraint on the inclination of the spacecraft's trajectory as it reentered the Earth's atmosphere. The penalty for this was an increase in the amount of aerodynamic heating experienced by the Command Module during entry.
- (vi) On the early Apollo lunar landing missions, the LM descent propulsion system was used to place the LM in a 110×15 -kilometer lunar orbit prior to the actual LM powered descent. Beginning with Apollo 14, it was decided that since the Service Module had excess capability, this burn would be performed with the SPS engine. The resulting decrease in the LM descent ΔV requirement made it possible to increase the LM landed weight by about 110 kilograms. This shows how a proper balance of the system could be maintained by transferring part of the total job from one stage to another. Although the maneuver could be performed more efficiently with the LM alone because the extra mass of the CSM was not involved, the overall objectives were better served by balancing the entire system.^{78,79}

It is informative to consider a specific example illustrating the surprising effects that a single small mass change could have. Assume that an experiment to be landed on the lunar surface and returned to Earth increased in mass by 10 kilograms. In order to maintain the same performance margins throughout the system, it would then have been necessary to add propellant to both stages of the LM, to the SM, and to one or more stages of the launch vehicle. The relative amounts are depicted by the bar graphs in Figs. 48 and 49.

Note that the launch vehicle propellant shown is the amount required if the propellant were added to only one stage, i.e., it would have been necessary to add either the S-IC, S-II, or S-IVB propellant shown. As a result of the leverage involved in the overall system, the 10-kilogram increase in the experiment mass would have caused a 57-kilogram increase in the total spacecraft mass and a 600-kilogram or more launch vehicle increase.

E.3 *Limit Masses*

The numerous tradeoff possibilities that existed sometimes made it difficult to evaluate and visualize the overall effects of changes to the

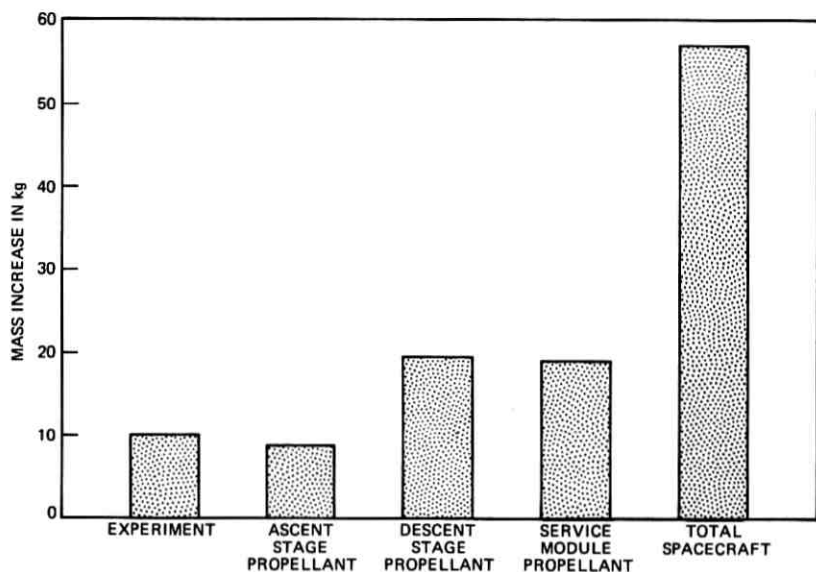


Fig. 48—Spacecraft mass increase resulting from increased experiment mass.

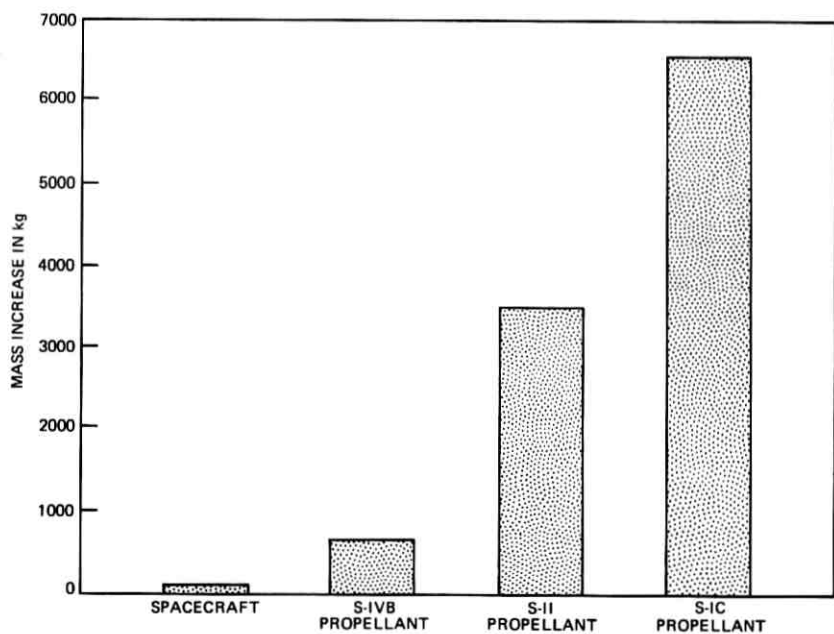


Fig. 49—Launch vehicle propellant increase resulting from increased spacecraft mass.

system. To facilitate such evaluations, a set of curves based on the concept of limit masses was developed. Stated simply, the limit mass of a given stage of the vehicle was the maximum allowable mass for that stage for a given set of constraints, requirements, and hardware parameters. The following paragraphs describe how limit masses were determined and discuss their use in program management. The discussion centers on the Lunar Module for illustrative purposes, but similar comments apply to other stages of the vehicle.

In generating a limit mass, two types of information had to be considered:

(i) *Requirements.* The requirements were determined primarily from the orbital mechanics of that portion of the trajectory under consideration. They could also be influenced by various operational considerations and constraints. For example, the requirement for a visibility phase during LM descent, in order to assure the astronauts a good view of the predicted landing site with adequate time to redesignate to another site if necessary, resulted in an increase in the ΔV requirement over the propellant optimum value. The requirements were stated in terms of the ΔV that had to be provided by the stage in question.

(ii) *Propulsion Capability.* The propulsion capability of the hardware could be characterized by two major factors: the propellant available and the hardware performance. The propellant that could be loaded depended upon the size of the tanks and the ullage required. However, part of the loaded propellant was trapped and unusable, or was budgeted for various dispersions and contingencies and was therefore not available to meet the ΔV requirements. The hardware performance depended on the design and fabrication of the engines and other portions of the propulsion systems. For calculating spacecraft limit masses, a single indicator of performance, the specific impulse, was used.

Once the performance requirements and propulsion capability were determined, limit masses could be calculated approximately by using the so-called rocket equation, which may be expressed as

$$\Delta V = I_{sp} G \ln \frac{M_i}{M_i - M_p},$$

where

ΔV = delta-velocity requirement

I_{sp} = specific impulse of engine

G = standard acceleration due to gravity

= 9.80665 meters/second/second

M_i = initial mass of the spacecraft

M_p = mass of propellant available.

Considering the LM ascent stage as an example, with $\Delta V = 1867$ meters per second, $I_{sp} = 309.6$ seconds and $M_p = 2273$ kilograms, the ascent stage limit mass at lunar liftoff was about 4951 kilograms.* However, in order to facilitate comparisons with other parts of the vehicle, it was desirable to convert this number into an equivalent value at another point in time, usually Earth launch. In order to do this, adjustments were made to account for the mass changes that occurred between Earth launch and lunar liftoff. In some cases, it was also convenient to express the limit mass as a stage mass without propellant. With these adjustments, the ascent stage limit mass (without propellant) at Earth launch was about 2467 kilograms. This was the maximum mass that the ascent stage could have and still meet its ΔV requirement with the stated hardware performance. This number was independent of the LM descent stage mass, as indicated by the horizontal ascent stage limit line shown in Fig. 50.

A similar procedure was used for the LM descent stage to determine the maximum allowable LM mass at the beginning of the powered descent phase of the mission. To find the descent stage limit mass at Earth launch, adjustments like those described in the previous paragraph were made. However, the ascent stage mass also had to be considered since it was part of the total LM mass at the beginning of the descent. Thus, the descent stage limit line, when plotted with the same axes as in Fig. 50, had a slope of -1 . The ascent and descent stage limit masses are both shown in Fig. 51. Charts such as this one proved to be effective management tools. By including a point indicating the current mass status, they could be used to show the current margin with respect to the limits and how well the margins (distance between the status point and the limit lines) were balanced between the two stages. The effects of actual, potential, or proposed changes in mass, mission requirements, or hardware capability showed up as shifts in either a limit line or the status point, so that many of the tradeoffs discussed earlier could be seen at a glance. Thus, a 10-second increase in the required hover time above the lunar surface would have increased the LM descent ΔV requirement by 16 meters per second and shifted the descent stage limit line about 85 kilograms to the left.

To complete the picture, a similar chart showing the relationship

* Limit masses, like actual masses, changed with time; however, the values shown here were typical.

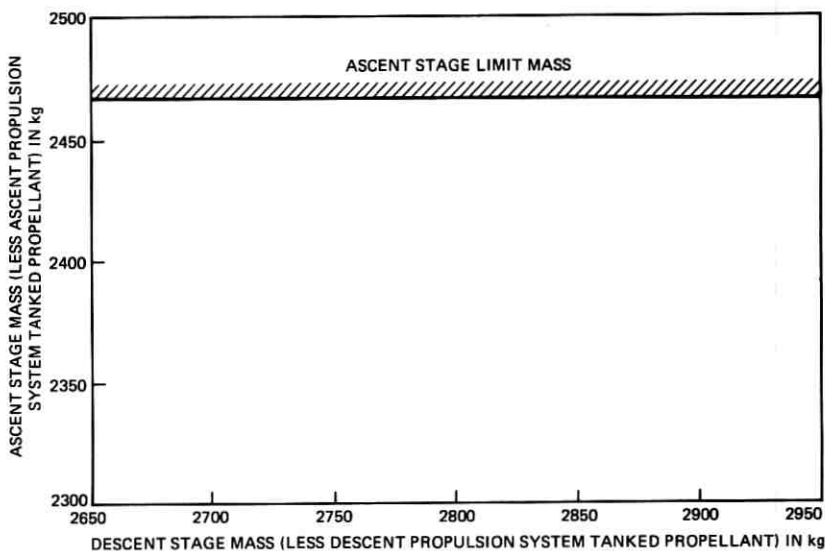


Fig. 50—LM performance status (Earth launch masses).

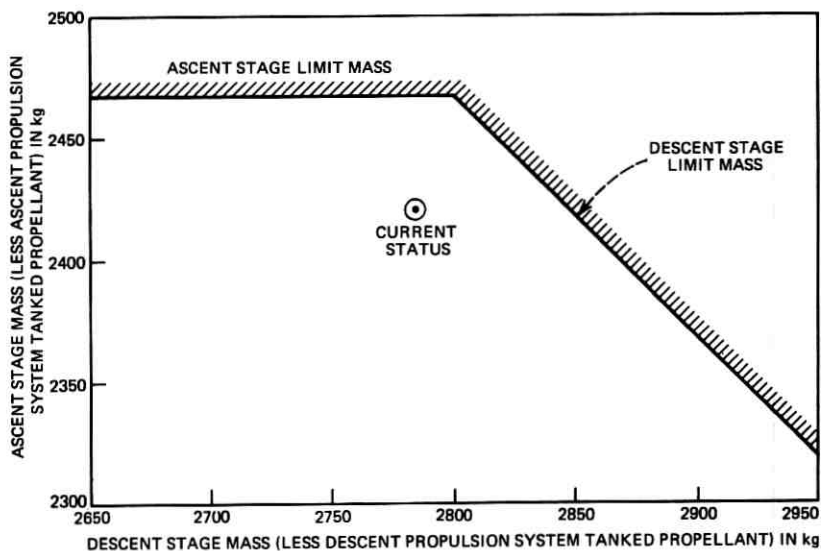


Fig. 51—LM performance status (Earth launch masses).

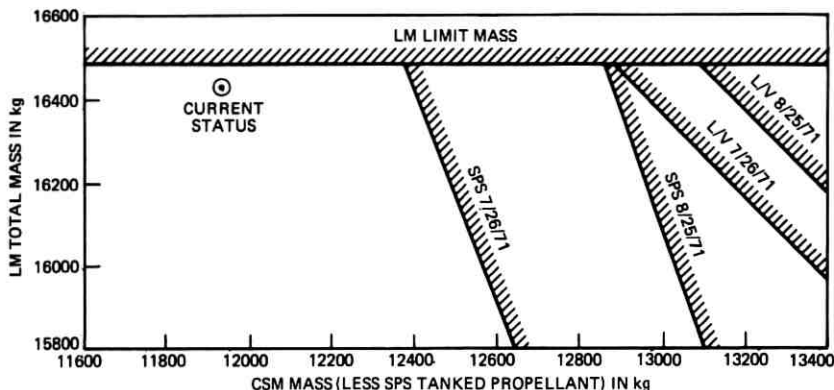


Fig. 52—CSM performance status for Hadley mission (Earth launch masses).

between the LM and the CSM was generated (Fig. 52). The abscissa is the CSM mass at Earth launch, less propellant, as in the previous chart. However, the total LM mass, including both stages and all LM propellant, was used as the ordinate, since customary usage resulted in this quantity being more convenient and familiar. The LM limit line is consistent with the data on the previous chart and represents the maximum total LM mass at Earth launch. Two CSM limit lines, with a slope of about -3 , are shown to illustrate the effect of a change in launch date. Also shown are limits imposed by the capability of the launch vehicle. Addition of a current status point again allows one to evaluate the current margins. When used together, these two types of charts gave a graphical display of the margins that existed in the system as a whole and provided a means for visualizing the overall effects of changes to either requirements or hardware capability. For example, Fig. 52 shows clearly, for the conditions examined, that CSM mass growth was more acceptable than LM mass growth, and that the spacecraft propulsion capability imposed a more severe constraint on CSM mass growth than did the launch vehicle.

The concepts described here were utilized as a management tool by NASA Headquarters. Charts of the type discussed were used in monthly reviews held by the Apollo Program Director. The material for these reviews was prepared and presented by Bellcomm and published each quarter in the NASA "Quarterly Weight and Performance Report".⁸⁰ In order to facilitate the preparation of this material, a flexible general purpose mass and performance program was developed.⁸¹

APPENDIX F

*Apollo Landing Sites*F.1 *Introduction*

As pointed out in Section 2.2, Apollo site selection was a continuous process, with the knowledge gained and the objectives achieved on each mission directly affecting the considerations for candidate sites for following missions. Consequently, specific sites could not be selected far in advance, as this would have eliminated the flexibility necessary to take advantage of the results from each successive mission. The purpose of this appendix is to describe in some detail the specific sites selected for Apollo 14, 15, 16, and 17, as well as other sites which were candidates for Apollo 17. The evolution of scientific objectives from mission to mission can be followed through these descriptions.

F.2 *Fra Mauro Region (Apollo 14)*

The Fra Mauro Formation (Fig. 53) is an extensive geologic unit that covers large portions of the lunar surface surrounding Mare Imbrium. The Formation in the area selected for the Apollo 14 landing is characterized by subparallel ridges radial to the Imbrium basin, and gentle swales that give it an undulating character. Most of the ridges are on the order of a hundred meters high and many can be traced for up to 90 kilometers. The general setting of this unit and its textural and structural characteristics suggest that it is part of the ejecta zone that surrounds Mare Imbrium. It is probably composed both of material ejected ballistically from the site of the Imbrium basin and of material carried by the base-surge of gas and debris produced by the giant impact that created the basin.

The major objective of Apollo 14 was to sample the Fra Mauro Formation so as to provide information on the nature of the ejecta from Imbrium, which should include samples from deep within the lunar interior, perhaps as deep as 200 kilometers. Age dating of these samples should establish the age of the pre-mare surface and/or the subsurface materials, as well as the time of formation of the Imbrium basin, thus providing important points on the lunar geologic time scale and insight into the early history of the Moon.

To achieve these objectives, a landing point was selected within walking distance of "Cone Crater," a 300-meter crater that is believed to have penetrated through the regolith (fragmental surface layer) and exposed the original Fra Mauro materials.

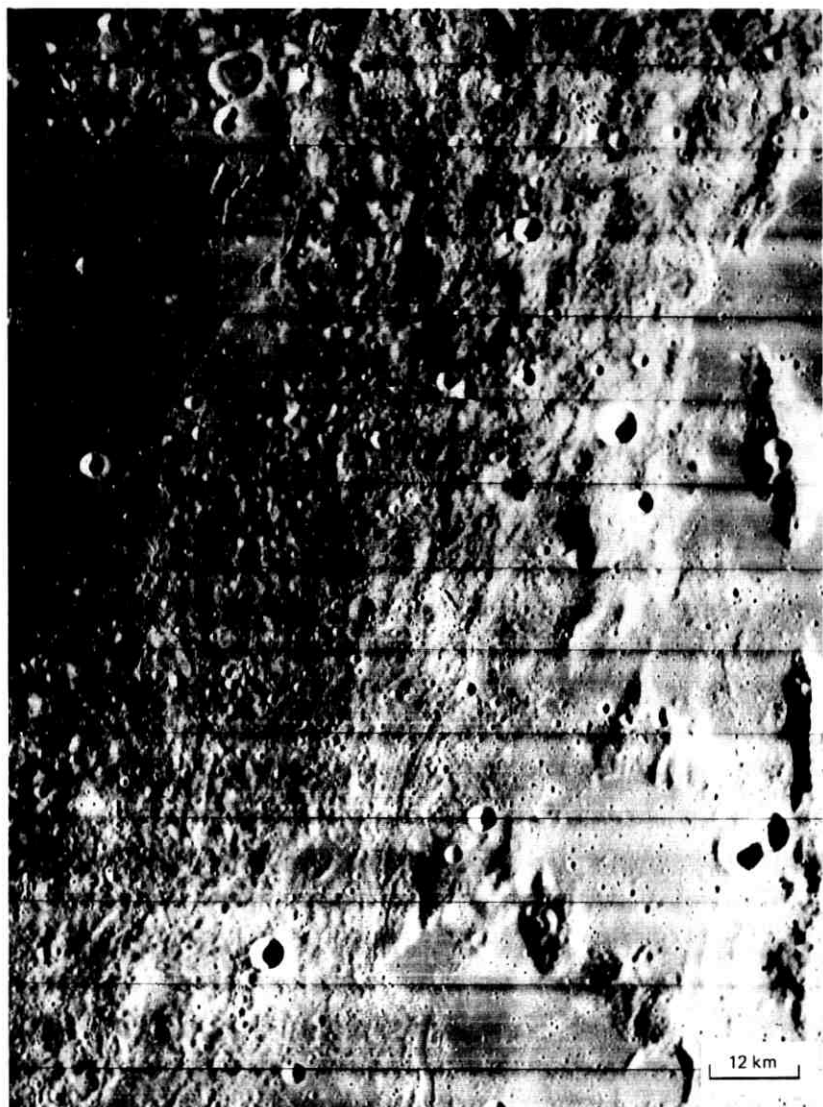


Fig. 53—The Fra Mauro Formation.

Material collected on Apollo 14 appeared to support premission interpretations. The majority of the rocks were breccias which must have originated as ejecta of a major impact event such as that which created Mare Imbrium.

F.3 *Hadley-Apennine Region (Apollo 15)*

The Apollo 15 site (Fig. 54) stands astride a mountain escarpment, the Apennine Mountains, and a sinuous rille, the Hadley Rille. In addition to these features, the site offered numerous interesting objectives in the surrounding mare material.

The Apennine Mountains front forms the arcuate southeastern rim of the Imbrium basin. It borders Palus Putredinis and rises from 2 to 4.5 kilometers above the mare surface. It is probably composed of materials that predate the excavation of the Imbrium basin, that is, pre-Imbrian rocks. Examination and collection of this ancient material was the prime objective of the mission to this site.

A second important objective was to study and sample the Hadley Rille, which runs parallel to the Apennine Mountains front and incises the Palus Putredinis mare material. The rille is a sinuous or meandering channel, much like river gorges on Earth. It displays a V-shaped cross section; however, it may once have had nearly vertical walls. It appears to originate in an elongate depression near the base of the mountain front in an area containing what seem to be constructional features of probable volcanic origin. In the area of the site, the rille is about 2 kilometers wide and 360 meters deep. The origin of lunar sinuous rilles such as the Hadley Rille is enigmatic; either the erosive action of some type of fluid was involved, or the collapse of the surface capping of a lava channel during or after emplacement of the mare material.

Secondary objectives included the examination and sampling of the constructional materials of Palus Putredinis, and that of a crater cluster which may have originated at the crater Autolycus, over 200 kilometers northwest of the site.

F.4 *Descartes Region (Apollo 16)*

The Descartes site (Figs. 55 and 56) is located on a topographic rise that forms a ridge which is a few kilometers higher than the surrounding highlands. Since the area is not associated with a known gravity anomaly, it probably represents a segment of the lunar crust which is thicker than that in the rest of the nearside highlands.

Constructional volcanics further increase the topographic expression of this ridge in the Descartes region. The bright material on the north



Fig. 54—The Hadley-Apennine region.

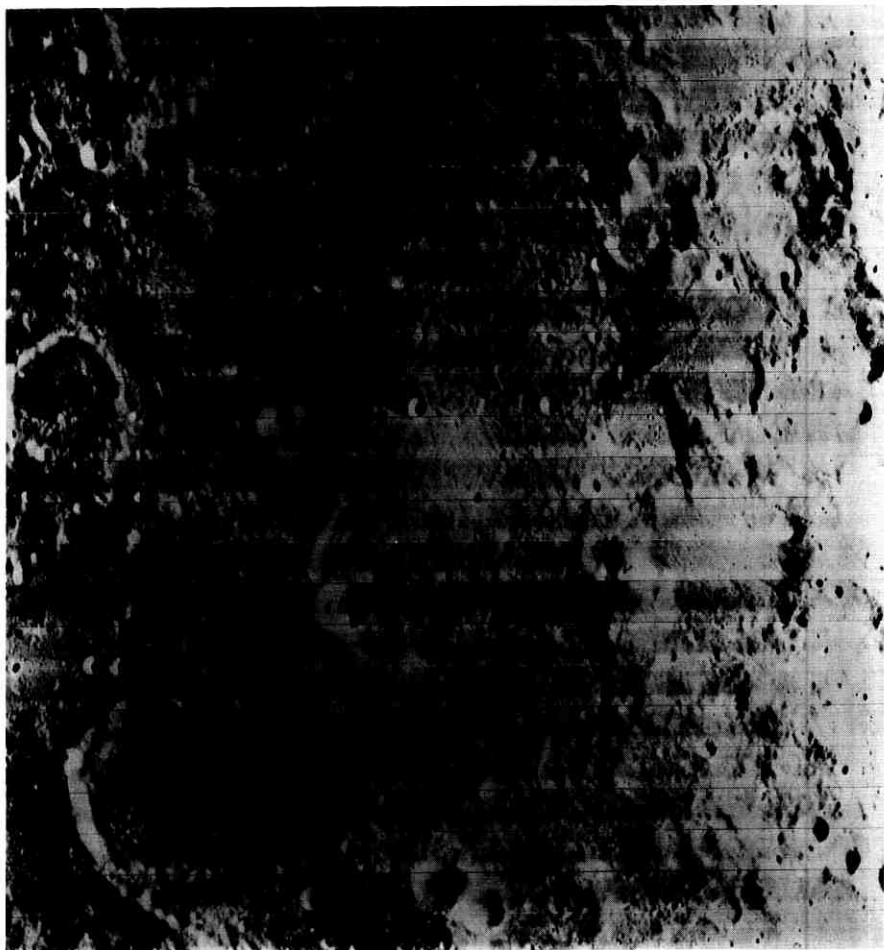


Fig. 55—Lunar Orbiter IV photograph of the Descartes region.

rim of the Crater Descartes is anomalous to both radar and IR and probably represents the focal point of upland volcanism in this region. Surrounding the bright material are constructional units which are similar to areas of upland volcanism west of Mare Humorum. There are also indications of similar units in the lunar farside highlands. They all appear to represent a younger stage of highland crustal evolution. The Descartes region might give the widest possible spread in compositional type and age of lunar highland materials.

There are four major geologic units at the Descartes site. Relative to the landing point selected, these units are to the north (sculptured terra), south (furrowed terra), east (hilly terra), and west (cratered plains), as shown in the geological sketch map (Fig. 56).

F.5 *Alphonsus (Apollo 17 Candidate Site)*

The crater Alphonsus (Fig. 57) is on the western borders of the central lunar highlands. The crater appears to be pre-Imbrian in age because its walls are cut by Imbrium sculpture. Therefore, the exposed crater walls must be pre-Imbrian shallow subsurface materials.

Alphonsus is typical of many upland craters, having a flat, heavily cratered floor, a central peak, and a broad sparsely cratered and subdued

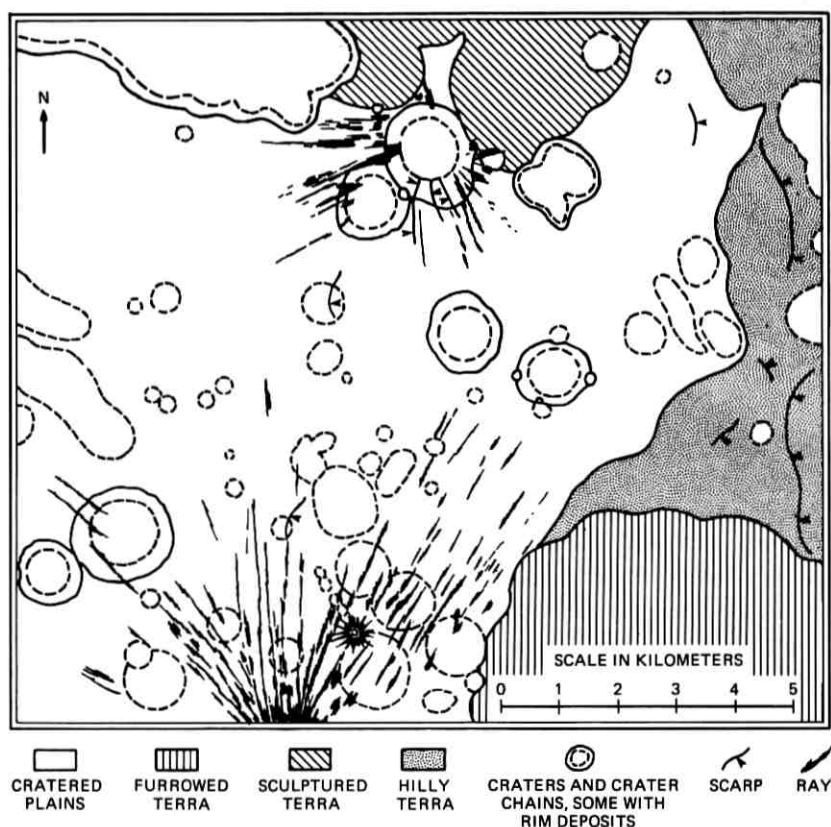


Fig. 56—Geological sketch map of the Descartes region.

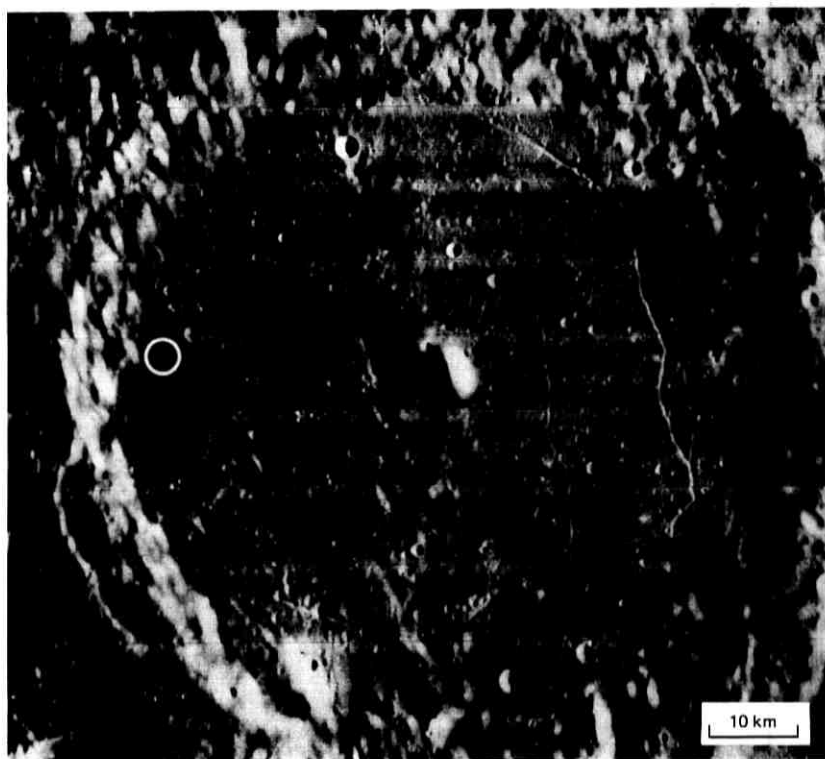


Fig. 57—Crater Alphonsus with candidate landing area shown by circle.

rim. Less typical features are a network of intersecting straight rilles cutting the floor and dark halo craters centered at the intersections and bends in these rilles. The dark halo craters are believed to be volcanic in origin, like cinder cones which have brought material from the lunar interior to the surface.

In addition to these features, there are deposits (ejecta of Arzachel) in the southern half of Alphonsus which were mapped by 3.8-centimeter radar as higher topographically than the rest of the crater floor. Consequently, Alphonsus is advantageous in providing access to pre-Imbrian materials as well as young volcanic deposits. These deposits must have also originated from deeper parts of the lunar interior.

F.6 *Gassendi (Apollo 17 Candidate Site)*

Gassendi (Fig. 58) is a 120-kilometer crater in the southwestern quadrant of the near side of the Moon, on the north rim of Mare

Humorum. The 500-kilometer diameter Humorum basin has clearly defined scarps and has a sizeable positive gravity anomaly (mascon). It is older than the Orientale, Imbrium, and Crisium basins. The floor of Gassendi apparently has been uplifted, producing the linear rilles (grabens) and making the central peaks as high as the crater rim. A ring of mare material occurs within Gassendi in a crescent-shaped zone along the south side of the warped crater floor. The proposed landing site lies at the base of the central peaks. Of the three high-priority candidates considered for Apollo 17, Gassendi is farthest removed from the Imbrium basin. Gassendi is interpreted to be of impact origin although other origins cannot be completely ruled out.

The main objective would be to sample material from the central peaks. From terrestrial analogues, this material should have come from depths of up to about 1/10 of the crater diameter or possibly as much

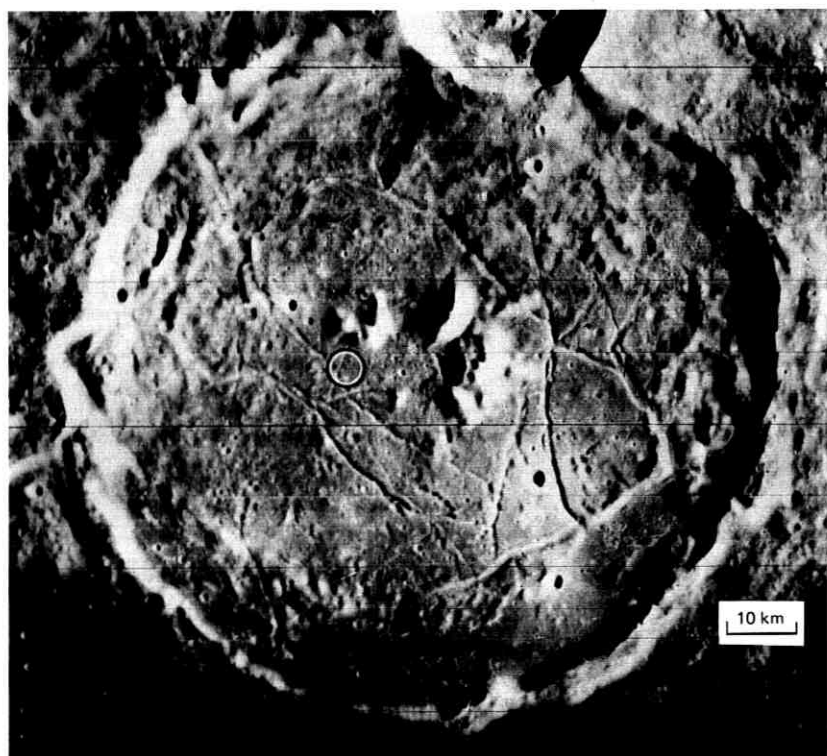


Fig. 58—Crater Gassendi with candidate landing area shown by circle.

as 10 kilometers. This is several times the depth of material exposed on a crater wall. Blocks at the base of the central peak should be ascribable to a source beneath the crater and should, in principle, be derived from the highland material below the Humorum ejecta blanket. Volcanism subsequent to the crater formation may have added a "non-highland" component to the central peaks, but continued mass wasting should produce original central peaks talus at the base. Material of the crater floor constitutes the second sampling objective. Gassendi was a favorable site from the orbital science point-of-view; its location in the southwestern part of the Moon made feasible photography and other remote sensing of new regions of the Moon, including Mare Orientale.

F.7 *Taurus-Littrow (Apollo 17)*

The Taurus-Littrow site (Fig. 59) is located on the southeastern rim of Mare Serenitatis on a flat cratered plain at the base of a series of

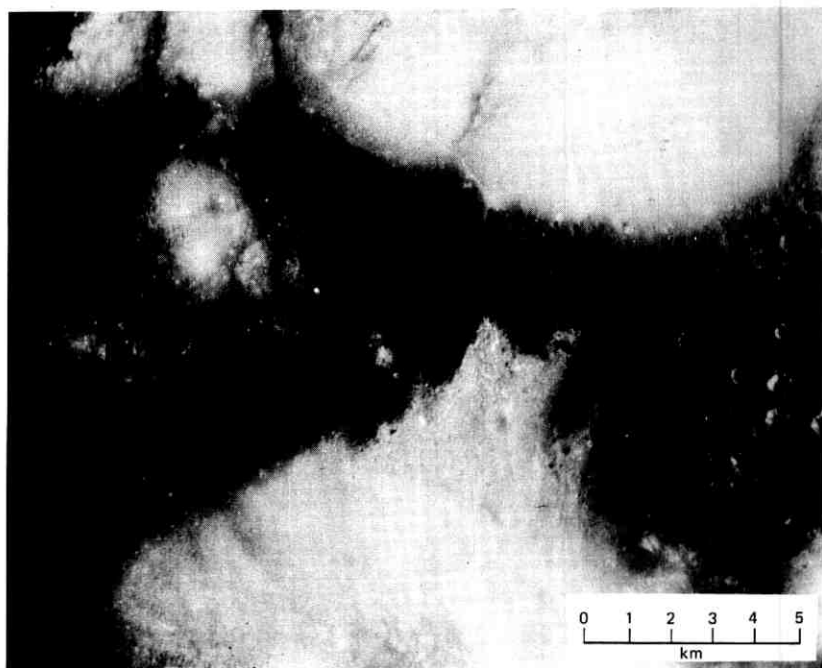


Fig. 59—Panoramic camera photograph of the Taurus-Littrow region showing the Apollo 17 landing point.

mountains forming the basin rim. Serenitatis mare material forms an embayment around the steep-sided mountains and both the mare material and parts of the highlands are mantled by dark deposits of probable volcanic (pyroclastic) origin. A fault (with wrinkle ridge-like features) cuts across both the dark deposits and highlands near the site and is partly mantled by a debris flow at the base of one of the massifs.

Highland massifs in the area of the landing site are steep-sided and rise almost 2 kilometers above the adjacent mare plain. Large blocky areas are seen in the massifs, and slopes in excess of 25 degrees are common. These highland massifs are believed to represent ancient highland crustal blocks structurally dissected by various basin forming events.

Dark mantle, a very low albedo unit which mantles pre-existing terrain and subdues underlying craters, is extensively developed in this area. Panoramic photography and Command Module Pilot observations on Apollo 15 documented the presence of a number of cinder cones which may be related to this unit. Radar maps indicate that this unit is anomalous in its paucity of block material. It may be composed of a young pyroclastic deposit. For this reason its sampling was of high priority since its age and composition would shed light on the thermal history of the Moon.

APPENDIX G

Aborts

Aborts were off-nominal mission segments following some kind of failure, usually with the only objective being to return safely to Earth. The Apollo missions presented many distinctly different families of abort opportunities, and much effort was spent in developing these into viable options in the rare event that one might be required. In some cases, preservation of certain abort opportunities resulted in constraints to the nominal mission.

Two broad classes of aborts were considered for the translunar coast and lunar orbit phases of a mission: minimum- ΔV and minimum-return-time. Table IV summarizes the maximum- ΔV capabilities of the various propulsion systems that might have been available for an abort during translunar coast and in lunar orbit prior to LM separation. In general, the more ΔV available, the faster the spacecraft could return to Earth.

The minimum- ΔV abort capability and the minimum-return-time capability represented the extremes of return-to-Earth time. In the

TABLE IV—MAXIMUM ΔV AVAILABLE FOR HADLEY MISSION,
LAUNCH JULY 26, 1971*

Option	Source of Propulsion†	Post-Abort Configuration†	ΔV (meters/second)		
			Post-TLI†	Post-LOI†	Post-DOI†
1	DPS	CSM + LM	620	870	900
2	SPS	CSM + LM	1520	620	560
3	DPS + SPS	CSM + LM	2640	1430	1690
4	DPS + SPS	CSM	3450	2190	2120
5	SPS	CSM	2830	1320	1220
6	SPS + DPS	CM + LM	3020	2120	2060
7	DPS	CM + LM	1500	1500	1500
8	DPS + APS	CSM + A/S	830	1190	1240
9	SM/RCS	CSM + LM	25		
10	SM/RCS	CSM	40		

* Spacecraft weights and propellant available were taken from the January 15, 1971, MSC Apollo Spacecraft Weight Status Summary.

† DPS: Descent Propulsion System, SPS: Service Propulsion System, APS: Ascent Propulsion System, SM/RCS: Service Module Reaction Control System; CSM: Command and Service Module, LM: Lunar Module, CM: Command Module, A/S: Ascent Stage; TLI: translunar injection, LOI: lunar orbit insertion, DOI: descent orbit insertion.

event of a contingency, a continuous range of return-to-Earth times between these extremes would have been available. The specific choice depended on real-time factors such as landing area, condition of the spacecraft systems, and condition of the crew.

The ability to return to Earth using only the CSM reaction control system was maintained throughout the translunar trajectory for Apollo missions 8, 10, and 11. For Apollo missions 12, 13, and 14,⁸² the spacecraft was on such a trajectory up to approximately 28 hours after translunar injection. For Apollo 15 and subsequent missions,⁸³ abort capability using the CSM reaction control system propulsion system was maintained for at least 5 hours following translunar injection.

Both minimum- ΔV and minimum-return-time aborts were considered during the translunar phase. Three types of minimum- ΔV aborts were usually considered. The first placed the spacecraft on a trajectory which returned to an unconstrained Earth landing point, the second initially placed the spacecraft on a trajectory which would return to an unconstrained Earth landing point and then executed a second maneuver at 2 hours after pericyinthian to assure landing in the mid-Pacific recovery area (150°W to 170°W), and the third maintained the nominal trajectory through pericynthian and then made a maneuver to place the spacecraft on a trajectory which landed in the mid-Pacific recovery area.

Typical minimum ΔV abort requirements are illustrated in Fig. 60.

Several abort modes were available in the event of an emergency which required the fastest safe return to Earth. Two strategies for fast Earth returns were: a direct return to Earth without going around the Moon, and an immediate minimum- ΔV maneuver to put the spacecraft on a circumlunar return trajectory, with a second maneuver executed 2 hours after pericynthian to speed up the vehicle. Typical return times for these types of aborts are illustrated in Fig. 61.

The minimum return time for direct aborts increased with time elapsed from translunar injection, while the return time for circumlunar aborts decreased. Thus, there was a point at which the return time was the same for both the circumlunar and the direct abort. This point was

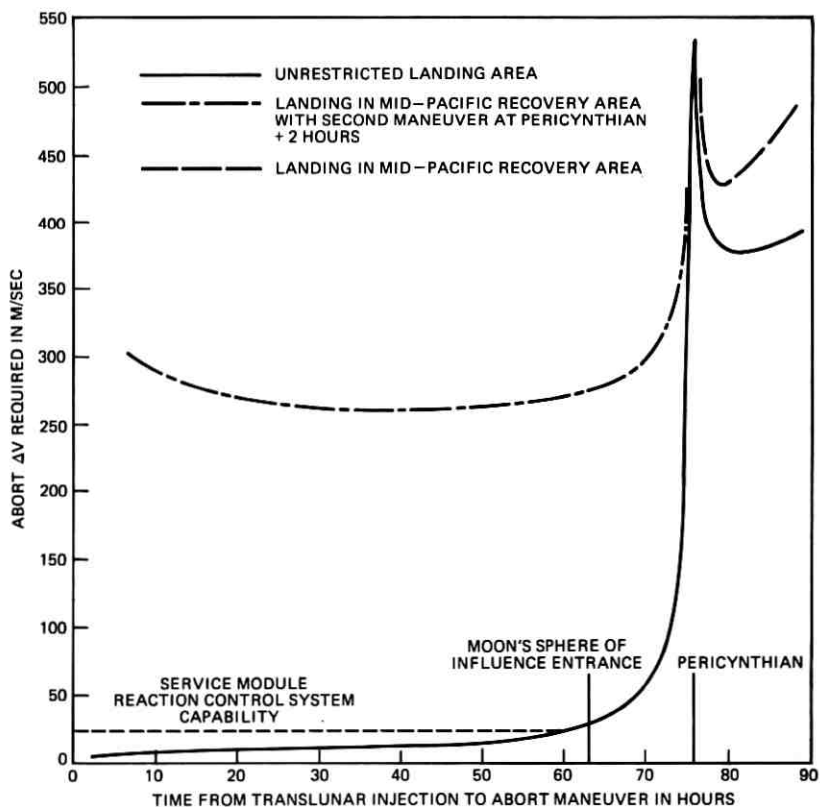


Fig. 60—Apollo 15 minimum ΔV abort requirements (July 26, 1971 launch date).

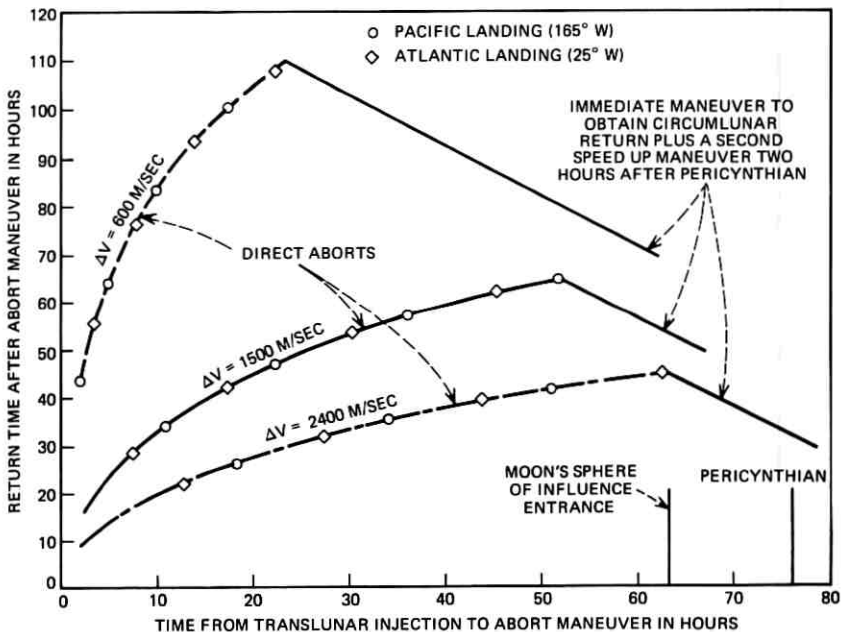


Fig. 61—Apollo 15 minimum return to Earth times for translunar aborts (July 26, 1971 launch date).

referred to as the critical point and represented the farthest point from Earth with respect to time.

The possibility of a CSM separation failure from the S-IVB was also considered in determining translunar abort capability. In this event, abort ΔV capability was provided by the CSM reaction control system and several S-IVB propulsion sources. Typically, the CSM reaction control system capability was found to provide the abort requirement for approximately 17 hours after translunar injection for a nominal translunar injection, while for a 3σ translunar injection underburn case the S-IVB propulsive sources (liquid oxygen and liquid hydrogen plus the Auxiliary Propulsion System) could provide the abort ΔV required for approximately 8 hours after translunar injection.

Beginning with Apollo 12, trajectory design was constrained to provide descent propulsion system abort capability, i.e., in the event lunar orbit insertion was not performed, a LM descent propulsion system maneuver 2 hours or more after pericynthian could return the spacecraft safely to Earth.

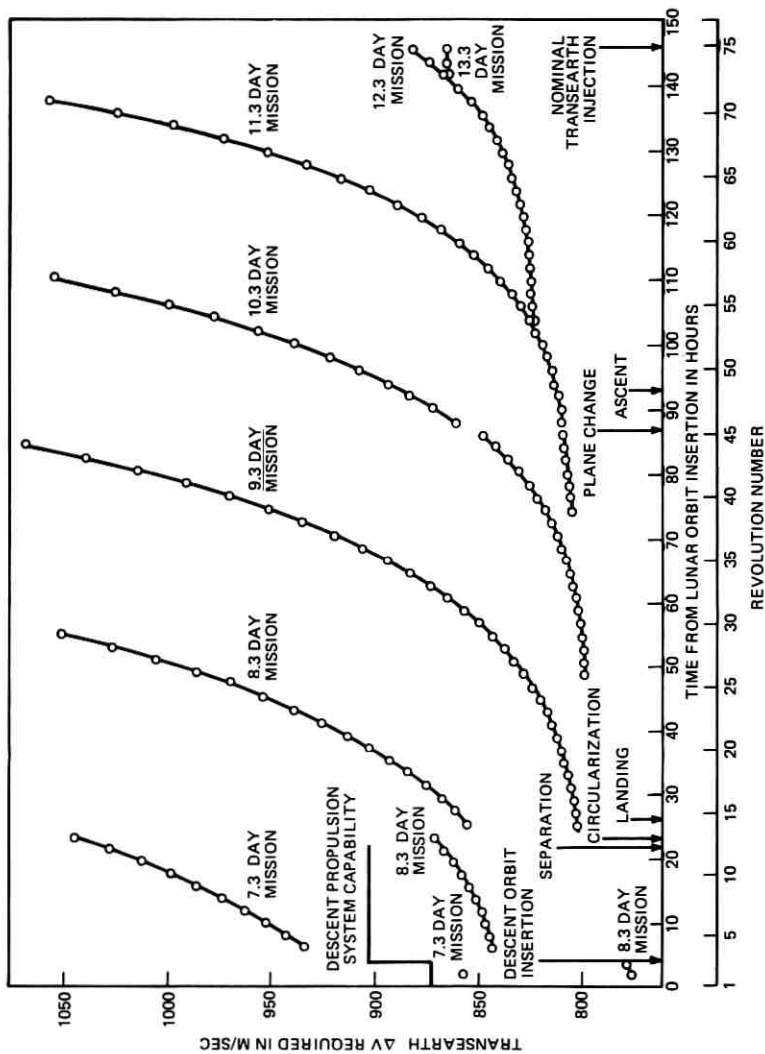


Fig. 62—Apollo 15 return to Earth requirements from lunar orbit (July 26, 1971 launch date).

Investigation of abort requirements and capabilities throughout the lunar orbit insertion burn and consideration of the operational restrictions involved in performing the abort maneuver led to the development of three post-lunar orbit insertion abort modes.¹⁷ Orbits resulting from very short lunar orbit insertion burns were either hyperbolic trajectories or ellipses (which impact the Moon). The procedure in this case was to perform the abort as soon as possible after shutdown. For lunar orbit insertion burns from approximately 127 to 182 seconds, a two-impulse mode was developed consisting of an initial corrective maneuver which transferred the spacecraft onto an intermediate orbit from which a low ΔV transearth injection maneuver could be made within a reasonably short time. When the vehicle arrived at the minimum fuel point (near pericynthian) the second maneuver was performed to return the vehicle to Earth. For lunar orbit insertion burn times greater than approximately 182 seconds (which gave stable nonimpacting ellipses), aborts were performed by waiting until the spacecraft reached the vicinity of pericynthian (behind the Moon) from which a low ΔV abort was performed. Regions of overlap existed at the transition times from one mode to another within which either mode could be used.

Abort from lunar orbit were more expensive than aborts from trans-lunar coast. Fig. 62 illustrates the return-to-Earth ΔV cost as a function of time in lunar orbit for Apollo 15.⁸³ Between lunar orbit insertion and descent orbit insertion the transearth injection cost was lowest. After the descent orbit insertion maneuver the ΔV cost to get out of orbit increased roughly by an amount equal to the descent orbit insertion maneuver of 60 meters/second. After circularization, the transearth injection cost dropped by 20 meters/second, equal to the circularization maneuver. All cases shown in Fig. 62 were targeted to the mid-Pacific landing area.

REFERENCES

Note: Although a number of the reports and memoranda cited as references are not generally available, they are included to show the chronology of the site selection process. Information as to the availability of reports and memoranda listed here may be obtained from: NASA Scientific and Technical Information Facility, P. O. Box 33, College Park, Maryland 20740.

1. Boyle, W. S., James, D. B., and Howard, B. T., "Apollo and the Unmanned Program," Bellcomm Memorandum for File, October 30, 1962.
2. Fudali, R. F., Powers, T. L., and Howard, B. T., "Analysis of the Value of the Lunar Logistics System. Part I: An Operations Research Study of a Strategy for Locating Lunar Landing Sites," Bellcomm Technical Report TR-63-207-4, March 14, 1963.
3. Pearse, C. A., "Photometry and Polarimetry of the Moon and their Relationship

- to Physical Properties of the Lunar Surface," Bellcomm Technical Report TR-63-211-6, August 23, 1963.
4. Thompson, W. B., "Lunar Landing Site Constraints. The Arguments for and against One Preselected Site versus Several Sites," Bellcomm Technical Report TR-64-211-4, January 31, 1964.
 5. James, D. B., "Lunar Site Survey for the Apollo Program by the Unmanned Program," Bellcomm Technical Memorandum TM-64-1112-3, April 24, 1964.
 6. Lloyd, D. D., "A Preliminary Evaluation of Alternate Strategies for Apollo Site Survey," Bellcomm Technical Memorandum TM-64-1012-5, October 28, 1964.
 7. Lloyd, D. D., and Fudali, R. F., "Lunar Orbiter Mission Planning," Bellcomm Technical Report TR-65-211-1, January 25, 1965.
 8. "Apollo Flight Mission Assignments," NASA Directive M-D MA 500-11, June 1971.
 9. Shoemaker, E. M., and Hackman, R. J., "Stratigraphic Basis for a Lunar Time Scale," from *The Moon*, edited by Kopal, Z., and Mikhailov, Z. K., London: Academic Press, 1962, pp. 289-300.
 10. Hinners, N. W., "The New Moon: A View," *Reviews of Geophysics and Space Physics*, 9, No. 3 (August 1971), pp. 447-552.
 11. "Apollo Operational Nominal Trajectory Ground Rules," NASA/MSC Internal Note No. 64-OM-4, March 14, 1964.
 12. Cappellari, J. O., Jr., "A Compendium of the Moon's Motion and Geometry, 1966 through 1985," Bellcomm Technical Report TR-68-310-1, January 1968.
 13. Young, K. A., and Alexander, J. D., "Apollo Lunar Rendezvous," NASA/MSC Internal Note No. 70-FM-47, March 25, 1970.
 14. Mummert, V. S., "Tracking Limitations on Apollo Western Lunar Landing Sites," Bellcomm Memorandum for File, December 13, 1965.
 15. Alexander, J. D., DuPont, A. L., Bell, J. A., and Spurlin, H. O., "Operational LM Abort and Rescue Plan for Apollo 13 (Mission H-2): Volume II-Rendezvous and Rescue," NASA/MSC Internal Note No. 70-FM-9, January 30, 1970.
 16. Klaasen, K. P., "Evaluation of SPS Weather Avoidance Delta-V Requirements," Bellcomm Memorandum for File, October 30, 1970.
 17. "Thirteenth Apollo Abort Working Group Meeting," NASA/MSC Internal Note No. 67-FM36-275, July 25, 1967.
 18. Caldwell, S. F., and Martersteck, K. E., "Optimization of Launch Azimuth Range to Adjust Launch Window Duration and Improve Vehicle Performance Margin," Bellcomm Memorandum for File, December 23, 1970.
 19. Anselmo, D. R., and Bass, R. A., "Feasibility of Hybrid Lunar Missions to Hadley, Copernicus, Davy, Marius Hills and Descartes from Early 1971 through 1974," Bellcomm Memorandum for File, June 2, 1970.
 20. Anselmo, D. R., "Feasibility of a Marius Hills Mission in the Period from July through October 1971," Bellcomm Memorandum for File, December 24, 1969.
 21. Baker, M. K., "SPS Requirements for a J2 Tycho Mission," Bellcomm Memorandum for File, September 17, 1970.
 22. Stern, R. J., "SPS Optimized Missions to Copernicus and Descartes during the J2 (3, 4, 5/72) and J3 (12/72, 1, 2/73) Mission Time Frames," Bellcomm Memorandum for File, February 22, 1971.
 23. Laugle, J. W., "Performance Scan Data for Marius Hills in 1972 (Apollo 17)," NASA/MSC Memorandum 71-FM55-04, January 5, 1971.
 24. McCaffety, O., "Performance Scans for Apollo 17," NASA/MSC Memorandum 71-FM-31, February 10, 1971.
 25. Stern, R. J., "The Effect of Approach Azimuth and Sun Elevation at LM Landing on Mission Design for Apollo 16 and 17, Descartes or Copernicus," Bellcomm Technical Memorandum TM71-2013-1, April 13, 1971.
 26. Mummert, V. S., "Lunar Landing Site Accessibility for July 1969," Bellcomm Technical Report TR-65-209-3, March 31, 1965.
 27. Cappellari, J. O., Jr., Kinney, W. D., Satterlee, A. A., and Tigner, R. D., "A Study of the Behavior of Lunar Accessibility over Extended Time Periods. Part I-Free Return Trajectories," Bellcomm Technical Report TR-65-209-4, May 28, 1965.
 28. Dudek, J. S., Kinney, W. D., and Smith, K., "A Study of Lunar Accessibility

- over Extended Time Periods. Part II-Non-Free Return Trajectories," Bellcomm Technical Report TR-65-310-1, October 22, 1965.
29. Cappellari, J. O., Jr., Dudek, J. S., and Kinney, W. D., "A Summary of Apollo Lunar Accessibility," Bellcomm Technical Report TR-66-310-2, January 18, 1966.
 30. Bass, R. A., and Stern, R. J., "Determination of Apollo Lunar Surface Accessibility Subject to DPS Abort and Lighting Constraints," Bellcomm Technical Memorandum TM-70-2013-2, March 31, 1970.
 31. Bass, R. A., and Wynn, S. C., "The Region of the Lunar Surface Accessible during March of 1972 (Apollo 16) and December of 1972 (Apollo 17)," Bellcomm Memorandum for File, April 29, 1971.
 32. Bush, G. L., Hoekstra, T. B., and LaPiana, F., "Ideas for Improvement of LM Descent Trajectory," Bellcomm Memorandum for File, June 30, 1969.
 33. Sorensen, J. A., "Look Angle Characteristics of a Proposed Apollo 15 LM Descent Trajectory," Bellcomm Memorandum for File, December 11, 1970.
 34. Sorensen, J. A., "Parameter Sensitivities of Preliminary Apollo 15 Trajectories," Bellcomm Memorandum for File, December 31, 1970.
 35. Farmer, G., and Hamblin, D. J., *First on the Moon*, Boston: Little, Brown and Company, 1970, p. 256.
 36. Graham, C. H., *Vision and Visual Perception*, New York: Wiley, 1965.
 37. Blackwell, H. R., "Contrast Thresholds of the Human Eye," *J. Opt. Soc. Am.*, *36*, No. 11 (November 1946), pp. 624-643.
 38. Taylor, J. H., "Use of Visual Performance Data in Visibility Prediction," *Appl. Opt.*, *3*, No. 5 (May 1964), pp. 562-569.
 39. Blackwell, H. R., "Specification of Interior Illumination Levels," *Illum. Eng.*, *54*, No. 6 (June 1959), pp. 317-353.
 40. Minnaert, M., "Photometry of the Moon," in *Planets and Satellites*, Vol. III (1961) of *The Solar System*, Kuiper, G. P., and Middlehurst, B. M., eds., Chicago: Univ. of Chicago Press.
 41. Herriman, A. G., Washburn, H. W., and Willingham, D. E., "Ranger Preflight Science Analysis and the Lunar Photometric Model," JPL Technical Report 32-384 (Rev.), March 11, 1963.
 42. Willingham, D., "The Lunar Reflectivity Model for Ranger Block III Analysis," JPL Technical Report 32-664, November 2, 1964.
 43. Van Diggelen, J., "Photometric Properties of Lunar Crater Floors," *Rech. Obs. Utrecht*, *14*, No. 2, 1959, pp. 1-114.
 44. Hapke, B. W., and Van Horn, H., "Photometric Studies of Complex Surfaces, with Applications to the Moon," *J. Geophys. Res.*, *68*, No. 15 (August 1, 1963), pp. 4545-4570.
 45. Hapke, B. W., "An Improved Theoretical Lunar Photometric Function," *Astron. J.*, *71*, No. 5 (June 1966), pp. 333-339.
 46. "Analysis of Apollo 8 Photography and Visual Observations," NASA SP-201, 1969.
 47. Gehrels, T., Coffeen, T., and Owings, D., "Wavelength Dependence of Polarization. III. The Lunar Surface," *Astron. J.*, *69*, No. 10 (December 1964), pp. 826-852.
 48. "Analysis of Apollo 10 Photography and Visual Observations," NASA SP-232, 1971.
 49. Byrne, C. J., "Lunar Photographic Orbiter: Lighting and Viewing Conditions," Bellcomm Technical Report TR-63-211-8, October 11, 1963.
 50. Hamza, V. and Radin, H. W., "Lighting and Approach Angle Considerations for Manned Lunar Landings," Bellcomm Technical Memorandum TM-65-1012-13, December 7, 1965.
 51. Anselmo, D. R., and Cavedo, D. A., "Evaluation of Lunar Lighting Constraint based on Photometric Derived Scene Contrast," Bellcomm Technical Memorandum TM-66-2013-1, April 29, 1966.
 52. Saulietis, I., "Visibility of Lunar Craters During the LEM Final Approach Phase," NASA/MSC Internal Note 66-EG-4, January 10, 1966.
 53. Feng, T., "A Study to Determine Optimum Lunar Lighting Conditions for Visual Selection of LEM Touchdown Point," Hughes Aircraft Company Report SSD 60293R, January 1967.

54. Ziedman, K., "Visibility during Lunar Landing," TRW Systems Report 05952-6195-R000, January 19, 1968.
55. Lewis, J. L., and Wheelwright, C. D., "Lunar Landing and Site Selection Study," NASA/MSC Technical Note TN D-2999, September, 1965.
56. Troester, R., "Reduction in Lunar Surface Visibility Due to Glare during a Landing into the Sun," Bellcomm Technical Memorandum TM-68-2013-5, September 30, 1968.
57. "Fra Mauro Lunar Landing—Visibility at High Sun Elevation Angles," NASA/MSC Report MSC-02583, January 20, 1971.
58. "Apollo Lunar Landing Mission Symposium," NASA Technical Memorandum TM-X-58006, Manned Spacecraft Center, Houston, Texas, June 25-27, 1966.
59. Moore, T. E., McSwain, G. G., and Montgomery, J. D., "Guidance Laws for Controlling Off-Nominal LM Powered Descent Trajectories Back to the Nominal," NASA/MSC Internal Note MSC-EG-69-9, February 28, 1969.
60. Moore, T. E., "System Performance with Proposed New Delta Guidance Reverted as Much as Possible to Apollo 11 LM Powered Descent Guidance," NASA/MSC Internal Note MSC-EG-69-42, October 31, 1969.
61. Sorensen, J. A., "The Use of Delta Guidance for Improved Trajectory Control and Fuel Cost during LM Descent," Bellcomm Technical Memorandum TM-70-2014-6, June 11, 1970.
62. Savely, R. T., "Free-Flight Analytic State Partial for Error Propagation," NASA/MSC Astrodynamics Conf., Houston, Texas, December 12-14, 1967.
63. Goodyear, W. H., "A General Method for the Computation of Cartesian Coordinates and Partial Derivatives of the Two-Body Problem," IBM, NASA Contractor Report CR-522, September 1966.
64. de Vezin, H. G., "Doppler Observable Modeling for the Apollo Real-Time Orbit Determination Program," NASA/MSC Astrodynamics Conf., Houston, Texas, December 12-14, 1967.
65. Wollenhaupt, W. R., "Apollo Orbit Determination and Navigation," AIAA 8th Aerospace Sci. Meeting, New York City, January 19-21, 1970.
66. Bellcomm Apollo Simulation Program Operations Manual, January 1, 1965, prepared by Bell Telephone Laboratories, Inc., Whippany, N. J., on behalf of Bellcomm, Inc., Washington, D. C.
67. Bellcomm Apollo Simulation Program Maintenance Manual, January 1, 1965, prepared by Bell Telephone Laboratories, Inc., Whippany, N. J., on behalf of Bellcomm, Inc., Washington, D. C.
68. Amman, R. J., "Mission Analysis and Open-Loop Trajectory Targeting Theory for the Bellcomm Apollo Simulation Program," Bell Telephone Laboratories, Inc., unpublished work.
69. Egorov, V. A., "Certain Problems of Moon Flight Dynamics," *Russian Literature of Satellites, Part I*, New York: International Physical Index, Inc., 1958.
70. Bass, R. A., "Optimization of Hybrid Trajectories for the Apollo Mission under a DPS Abort Constraint," Bellcomm Memorandum for File, February 7, 1969.
71. Kerr, M. R., "Parametric Analysis of Three-Impulse Transfer between a Hyperbolic Lunar Orbit and a Circular Lunar Parking Orbit," Bellcomm Technical Memorandum TM-70-2013-1, March 18, 1970.
72. Sun, F. T., "Analysis of the Optimum Two-Impulse Orbital Transfer under Arbitrary Conditions," AIAA J., 6, (November 1968), pp. 2145-53.
73. Bass, R. A., "J-Mission Lunar Accessibility during November and December 1971," Bellcomm Memorandum for File, July 7, 1970.
74. Kerr, M. R., and Stern, R. J., "An Improved Determination of Optimal Moon-to-Earth Trajectories for BCMASP," Bellcomm Memorandum for File, April 20, 1970.
75. Klaasen, K. P., "Calibration of the Descent Propulsion System Propellant Tanks and Propellant Quantity Gauging System," Bellcomm Memorandum for File, March 11, 1970.
76. Klaasen, K. P., "Effects of LM Descent Propellant Gauging Inaccuracy on Propellant Budgeting," Bellcomm Memorandum for File, January 12, 1971.
77. Estberg, D. G., and Klaasen, K. P., "Saturn V Payload Capability Increase

- from S-IC Pitch Profile Optimization," Bellcomm Technical Memorandum TM-71-2013-2, April 21, 1971.
78. Anselmo, D. R., and Marshall, J. L., Jr., "Spacecraft Payload and Mission Profile Changes for Lunar Exploration Missions," Bellcomm Memorandum for File, March 17, 1969.
 79. Estberg, D. G., "Effect of Lower CSM Parking Orbit on Rescue after Abort during LM Descent," Bellcomm Memorandum for File, December 18, 1969.
 80. "Quarterly Weight and Performance Report—March 1970 through June 1970," NASA Headquarters Document SE 015-002-1, July 1, 1970.
 81. Marshall, J. L., Jr., "WAP—A General Purpose Weight and Performance Analysis Program," Bellcomm Memorandum for File, December 30, 1971.
 82. Anselmo, D. R., and Baker, M. K., "Translunar and Lunar Orbit Abort Trajectories for Apollo 14," Bellcomm Memorandum for File, December 7, 1970.
 83. Baker, M. K., "Apollo 15 Translunar and Lunar Orbit Aborts for the Nominal Launch—7/26/71," Bellcomm Memorandum for File, March 7, 1971.

Contributors to This Issue

Many people were involved in the Apollo lunar landing site selection process over the years. However, only the names of the few who contributed directly to the preparation of this issue have been included in the following list of contributors:

Bass, R. A.	Hoekstra, T. B.
Boysen, A. P., Jr.	Klaasen, K.
Cappellari, J. O., Jr.	Marshall, J. L., Jr.
El-Baz, F.	Martersteck, K. E.
Ennis, W. W.	Piotrowski, W. L.
Estberg, D. G.	Reynolds, P. E.
Ferrari, A. J.	Stern, R. J.
Head, J. W.	Troester, R. A.
Heffron, W. G.	Wagner, R. L.
Hinners, N. W.	Wynn, Mrs. S. C.

3406-7-2 N.Z.

Contributors to This Issue

Many people were involved in the Apollo lunar landing site selection process over the years. However, only the names of the few who contributed directly to the preparation of this issue have been included in the following list of contributors:

Bass, R. A.	Hoekstra, T. B.
Boysen, A. P., Jr.	Klaasen, K.
Cappellari, J. O., Jr.	Marshall, J. L., Jr.
El-Baz, F.	Martersteck, K. E.
Ennis, W. W.	Piotrowski, W. L.
Estberg, D. G.	Reynolds, P. E.
Ferrari, A. J.	Stern, R. J.
Head, J. W.	Troester, R. A.
Heffron, W. G.	Wagner, R. L.
Hinners, N. W.	Wynn, Mrs. S. C.

3406-7-2 N.Z.